Sepsis-associated Pathways Segregate Cancer Groups

Himanshu Tripathi+, Samanwoy Mukhopadhyay+, Saroj Kant Mohapatra*

+ These authors contributed equally to this work.

* skm1@nibmg.ac.in

Abstract

Background: Sepsis and cancer are both leading causes of death, and occurrence of any one, increases the likelihood of the other. While cancer patients are susceptible to sepsis, survivors of sepsis are also susceptible to develop certain cancers. This mutual dependence for susceptibility suggests shared biology between the two disease categories. Earlier analysis had revealed cancer-related pathway to be up-regulated in Septic Shock (SS), an advanced stage of sepsis. This has motivated a more comprehensive comparison of the transcriptomes of SS and cancer.

Methods: Gene Set Enrichment Analysis was performed to detect the pathways enriched in SS and cancer. Thereafter, hierarchical clustering was applied to identify relative segregation of 17 cancer types in to two groups *vis-a-vis* SS. Biological significance of the selected pathways was explored by network analysis. Clinical significance of the pathways was tested by survival analysis. A robust classifier of cancer groups was developed based on machine learning.

Results: A total of 66 pathways were observed to be enriched in both SS and cancer. However, clustering segregated cancer types into two categories based on the direction of transcriptomic change. In general, there was up-regulation in SS and one group of cancer (termed Sepsis-Like Cancers, or SLC), but not in other cancers. SLC group mainly consisted of malignancies of the gastrointestinal tract (head and neck, oesophagus, stomach, liver and biliary system) often associated with infection. Machine learning classifier successfully segregated the two cancer groups with high accuracy (> 98%). Additionally, pathway up-regulation was observed to be associated with survival in the SLC group of cancers.

Conclusion: Transcriptome-based systems biology approach segregates cancer into two groups (SLC and CA) based on similarity with SS. Host response to infection plays a key role in pathogenesis of SS and SLC. However, we hypothesize that some component of the host response is protective in both SS and SLC.

Keywords: Sepsis, Septic shock, Cancer, KEGG Pathway, TCGA, GEO

Background

Sepsis is a potentially life-threatening complication caused by dysregulated host response to infection, often leading to organ failure and death. Estimated global burden of sepsis is more than 48.9 million people in 2017 with 11 million deaths [1]. Septic shock is the advanced stage of sepsis with metabolic dysregulation and uncontrolled hypotension. Several epidemiological studies have linked sepsis and cancer [2, 3]. Liu *et al.* [2] conducted an association study between sepsis and ensuing risk of cancer in elderly adult population of the United States, and observed that sepsis is significantly associated with increased risk for many cancers including chronic myeloid leukemia, myelodysplastic syndrome, acute myeloid leukemia, cancers of the cervix, liver, lung, rectum, colon. Another association study revealed 2.5 fold increased risk of sepsis in survivors of cancer in

community-dwelling adults (the risk is increased up to 10 times in hospitalized cancer patients) [3]. Co-occurrence of cancer with sepsis is associated with higher mortality than sepsis alone without cancer [4]. On the other hand, sepsis is a common cause of death in critically ill patients with cancer, with high ICU and hospital mortality [5–7]. Interestingly, mortality due to sepsis varies widely from 42 to 82% across cancer tissue types [8], suggesting varying likelihood of survival of patients suffering from different cancers.

This study is motivated by multiple shared features of septic shock (SS) and cancer. There is co-occurrence of the two entities, with synergistic effect on mortality. Both are associated with inflammation at some stage of the disease. Inflammation is well understood to promote malignant growth with participation of diverse immune cells and molecules, such as, cytokines [9]. Similarly, sepsis is understood as a non-resolving inflammatory response to infection that leads to organ dysfunction [10]. Both the diseases are associated with anaerobic metabolism with lactic acidosis being a hallmark of septic shock [9, 11]. In our earlier work, we have observed a cancer associated pathway to be significantly up-regulated in septic shock [12]. Additionally, there are previous reports on shared molecular changes in sepsis and cancer. Bergenfelz *et al.* [13] reported that Wnt5a induces immunosuppressive phenotype of macrophages in sepsis and breast cancer patients. HMGB1, a key late inflammatory mediator of systemic inflammatory response syndrome associated with bacterial sepsis, is also implicated in tumorigenesis and disease progression [14]. Muscle wasting - observed in patients with cancer, severe injury and sepsis - is associated with increased expression of several genes, particularly transcription factors and nuclear cofactors, regulating different proteolytic pathways [15]. Methodologically, all of these studies employed gene-level analysis, i.e., considering gene as the functional unit. On the other hand, a gene set or pathway represents coordinated molecular activity and represents a higher-order functional unit in a tissue or cell. Pathway-level analysis allows detection of a cumulative signal that is not accessible at the gene-level. To our knowledge, there is no report in literature on pathway-level comparison between sepsis and cancer. In the present study, we have performed unbiased analysis of SS and cancer datasets to discover shared patterns of pathway-level transcriptional alteration underlying the two illnesses.

Methods

Gene expression data

TCGA data: Gene expression data as FPKM (Fragments Per Kilobase of transcript per Million mapped reads) values were retrieved from The Cancer Genome Atlas (TCGA) database (https://portal.gdc.cancer.gov/) on July 5, 2018 for 17 different human cancers i.e., bladder urothelial carcinoma (BLCA), breast invasive carcinoma (BRCA), cholangiocarcinoma (CHOL), colon adenocarcinoma (COAD), esophageal carcinoma (ESCA), head and neck squamous cell carcinoma (HNSC), kidney chromophobe (KICH), kidney renal clear cell carcinoma (KIRC), kidney renal papillary cell carcinoma (KIRP), liver hepatocellular carcinoma (LIHC), lung adenocarcinoma (LUAD), lung squamous cell carcinoma (LUSC), prostate adenocarcinoma (PRAD), rectum adenocarcinoma (READ), stomach adenocarcinoma (STAD), thyroid carcinoma (THCA) and uterine corpus endometrial carcinoma (UCEC). For each cancer type, TCGA project code was provided in the search field and RNA-seq data for paired samples (each pair consisting of tissue from tumour zone and tissue from adjacent unaffected zone in the same individual) were downloaded. In all, gene expression data were derived from 687 patients with cancer. Data were transformed to logarithmic scale (base 2).

GEO data: Six studies of septic shock (SS) were selected following the procedure described earlier [12]. Normalized gene expression data from the series matrix files were retrieved from NCBI Gene

Expression Omnibus (GEO) database (https://www.ncbi.nlm.nih.gov/geo/) on April 10, 2019. Data were transformed to logarithmic scale (base 2). Expression intensity for each Entrez gene ID was calculated after removing duplicated probe sets. Genes common to all SS studies were included in the analysis. In all, gene expression data were derived from 445 patients with SS and 116 control subjects. Redundant samples (other than control and SS) were excluded from analysis.

Characteristics of 23 distinct data sets used in the current study (6 of SS and 17 of cancer) are listed in Table 1. Each data set consisted of transcriptome-wide expression data from a number of patients suffering from a single disease (SS or cancer). For SS, each data set consisted of blood transcriptome data. For cancer, each data set consisted of transcriptome data from a tissue. Control was defined as adjacent normal tissue for cancer (TCGA), and a healthy subject for SS (GEO).

Table 1: Characteristics (such as tissue of origin, source database, disease type, sample size of each study and details about the platform technology used to generate the data) of the 23 data sets (17 cancer + 6 septic shock) included in the analysis. Study_code refers to the code assigned by the source database (either TCGA or GEO) to the data set. TCGA stands for The Cancer Genome Atlas. GEO stands for NCBI Gene Expression Omnibus. Paired control refers to adjacent normal tissue in the same cancer patient. Technology for transcriptome assay is either sequencing (RNA-seq) or hybridization-based microarray (Affymetrix).

Study_Code	Data source	Disease	Tissue	Number of samples	Paired control	Technology
BLCA	TCGA	Cancer	Bladder	38	Yes	RNA-seq (Illumina)
BRCA	TCGA	Cancer	Breast	220	Yes	RNA-seq (Illumina)
CHOL	TCGA	Cancer	Gallbladder, liver and parts of biliary tract	18	Yes	RNA-seq (Illumina)
COAD	TCGA	Cancer	Colon and rectosigmoid junction	82	Yes	RNA-seq (Illumina)
ESCA	TCGA	Cancer	Esophagus	16	Yes	RNA-seq (Illumina)
HNSC	TCGA	Cancer	Base of tongue, floor of mouth, gum, hypo- and oro-pharynx, larynx, etc.	86	Yes	RNA-seq (Illumina)
KICH	TCGA	Cancer	Kidney	48	Yes	RNA-seq (Illumina)
KIRC	TCGA	Cancer	Kidney	144	Yes	RNA-seq (Illumina)
KIRP	TCGA	Cancer	Kidney	64	Yes	RNA-seq (Illumina)
LIHC	TCGA	Cancer	Liver and intrahepatic bile ducts	100	Yes	RNA-seq (Illumina)
LUAD	TCGA	Cancer	Bronchus and lung	114	Yes	RNA-seq (Illumina)
LUSC	TCGA	Cancer	Bronchus and lung	98	Yes	RNA-seq (Illumina)
PRAD	TCGA	Cancer	Prostate gland	104	Yes	RNA-seq (Illumina)
READ	TCGA	Cancer	Rectum rectosigmoid junction	20	Yes	RNA-seq (Illumina)

STAD	TCGA	Cancer	Stomach	62	Yes	RNA-seq (Illumina)
THCA	TCGA	Cancer	Thyroid gland	116	Yes	RNA-seq (Illumina)
UCEC	TCGA	Cancer	Corpus uteri	46	Yes	RNA-seq (Illumina)
GSE4607	GEO	Septic Shock	Whole Blood	84	No	Microarray (Affymetrix HGU 133 Plus 2.0)
GSE8121	GEO	Septic Shock	Whole Blood	75	No	Microarray (Affymetrix HGU 133 Plus 2.0)
GSE9692	GEO	Septic Shock	Whole Blood	45	No	Microarray (Affymetrix HGU 133 Plus 2.0)
GSE13904	GEO	Septic Shock	Whole Blood	124	No	Microarray (Affymetrix HGU 133 Plus 2.0)
GSE26378	GEO	Septic Shock	Whole Blood	103	No	Microarray (Affymetrix HGU 133 Plus 2.0)
GSE26440	GEO	Septic Shock	Whole Blood	130	No	Microarray (Affymetrix HGU 133 Plus 2.0)

Pathway Enrichment Analysis

Pathway (gene set) enrichment analysis was performed using the algorithm previously described [12, 16]. Gene sets were defined based on pathways annotated at KEGG [17]. Any pathway with small number (10 or less) of genes was discarded from analysis. For each gene, t-statistic was computed to denote change in gene expression in case group compared to the control group. For each pathway, a score was calculated by weighted averaging (i.e., sum of the gene-level t-statistics divided by the square root of the number of genes in the pathway) of all gene-level t-statistic for the pathway. Significance of the observed pathway score was calculated by permutation testing performed in the following manner. In each permutation, the samples were randomly re-labelled as case and control, with calculation of a simulated pathway score. This was done 10000 times generating 10000 simulated values representing the null distribution of the pathway score. Deviation of the observed pathway score from the null distribution was quantified by the fraction of times that the simulated score was more extreme than the observed score. This result was assigned as permutation p-value of the observed pathway score. Pathway enrichment analysis was performed using code modified from the R function *gseattperm()* of the package **Category** [18].

Cluster Analysis

Pathway scores of all 23 studies (6 SS + 17 cancer) were subjected to hierarchical clustering in the following manner. First, the Euclidean distance matrix was computed to capture the pair-wise dissimilarity among the studies. Thereafter, the distance matrix was subjected to agglomerative hierarchical cluster analysis, with “complete” linkage method. Distance matrix computation and cluster analysis were performed using the R functions *dist()* and *hclust()* respectively. Output of the cluster analysis was plotted as a dendrogram.

Visualization of Pathway-level and Gene-level Expression Scores

A pathway was selected if it was significantly enriched (permutation $p < 0.01$) in 80% or more of the studies in one or both of the cancer groups (SLC, CA). Pathway score matrix was generated for all selected pathways across all 23 data sets. Heat map was generated with the R function *heatmap.2()* of the package **gplots** [19]. For each pathway, mean pathway score across the disease group was calculated separately. Boxplot of the pathway scores for the three disease groups

(SS, SLC and CA) was drawn using R function *boxplot()*.

For generating gene-level heat map of individual pathway, the following steps were followed. First, average log-expression level was calculated for case group and control group separately. Log2(fold -change) or LFC was calculated by subtracting the average control value from the average case value. This was done for each gene. For each disease type (SS, SLC or CA), median LFC was calculated across the studies in that disease group. Combined heat map was generated based on the pathway genes and the three disease groups. Only those genes with similar LFC directionality in SLC and SS were included in visualization.

Network analysis

Firstly, a background network was constructed by including all the pathways (KEGG) [17] with overlapping gene memberships, i.e., for a pathway to be included, it must share at least 5% of the total number of genes with another pathway. Pathways connected to less than 3 other pathways each were dropped from network analysis. In this network, each pathway was considered a node, and the edge between two nodes represented overlap between the two pathways. In this way, a network was constructed with 244 nodes and 5304 edges. Degree distribution of the network was calculated using the function *degree_distribution()* of the package **igraph** [20]. Plot of the degree distribution of the network was drawn. For each node in the network, degree and betweenness centrality were calculated with the R functions *degree()* and *betweenness()* respectively. In the network diagram, selected pathways were shown as nodes coloured in red. Box plot was drawn to show the difference of degrees between selected set and other pathways.

Sample-level pathway score

Individual pathway scores for the cancer patients were computed in the following manner. For each subject, two genome-wide expression vectors were retrieved from TCGA: one for the tumour tissue (T) and another for the adjacent normal tissue (N). Normalized gene expression vector (E) was then calculated by subtracting the normal expression values from the tumour expression values (E = T - N). For each of the selected 66 pathways, a score (Z) was calculated as the weighted average of the expression of the genes in the pathway (i.e., sum of the individual gene expression scores divided by the square root of the number of genes in the pathway). This resulted in 66 pathway scores for each patient. These individual pathway scores were used for survival analysis.

Machine learning

For the machine learning-based prediction, we retrieved additional transcriptome data for SLC and CA cancers from NCBI GEO. Six datasets containing 542 cancer subjects (of both SLC and CA) and 180 healthy control subjects were included (Additional File 7: Table S4.). The additional validation data sets were required because the TCGA data sets were used for feature selection (i.e., 66 pathways) and segregation of cancer groups (SLC and CA). For each cancer sample, pathway scores were generated by weighted averaging of the gene-level t-statistic between the case group and control group, (i.e., sum of the individual t-statistic divided by the square root of the number of genes in the pathway). The scores of the sixty-six pathways were used as input and the cancer group label (SLC or CA) as output in machine learning-based classification of cancer patients. Support vector machine (SVM) and neural net (NN) classifiers were implemented using R package **MLInterfaces** [21]. SVM was used through function call *Mlearn()* with learning function svmI. Neural Network was used through function call *MLearn()* with learning function nnetI and three nodes in the hidden layer, with weight decay set to 0.01. Confusion matrix from the classifier output of five-fold cross-validation was collected for calculation of misclassification rate (fraction of samples wrongly predicted by the algorithm) and accuracy.

Survival Analysis

Based on the number of cases and available survival information, three SLC cancer types (HNSC, KIRC and LIHC) were selected for survival analysis. The following clinical metadata were collected as provided by TCGA: days (to death or last follow-up) and outcome (survivor or non-survivor). Patient-level (sample-level) pathway score was used for analysis. For each cancer type, the patients were divided into two groups (high-score and low-score) by applying the median pathway score as threshold. Survival plots were generated using the functions in the R package **survival** [22] as described here. First, a survival object was created applying the function *Surv()*, with day and outcome. The output, i.e., the fitted model, was passed to the function *survfit()* that created two survival curves, based on the level of pathway score (high or low). Survival plots were displayed using the function *ggsurvplot()* from the package **survminer** [23]. Significance of the difference between the survival plots of the two curves was calculated by the function *surv_pvalue()* from the same package.

Code and data availability

All programming was done in the R programming language [24]. Data and R code are available at the following link: https://figshare.com/ (https://doi.org/10.6084/m9.figshare.8118413.v3, https://doi.org/10.6084/m9.figshare.8118647.v5). The whole data can be downloaded as a single zip file (tcnibmgdoc.zip). Upon uncompressing the zip, instructions for running the code and generating the figures of this manuscript are available in the file howto.pdf.

Selection of the transcriptome data sets and analysis workflow leading to the final list of 66 significant pathways are described in Fig. 1. The study characteristics of the data sets are listed in Table 1.

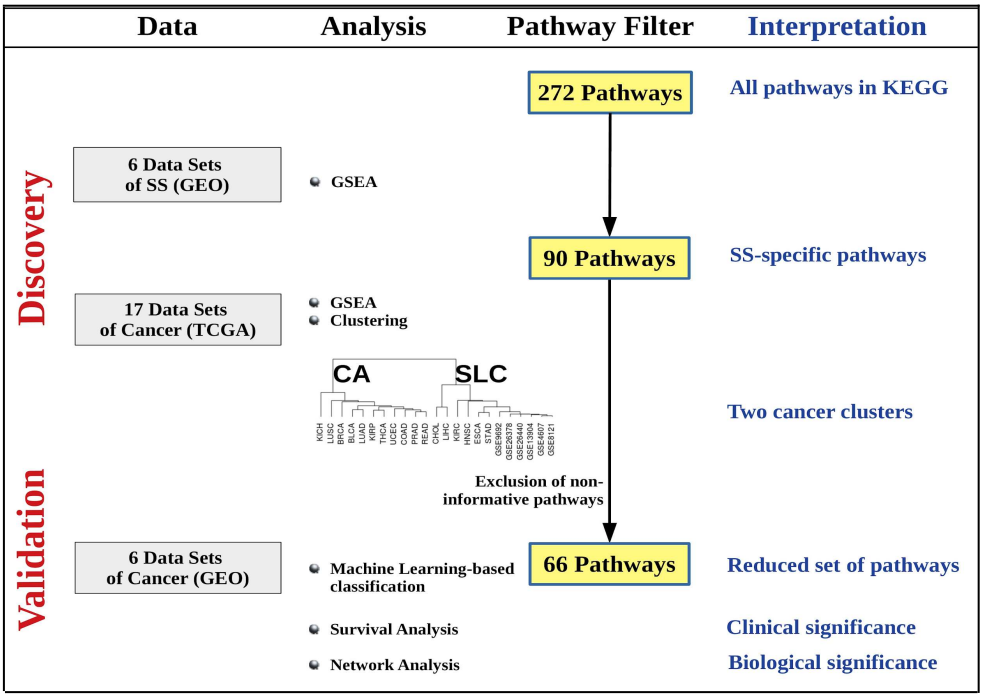

Fig. 1: Selection of data and analysis workflow. Left-most column shows the source of data from GEO for SS and TCGA for cancer. Data for SS were applied first followed by data from TCGA. Next column describes the processing of the data that form a progressive filter for narrowing down the number of pathways of relevance. KEGG contains 272 pathways of which 90 were assigned significant pathway score by Gene Set Enrichment Analysis (details in the main text). The right-most column lists the interpretations

made at each horizontal step.

Results

The transcriptomic data for 23 studies (17 cancer and 6 SS) consisted of 687 patients with cancer and 445 with SS. The data were subjected to progressive analysis and pathway filtering (Fig. 1).

Hierarchical clustering revealed two groups of cancers

At the outset, independent of our data, there were a total of 272 pathways in the KEGG database. Application of permutation-based testing of each pathway, revealed that 90 of these were significantly ($p < 0.01$) enriched in each of the 6 SS data sets, thus constituting a robust set of SS-specific pathways. Hierarchical clustering on combined cancer and sepsis data sets for these 90 pathways revealed two groups of cancers, with one group segregating with SS (Additional File 1: Figure S1). The 6 cancers (HNSC, ESCA, STAD, LIHC, CHOL, KIRC) belonging to the SS clade were termed Sepsis-Like Cancer (SLC). The other 11 cancers (BLCA, BRCA, COAD, KICH, KIRP, LUAD, LUSC, PRAD, READ, THCA and UCEC) formed the other clade and were termed the CA (Cancer Alone) group.

In order to exclude those pathways that may be irrelevant to cancer biology, the 90 pathways were tested for enrichment in any or both of the cancer groups (i.e., significantly enriched in at least 80% of a group of cancer). 24 out of the 90 SS-specific pathways were observed not to be associated with any of the two cancer groups. Exclusion of these 24 non-significant pathways resulted in retention of 66 pathways significantly associated with both SS and cancer. Pathway score matrix of these 66 pathways across all diseases (including SS, SLC, CA) was visualized as a heat map (Fig. 2A). The sample dendrogram of this heat map recapitulated the segregation of the cancer groups as observed earlier with 90 pathways (Additional File 1: Figure S1). In general, the heat map demonstrated up-regulation of the pathways in SS and SLC. Further, for each pathway, mean score was calculated across all data sets in one disease group (SS, SLC or CA). Box plot of these scores clearly demonstrated the shared directionality in pathway dysregulation in SS and SLC, i.e., in both these conditions there was up-regulation of the pathway (Fig. 2B). Additionally, the average number of pathways up-regulated in a disease group was observed to be 63, 58 and 11 for SS, SLC and CA respectively (Additional File 4: Table S1), thus establishing general agreement in the direction of pathway transcriptional change between SS and SLC. The overall trend in pathway dysregulation was also reflected in the gene-level heat map for individual pathways (Additional File 2: Figure S2).

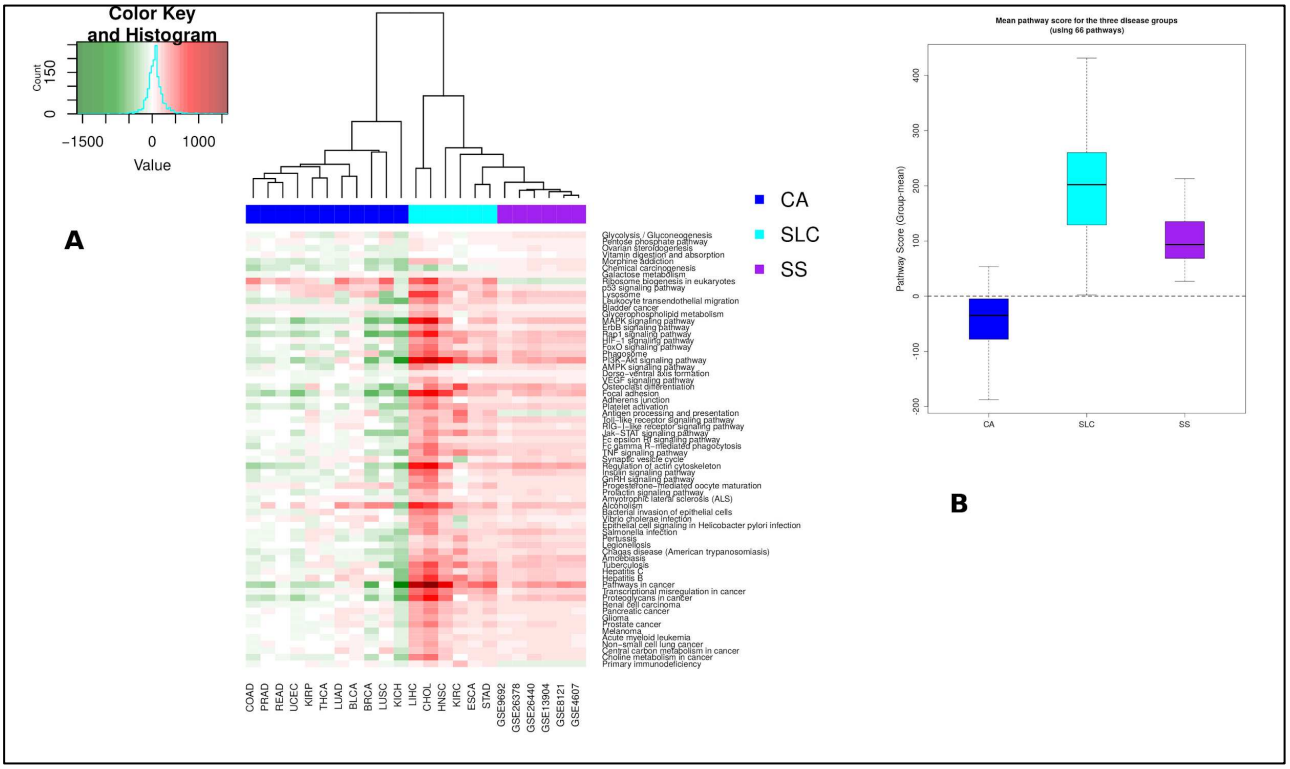

Fig. 2: (A) Pathway heat map for 66 selected KEGG pathways where each pathway is significantly perturbed in at least 80% of the studies in one or both of the two groups of cancers. Colour of the cell is explained by the colour key histogram provided on the top left. Green indicated down-regulation of pathway, red indicates up-regulation. In the column-sidebar, purple indicates SS group, cyan indicates SLC group and blue indicates CA group. Positive pathway score is presented in red, negative pathway score in green. (B) Box plot shows group-mean pathway scores for the three groups of diseases. In general, there is pathway up-regulation in SLC group, even higher than that in SS, while down-regulation in CA group.

Network analysis

Genome-level biological significance of the selected pathways was revealed by network analysis. Here, the network consisted of all KEGG pathways as nodes and substantial pairwise gene-overlap among pathways as edges. The centrality of the selected pathways was further quantified in terms of degree and betweenness centrality. Degree captures short-range connectivity of a node (i.e., how many nodes are connected to this node?), while betweenness centrality captures long-range centrality (i.e., how often this node falls on the shortest path between any two other nodes?) Degree captures the number of immediate neighbours of a node, while betweenness captures the essentiality of a node to the structure of the network. The degree and betweenness values for the selected 66 pathways were recorded (Additional File 5: Table S2).

The degree distribution of the network showed scale-free property of a biological network, i.e., many nodes with few edges and a few nodes with large number of edges (Additional File 3: Figure S3 - panel A). Visual exploration revealed the selected pathways at the core of the network (Fig. 3), and this was confirmed by comparing the degree of these 66 pathways with other pathways in the human genome. As shown in Additional File 3: Figure S3 (panel B), selected pathways had higher degree than the other pathways.

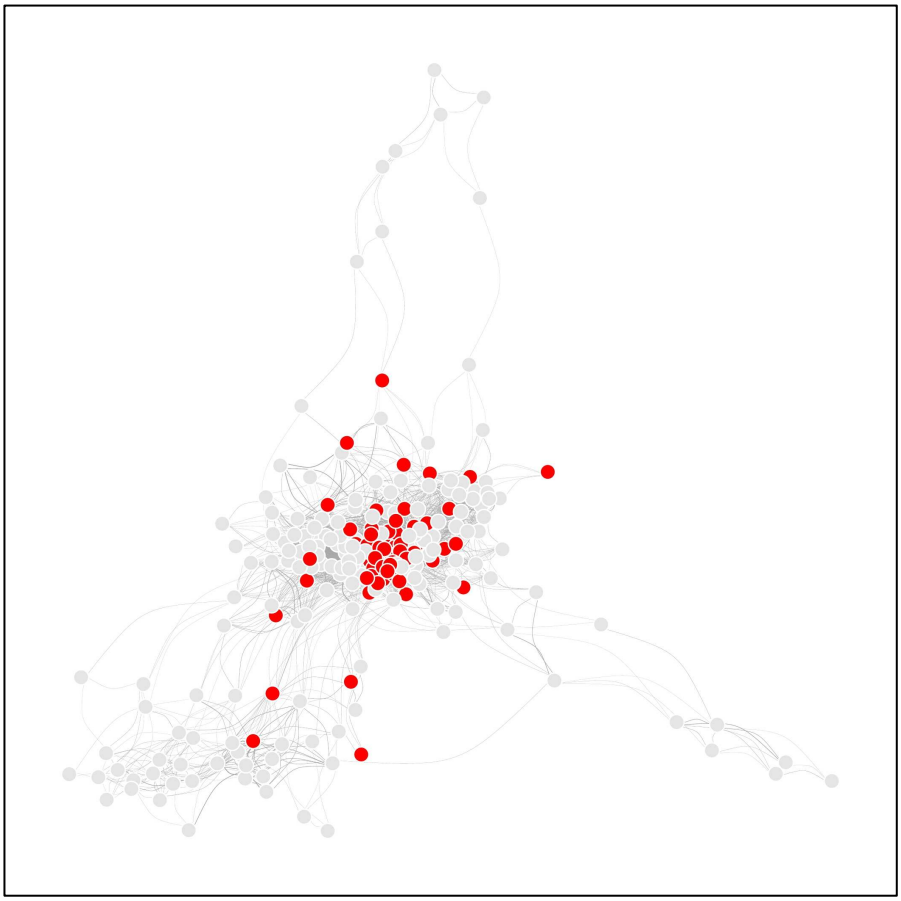

Fig. 3: KEGG overlap network is constructed with each KEGG pathway as a node and overlapping gene membership between two pathways as an edge. The selected 66 pathways are shown in red, while the other pathways are shown in grey. Red nodes (selected pathways) have more connecting edges than the grey nodes, thus representing hub-like nature of selected pathways. This suggests that key biological processes are perturbed in both SS and SLC.

Machine learning-based prediction of cancer group (SLC/CA) from 66 pathway scores

In order to assess the clinical relevance of the selected pathways, we asked if it is possible to predict (by a machine learning algorithm) the cancer group based on the selected pathway scores of an individual patient of cancer. For each patient, 66 pathway scores were input for the classifier, with the expected output being SLC or CA. Five-fold cross-validation was employed with balanced partitioning in each fold. Both algorithms - Support Vector Machine (SVM) and Neural Net (NN) – performed with high accuracy in assigning the samples to their respective cancer groups. SVM correctly assigned 537 (99.08%) out of 542 patients , while NN correctly assigned 536 (98.89%) out of 542 patients, with a misclassification rate of 0.9% and 1.1% respectively (Table 2). This independent validation showed the clinical relevance of the selected 66 pathways for prediction of cancer group from individual patient-level data.

Table 2: Two machine learning algorithms - Support Vector Machine (SVM) and Neural Network (NN) - were implemented through the function call MLearn (of R package MLInterfaces). SVM was applied with default parameters. Neural Network applied with three nodes in the hidden layer, with weight decay set to 0.01. Five-fold cross-validation was performed by generating a partition function (for cross-validation, where the partitions are approximately balanced with respect to the distribution of cancer tissue types (SLC or CA) in training and test sets in each fold. Confusion matrix from the classifier output was collected for calculation of misclassification rates.

Support Vector Machine		**Predicted**	
		CA	**SLC**
Given	**CA**	**349**	**1**
	SLC	**4**	**188**
Misclassification rate			**0.9**
Neural Network		**Predicted**	
		CA	**SLC**
Given	**CA**	**347**	**3**
	SLC	**3**	**189**
Misclassification rate			**1.1**

Survival analysis

Another measure of clinical relevance of pathway signature was provided by its association with survival. For a given pathway, the patients were divided into two groups of subjects (high-scoring and low-scoring) based on the level of pathway score. Survival probability for these two groups was assessed both graphically and statistically. For many of the pathways, there was a higher pathway score in survivors compared to non-survivors in SLC. This directionality was also maintained in SS, i.e., higher pathway score in survivors compared to non-survivors (Additional File 6: Table S3). The number of pathways associated ($p < 0.1$) with survival varied: 9 (14%) in HNSC, 28 (42%) in LIHC and 34 (52%) in KIRC (Fig. 4A). Representative plots were drawn to show survival difference between high-score and low-score patients for the pathway “Fc gamma R-mediated phagocytosis” (Fig. 4B-D).

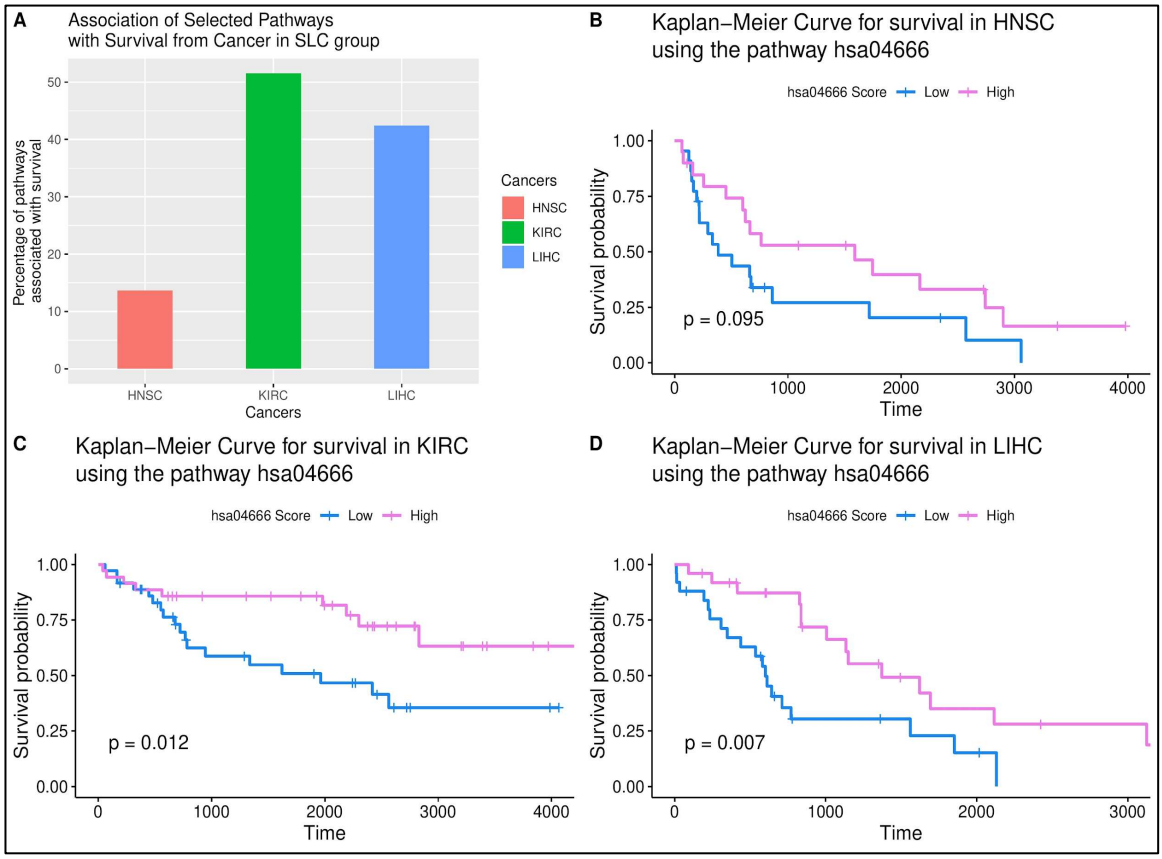

Fig. 4: (A) Three SLC studies were selected for survival analysis. For each cancer, association with survival was accepted at threshold of $p < 0.1$. For each cancer type, proportion of pathways associated with survival was calculated and converted to a percentage. The percentage values are presented in this bar plot. As shown, up to 50% of the pathways are associated with survival in the SLC group. (B-D) Kaplan-Meier plot showing significant association between pathway score and survival from the three SLC cancer types: HNSC (B), KIRC (C) and LIHC (D).

Functional classification of the pathways

The selected 66 pathways were divided into categories based on their functional relevance. The categories included: immune system, infection, cancer, catabolism, signal transduction, ribosome biogenesis and carbohydrate metabolism (Additional File 8: Text S1).

Viral integration in TCGA samples

Out of the 687 cancer samples from TCGA analysed by us, there was overlap of 425 (61.9%) samples with the samples analysed for viral integration by Tang *et al*. [25]; of the 425 samples, 120 belonged to SLC group, and 305 belonged to CA group. Viral integration was observed in 9 (7.5%) SLC samples and 2 (0.66%) CA samples, showing significantly ($p = 0.0003$) higher viral integration in SLC. In another study by Cao *et al.* [26], there was an overlap of 533 (77.6%) of 687 samples analysed by us. Of the 533, 200 (37.5%) were SLC while 333 (62.5%) were CA cancers. There was significantly ($p = 0.001$) higher viral integration in SLC (30%) compared to CA (17.4%). The report by Kazemian *et al.* [27] was not associated with supplementary sample-level data. However, re-analysis of summary data provided (Additional File 8: Table S5) led to the finding of significantly ($p = 4.10E-13$) higher viral integration in SLC (18.7%) compared to CA (5.6%). Over all, the findings were consistent with SLC cancers to have greater likelihood of prediction of viral integration.

Discussion

Comprehensive system-level analysis reveals shared transcriptomic response between septic shock (SS) and a subset of cancers (SLC). The SLC group predominantly consists of cancer of the upper GI tract, including head and neck, oesophagus, stomach, liver and biliary tract. The striking segregation of the SLC group with SS suggests shared elements of pathophysiology operational in these disorders. Sixty-six pathways differentially expressed in both SS and SLC represent critical biological processes, such as metabolism, immune response and protection against infection. Network analysis reveals the selected pathways as a core functional module (Figure 3) of the genome-scale network dysregulated in both SS and SLC. Many of these processes, such as metabolism and inflammatory response are known to contribute to the pathogenesis of both sepsis and cancer [9].

The segregation of cancer into two groups (SLC and CA) prompted us to investigate the prospect of the selected pathways as a classifier. Machine learning-based validation of an independent data set proved that the pathways indeed consist of a robust sample-level signature of the cancer groups. It is thus possible to predict, with high accuracy, whether a patient belongs to a particular cancer group (SLC or not). With plummeting costs and increasing acceptability of clinical transcriptomics, this signature may be useful in future for patient stratification.

Similarity in the direction of change in pathway activity immediately evokes an explanation in terms of shared immunological response in either case. SLC are often associated with infection (i.e., human papilloma virus in “head and neck”, *H. pylori* in stomach, hepatitis viruses in liver). In fact, TCGA data analysed for the presence of viral sequence reads in RNA-seq datasets of several cancers have revealed infection status of the samples. Interestingly, the majority of the infected samples belong to the GI associated cancers including head and neck (HNSC), oesophagus (ESCA), stomach (STAD) and liver (LIHC) [25–29]. Cao et al. (2016) [26] estimated high percentage of infected samples in TCGA datasets for liver (21.2%), head and neck (16.6%), stomach (14.8%) and oesophagus (12%). It is known that sepsis starts out as an infection, but it is the uncontrolled host response that drives the phase of shock. Similarly, in cancers with an infectious origin, host response (e.g., inflammation) plays a role in malignant transformation [9]. Pathways related to immune response are consistently differentially expressed in both SS and SLC. Although the time scale of pathogenesis is much shorter in SS compared to cancer, our finding calls for greater attention into the shared cellular processes underlying these two distinct clinical phenotypes.

The finding of pathway up-regulation associated with survival brings new insight into the relationship between the shared transcriptomic patterns and disease outcome. Sepsis is a highly lethal dysregulated host response to infection, and SLC, by extension, appears to share a part of that response. Since the pathways are selected on the basis of up-regulation in both SLC and SS (compared to control), plausible explanation is that the pathway up-regulation is protective rather than detrimental to the human host. It is worth mentioning that viral integration or bacterial infection in a setting of cancer has been reported to favour survival in SLC cancers of oropharyngeal [30], liver [31] and kidney [32].

Alteration of intestinal permeability is known in both sepsis and cancer [33]. It may be speculated that anatomical proximity increases the likelihood of the liver and upper gastrointestinal tissue to be exposed to the translocated microbial products through a permeable gut, eliciting a host response in both SS and SLC. Significant association between survival and up-regulation of phagocytosis-associated pathway (i.e., Fc gamma R-mediated phagocytosis) lends support to this view. In general, sepsis is less lethal in patients with cancer of the digestive system than cancer of other organs [8]. The role of gut in survival from sepsis and cancer is an active area of research with translational potential.

Conclusions

Firstly, transcriptome-based systems biology approach segregates cancer into two groups (SLC and CA) based on similarity with SS. Secondly, the similarity is based on a set of pathways associated with pathogenesis of sepsis and cancer. These pathways form a robust signature of a novel cancer grouping. Lastly, up-regulation of the pathways is protective rather than detrimental to the patient. A mechanism of the shared protective host response is hypothesized in terms of immunocompetence induced by microbial products from the permeable gut. This work is the first step towards a systems biology-based patient stratification. It is hoped that future work in this direction shall generate actionable knowledge for clinical management of both cancer and septic shock.

List of abbreviations:

BLCA: Bladder Urothelial Carcinoma
BRCA: Breast invasive carcinoma
CA: Cancer Alone
CHOL: Cholangiocarcinoma
COAD: Colon adenocarcinoma
ESCA: Esophageal carcinoma
FPKM: Fragments Per Kilobase of transcript per Million mapped reads
GEO: Gene Expression Omnibus
HNSC: Head and Neck squamous cell carcinoma
ICU: Intensive Care Unit
KEGG: Kyoto Encyclopaedia of Genes and Genomes
KICH: Kidney Chromophobe
KIRC: Kidney renal clear cell carcinoma
KIRP: Kidney renal papillary cell carcinoma
LFC: log2(fold change)
LIHC: Liver hepatocellular carcinoma
LUAD: Lung adenocarcinoma
LUSC: Lung squamous cell carcinoma
NCBI: National Center for Biotechnology Information
NN: Neural Net
PRAD: Prostate adenocarcinoma
READ: Rectum adenocarcinoma
SLC: Sepsis-Like Cancers
SS: Septic shock
STAD: Stomach adenocarcinoma
SVM: Support Vector Machine
TCGA: The Cancer Genome Atlas
THCA: Thyroid carcinoma
UCEC: Uterine Corpus Endometrial Carcinoma

Declarations

- **Ethics approval and consent to participate**

  In this study, patient data from public databases (GEO and TCGA) have been analysed. We have not used any patient data that are not already available in the public domain.

- **Consent to publish**
  Not applicable.
- **Availability of data and materials**
  All programming was done in the R programming language [20]. Data and R code are available at the following link: https://figshare.com/ (https://doi.org/10.6084/m9.figshare.8118413.v3, https://doi.org/10.6084/m9.figshare.8118647.v5**)**. The whole data can be downloaded as a single zip file (tcnibmgV3doc.zip). Upon uncompressing the zip, instructions for running the code and generating the figures of this manuscript are available in the file howto.pdf.
- **Competing interests**
  The authors declare that they have no competing interests.
- **Funding**
  This work was supported by an extramural grant (No. BT/PR16536/BID/7/652/2016, duration of 3 years, sanctioned on 30-03-2017) from the Department of Biotechnology, Government of India.
- **Authors' contributions**
  SKM conceptualized the study and contributed to Funding Acquisition, Project Administration, Resources, Supervision. HT contributed to Data Curation. SM contributed to Data Curation, Software, Validation, Visualization. All authors contributed to Formal Analysis, Investigation, Methodology, Manuscript writing and approved of the final manuscript.
- **Acknowledgements**
  We thank the National Cancer Institute for making TCGA data available in the public domain. We thank the National Center for Biotechnology Information for making GEO data available in the public domain. This study would not have been possible without data from these two resources. We thank the Director of National Institute of Biomedical Genomics for making the computational resources accessible to us. HT and SKM thank the Department of Biotechnology, Government of India for financial support to carry out the analysis.
- **Authors' information**
  HT and SM are co-first authors. All authors are affiliated to the National Institute of Biomedical Genomics, P.O. NSS, Kalyani, Nadia, West Bengal, India. 741251.

References:

1. Rudd KE, Johnson SC, Agesa KM, Shackelford KA, Tsoi D, Kievlan DR, et al. Global, regional, and national sepsis incidence and mortality, 1990–2017: analysis for the Global Burden of Disease Study. The Lancet. 2020;395:200–11.

2. Liu Z, Mahale P, Engels EA. Sepsis and risk of cancer among elderly adults in the United States. Clinical Infectious Diseases. 2019;68:717–24.

3. Moore JX, Akinyemiju T, Bartolucci A, Wang HE, Waterbor J, Griffin R. A prospective study of cancer survivors and risk of sepsis within the REGARDS cohort. Cancer Epidemiology. 2018;55 April:30–8.

4. Abou Dagher G, El Khuri C, Chehadeh AAH, Chami A, Bachir R, Zebian D, et al. Are patients with cancer with sepsis and bacteraemia at a higher risk of mortality? A retrospective chart review of patients presenting to a tertiary care centre in Lebanon. BMJ Open. 2017;7:1–8.

5. Torres VBL, Azevedo LCP, Silva UVA, Caruso P, Torelly AP, Silva E, et al. Sepsis-associated outcomes in critically ill patients with malignancies. Annals of the American Thoracic Society. 2015;12:1185–92.

6. Rosolem MM, Rabello LSCF, Lisboa T, Caruso P, Costa RT, Leal JVR, et al. Critically ill patients with cancer and sepsis: Clinical course and prognostic factors. Journal of Critical Care. 2012;27:301–7.

7. Aygencel G, Turkoglu M, Turkoz Sucak G, Benekli M. Prognostic factors in critically ill cancer patients admitted to the intensive care unit. Journal of Critical Care. 2014;29:618–26.

8. Wang Y, Zhou J, Wu K. High 28-day mortality in critically ill patients with sepsis and concomitant active cancer. Journal of International Medical Research. 2018;46:5030–9.

9. Hanahan D, Weinberg RA. Hallmarks of cancer: The next generation. Cell. 2011;144:646–74.

10. Vincent J-L, Opal SM, Marshall JC, Tracey KJ. Sepsis definitions: time for change. Lancet. 2013;381:774–5.

11. Angus DC, van der Poll T. Severe Sepsis and Septic Shock. New England Journal of Medicine. 2013;369:840–51.

12. Mukhopadhyay S, Thatoi PK, Pandey AD, Das BK, Ravindran B, Bhattacharjee S, et al. Transcriptomic meta-analysis reveals upregulation of gene expression functional in osteoclast differentiation in human Septic shock. PLoS ONE. 2017;12:1–17.

13. Bergenfelz C, Medrek C, Ekström E, Jirström K, Janols H, Wullt M, et al. Wnt5a Induces a Tolerogenic Phenotype of Macrophages in Sepsis and Breast Cancer Patients. The Journal of Immunology. 2012;188:5448–58.

14. Diener KR, Al-Dasooqi N, Lousberg EL, Hayball JD. The multifunctional alarmin HMGB1 with roles in the pathophysiology of sepsis and cancer. Immunology and Cell Biology. 2013;91:443–50.

15. Aversa Z, Alamdari N, Hasselgren PO. Molecules modulating gene transcription during muscle wasting in cancer, sepsis, and other critical illness. Critical Reviews in Clinical Laboratory Sciences. 2011;48:71–86.

16. Jiang Z, Gentleman R. Extensions to gene set enrichment. Bioinformatics. 2007;23:306–13.

17. Ogata H, Goto S, Sato K, Fujibuchi W, Bono H, Kanehisa M. KEGG: Kyoto encyclopedia of genes and genomes. Nucleic Acids Research. 1999;27:29–34.

18. Gentleman R. Category: Category Analysis. R package version 2.50.0.

19. Warnes GR, Bolker B, Bonebakker L, Gentleman R, Liaw WHA, Lumley T et. al. gplots:

Various R Programming Tools for Plotting Data. 2019. https://CRAN.R-project.org/package=gplots.

20. Csardi G NT. The igraph software package for complex network research. 2006. http://igraph.org.

21. Carey V, Gentleman. Carey V, Gentleman R, Mar J, Vertrees J, Gatto L. MLInterfaces: Uniform interfaces to R machine learning procedures for data in Bioconductor containers. R package version. 2018; 1.58.1.

22. Patricia M. Grambsch Terry M. Therneau. Modeling Survival Data: Extending the Cox Model. New York: Springer.

23. Alboukadel Kassambara, Marcin Kosinski, Przemyslaw Biecek. survminer: Drawing Survival Curves using “ggplot2”. 2019. https://CRAN.R-project.org/package=survminer.

24. Team RC, others. R: A language and environment for statistical computing. 2013.

25. Tang KW, Alaei-Mahabadi B, Samuelsson T, Lindh M, Larsson E. The landscape of viral expression and host gene fusion and adaptation in human cancer. Nature Communications. 2013;4:1–9.

26. Cao S, Wendl MC, Wyczalkowski MA, Wylie K, Ye K, Jayasinghe R, et al. Divergent viral presentation among human tumors and adjacent normal tissues. Scientific Reports. 2016;6 June:1–12.

27. Kazemian M, Ren M, Lin J-X, Liao W, Spolski R, Leonard WJ. Possible Human Papillomavirus 38 Contamination of Endometrial Cancer RNA Sequencing Samples in The Cancer Genome Atlas Database. Journal of Virology. 2015;89:8967–73.

28. Cantalupo PG, Katz JP, Pipas JM. Viral sequences in human cancer. Virology. 2018;513:208–16.

29. Salyakina D, Tsinoremas NF. Viral expression associated with gastrointestinal adenocarcinomas in TCGA high-throughput sequencing data. Human Genomics. 2013;7:1–12.

30. Chaturvedi AK, Engels EA, Pfeiffer RM, Hernandez BY, Xiao W, Kim E, et al. Human Papillomavirus and Rising Oropharyngeal Cancer Incidence in the United States. JCO. 2011;29:4294–301.

31. Chao JS, Zhao SL, Ou-Yang SW, Qian YB, Liu AQ, Tang HM, et al. Post-transplant infection improves outcome of hepatocellular carcinoma patients after orthotopic liver transplantation. World Journal of Gastroenterology. 2019;25:5630–40.

32. Chen J, Lv Y, Mu F, Xu K. Long-term response of metastatic renal clear cell carcinoma following a subcutaneous injection of mixed bacterial vaccine: a case report. Onco Targets Ther. 2019;12:2531–8.

33. Bindels LB, Neyrinck AM, Loumaye A, Catry E, Walgrave H, Cherbuy C, et al. Increased gut permeability in cancer cachexia: Mechanisms and clinical relevance. Oncotarget. 2018;9:18224–38.

Supplementary Information

Supplementary Figure S1. For the 90 pathways significantly associated with SS, pathway scores were computed for the cancer studies. Scores for SS (6 studies) and cancer (17 studies) were subjected to hierarchical clustering (details in main text). As shown in this dendrogram, there is clear segregation of the cancer studies into two groups: sepsis–like (SLC) and other cancer (CA).

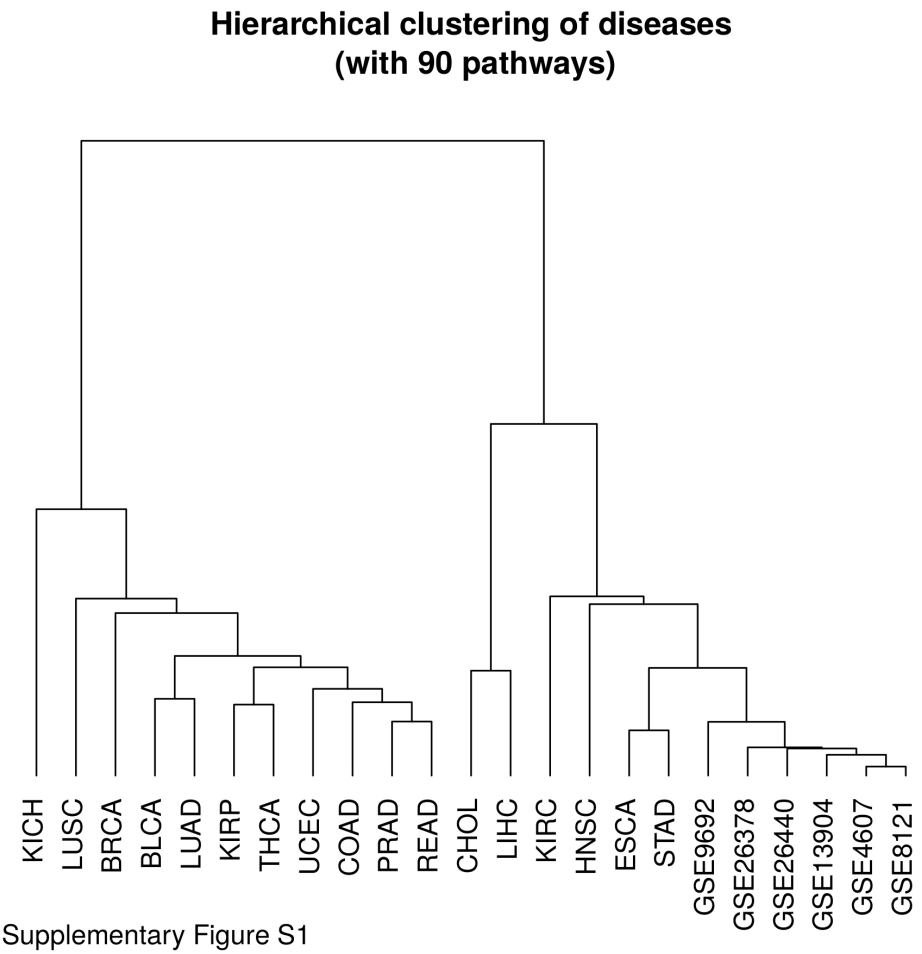

Supplementary Figure S1
For the 90 pathways significantly associated with SS, pathway scores were computed for the cancer studies. Scores for SS (6 studies) and cancer (17 studies) were subjected to hierarchical clustering (details in main text). As shown in this dendrogram, there is clear segregation of the cancer studies into two groups: sepsis–like (SLC) and other cancer (CA).

Supplementary Figure S2. Gene level heat map of each of the selected 66 pathways. LFC for each gene was calculated from disease and normal samples (disease-normal) for all studies. For each disease type (CA, SLC or SS), median LFC was calculated across the studies in that disease type. Combined heat map was generated based on the pathway genes and the three disease groups. We considered only those genes which have similar LFC directionality in SLC and SS. Red colour represents up-regulation in disease compared to control, while green colour represents down-regulation. Pathway names with KEGG identifiers are shown on the top, gene symbol and names are row-labels of heat map. The major class (to which the pathway belongs) is shown at the bottom.

(Go to the last part of the document after page 30)

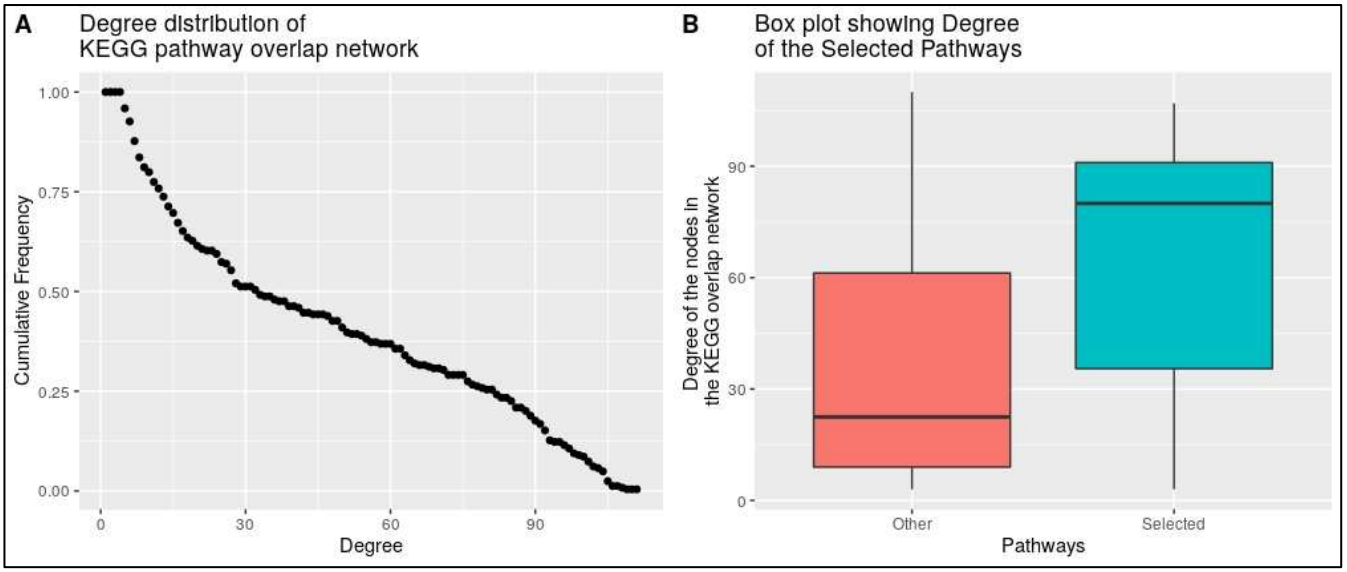

Supplementary Figure S3. (A) This is the degree distribution of the network generated by overlapping KEGG pathways. This shows that there are many nodes with very low connectivity but a few nodes with very high connectivity. This is consistent with the scale-free property of biological networks. (B) Box plot showing comparison of degree between two groups of nodes in this network - selected 66 and others. The higher value of the selected 66 nodes suggests that these are highly overlapping pathways forming a functional core of the human genome.

Supplementary Table S1 . Selected 66 pathways with their significance and direction of regulation in all the studies. Coloured cells are a representation of pathway scores. Red indicates significant up-regulation, green indicates significant down-regulation and grey indicates non-significant change in pathway. Number of up- and down-regulated pathways in each study is shown at the top. Group membership (to CA, SLC or SS) is shown as a label on top of the code of the data set. First three columns of the sheet are pathway name, annotation (functional class) and KEGG ID respectively.

Average number of up-regulated pathways			**11**											**58**						**63**					
# Up-regulated			**30**	**10**	**5**	**1**	**13**	**19**	**19**	**3**	**4**	**9**	**13**	**63**	**63**	**57**	**42**	**62**	**60**	**63**	**63**	**63**	**63**	**63**
# Down-regulated			**0**	**39**	**34**	**65**	**20**	**14**	**32**	**9**	**6**	**12**	**32**	**1**	**1**	**0**	**8**	**1**	**0**	**3**	**3**	**3**	**3**	**3**
			CA											**SLC**						**SS**					
Pathway name	**Annotation**	**Pathway_id**	**BLCA**	**BRCA**	**COAD**	**KICH**	**KIRP**	**LUAD**	**LUSC**	**PRAD**	**READ**	**THCA**	**UCEC**	**LIHC**	**CHOL**	**HNSC**	**KIRC**	**ESCA**	**STAD**	**GSE13904**	**GSE26378**	**GSE26440**	**GSE4607**	**GSE8121**
Pathways in cancer	Cancer	hsa05200																						
Transcriptional misregulation in cancer	Cancer	hsa05202																						
Proteoglycans in cancer	Cancer	hsa05205																						
Renal cell carcinoma	Cancer	hsa05211																						
Pancreatic cancer	Cancer	hsa05212																						
Glioma	Cancer	hsa05214																						
Prostate cancer	Cancer	hsa05215																						
Melanoma	Cancer	hsa05218																						
Bladder cancer	Cancer	hsa05219																						
Acute myeloid leukemia	Cancer	hsa05221																						
Non-small cell lung cancer	Cancer	hsa05223																						
Central carbon metabolism in cancer	Cancer	hsa05230																						
Choline metabolism in cancer	Cancer	hsa05231																						
Chemical carcinogenesis	Cancer	hsa05204																						
Galactose metabolism - Homo sapiens (human)	Carbohydrate metabolism	hsa00052																						
Glycolysis / Gluconeogenesis	Carbohydrate metabolism	hsa00010																						
Pentose phosphate pathway	Carbohydrate metabolism	hsa00030																						
Insulin signaling pathway	Endocrine system	hsa04910																						
GnRH signaling pathway	Endocrine system	hsa04912																						
Progesterone-mediated oocyte maturation	Endocrine system	hsa04914																						
Prolactin signaling pathway	Endocrine system	hsa04917																						
Ovarian steroidogenesis	Endocrine system	hsa04913																						
Platelet activation	Immune system	hsa04611																						
Antigen processing and presentation	Immune system	hsa04612																						
Toll-like receptor signaling pathway	Immune system	hsa04620																						
RIG-I-like receptor signaling pathway	Immune system	hsa04622																						
Fc epsilon RI signaling pathway	Immune system	hsa04664																						
Fc gamma R-mediated phagocytosis	Immune system	hsa04666																						
Leukocyte transendothelial migration	Immune system	hsa04670																						
Bacterial invasion of epithelial cells	Infectious disease	hsa05100																						
Vibrio cholerae infection	Infectious disease	hsa05110																						
Epithelial cell signaling in Helicobacter pylori inf	Infectious disease	hsa05120																						
Salmonella infection	Infectious disease	hsa05132																						
Pertussis	Infectious disease	hsa05133																						
Legionellosis	Infectious disease	hsa05134																						
Chagas disease (American trypanosomiasis)	Infectious disease	hsa05142																						
Amoebiasis	Infectious disease	hsa05146																						
Tuberculosis	Infectious disease	hsa05152																						
Hepatitis C	Infectious disease	hsa05160																						
Hepatitis B	Infectious disease	hsa05161																						
Glycerophospholipid metabolism	Other	hsa00564																						
Ribosome biogenesis in eukaryotes	Other	hsa03008																						
p53 signaling pathway	Other	hsa04115																						
Dorso-ventral axis formation	Other	hsa04320																						
Osteoclast differentiation	Other	hsa04380																						
Focal adhesion	Other	hsa04510																						
Adherens junction	Other	hsa04520																						
Synaptic vesicle cycle	Other	hsa04721																						
Regulation of actin cytoskeleton	Other	hsa04810																						
Amyotrophic lateral sclerosis (ALS)	Other	hsa05014																						
Alcoholism	Other	hsa05034																						
Primary immunodeficiency	Other	hsa05340																						
Vitamin digestion and absorption	Other	hsa04977																						
Morphine addiction	Other	hsa05032																						
MAPK signaling pathway	Signal transduction	hsa04010																						
ErbB signaling pathway	Signal transduction	hsa04012																						

Supplementary Table S2: This table contains the property of each node of the network. Degree of a node is the number of edges connected to a node. Betweenness centrality is a measure of how much information flows through a specific node, i.e., average number of shortest paths passing through the node. Degree refers to the number of neighbours of a node while betweenness centrality refers to how important the node is for maintaining the overall structure of that network. The two nodes with highest betweenness centrality (Glycolysis/Gluconeogenesis, Lysosome) in the network are highlighted.

KEGG Pathway Names	**KEGG ID**	**Degree**	**Betweenness Centrality**
Vitamin digestion and absorption	hsa04977	NA	NA
Ribosome biogenesis in eukaryotes	hsa03008	NA	NA
Glycolysis / Gluconeogenesis	hsa00010	26	1599.07
Lysosome	hsa04142	7	680.2
Insulin signaling pathway	hsa04910	89	560.44
Epithelial cell signaling in Helicobacter pylori infection	hsa05120	49	520.57
AMPK signaling pathway	hsa04152	62	520.28
Vibrio cholerae infection	hsa05110	37	439.59
Choline metabolism in cancer	hsa05231	90	433.04
Tuberculosis	hsa05152	87	410.94
Central carbon metabolism in cancer	hsa05230	81	403.15
Ovarian steroidogenesis	hsa04913	48	387.79
GnRH signaling pathway	hsa04912	107	383.52
Hepatitis B	hsa05161	106	347.57
Chagas disease (American trypanosomiasis)	hsa05142	104	328.8
HIF-1 signaling pathway	hsa04066	80	323.29
Fc epsilon RI signaling pathway	hsa04664	102	317.94
Pertussis	hsa05133	67	295.91
Progesterone-mediated oocyte maturation	hsa04914	103	287.93
Pathways in cancer	hsa05200	98	286.47
VEGF signaling pathway	hsa04370	103	265.42

Amoebiasis	hsa05146	99	248.79
Proteoglycans in cancer	hsa05205	100	230.53
FoxO signaling pathway	hsa04068	90	206.86
Phagosome	hsa04145	31	195.33
PI3K-Akt signaling pathway	hsa04151	80	176.5
Fc gamma R-mediated phagocytosis	hsa04666	83	170.39
MAPK signaling pathway	hsa04010	90	167.12
Platelet activation	hsa04611	100	166.21
Toll-like receptor signaling pathway	hsa04620	91	156.38
Rap1 signaling pathway	hsa04015	96	153.11
Morphine addiction	hsa05032	46	152.64
Prostate cancer	hsa05215	95	150.98
Glioma	hsa05214	97	145.97
TNF signaling pathway	hsa04668	91	136.56
Hepatitis C	hsa05160	91	131.46
Antigen processing and presentation	hsa04612	26	123.22
Bacterial invasion of epithelial cells	hsa05100	56	116.33
Pancreatic cancer	hsa05212	91	101.47
Osteoclast differentiation	hsa04380	87	97.12
Focal adhesion	hsa04510	80	90.01
Acute myeloid leukemia	hsa05221	84	78.81
Chemical carcinogenesis	hsa05204	14	75.3
Leukocyte transendothelial migration	hsa04670	66	72.24
Non-small cell lung cancer	hsa05223	86	64.38
Salmonella infection	hsa05132	48	61.81
Alcoholism	hsa05034	46	60.62
Regulation of actin cytoskeleton	hsa04810	62	60.6
Jak-STAT signaling pathway	hsa04630	61	58.74
Prolactin signaling pathway	hsa04917	91	57.33

Renal cell carcinoma	hsa05211	84	56.81
ErbB signaling pathway	hsa04012	91	56.53
Melanoma	hsa05218	81	45.43
Synaptic vesicle cycle	hsa04721	10	42.04
Galactose metabolism	hsa00052	8	41.96
Amyotrophic lateral sclerosis (ALS)	hsa05014	30	39.8
Glycerophospholipid metabolism	hsa00564	14	26.42
Bladder cancer	hsa05219	53	18.91
Adherens junction	hsa04520	27	17.54
RIG-I-like receptor signaling pathway	hsa04622	39	17.21
Legionellosis	hsa05134	27	9.08
Dorso-ventral axis formation	hsa04320	26	2
p53 signaling pathway	hsa04115	14	1.21
Transcriptional misregulation in cancer	hsa05202	6	0.78
Primary immunodeficiency	hsa05340	5	0.29
Pentose phosphate pathway	hsa00030	3	0

Supplementary Table S3: Three SLC cancers were selected for survival analysis. The value in each cell corresponds to the p-value for association of the pathway with the cancer type. At a threshold of $p < 0.1$, the cell has been high-lighted, noting significant association of the pathway with survival from cancer. Direction of pathway expression score was estimated from visual inspection of survival plot in the SLC cancers. For each cancer, proportion of pathways associated with survival was calculated and converted to percentage (bottom row of the table). For septic shock, pathway score was calculated in the survivor group compared to the non-survivor group, as described in the Methods. A direction of "High" was assigned, if the pathway was observed to be higher in the survivor group for four or more of the eight septic shock data sets tested. Otherwise, the direction of "Low" was assigned.

	P-value			**Direction in Survivors**			
Association with survival	**SLC group**			**SLC group**			**Septic Shock**
	HNSC	**KIRC**	**LIHC**	**HNSC**	**KIRC**	**LIHC**	
Glycolysis / Gluconeogenesis | hsa00010	0.07	0.84	0.24	Low	-	Low	High
Pentose phosphate pathway | hsa00030	0.81	0.74	0.26	-	-	Low	High
Galactose metabolism | hsa00052	0.99	0.61	0.99	-	High	-	High
Glycerophospholipid metabolism | hsa00564	0.63	0.65	0.88	-	-	-	High
Ribosome biogenesis in eukaryotes | hsa03008	0.26	0.40	0.62	High	-	-	High
MAPK signaling pathway | hsa04010	0.53	0.12	0.04	-	High	High	High
ErbB signaling pathway | hsa04012	0.08	0.08	0.22	High	High	-	High
Rap1 signaling pathway | hsa04015	0.51	0.03	0.01	-	High	High	High
HIF-1 signaling pathway | hsa04066	0.22	0.04	0.16	Low	High	-	High
FoxO signaling pathway | hsa04068	0.27	0.00	0.74	Low	High	-	High
p53 signaling pathway | hsa04115	0.50	0.24	0.44	-	High	-	Low
Lysosome | hsa04142	0.55	0.31	0.13	-	High	High	High
Phagosome | hsa04145	0.98	0.92	0.15	-	-	High	High
PI3K-Akt signaling pathway | hsa04151	0.88	0.15	0.00	-	High	High	High
AMPK signaling pathway | hsa04152	0.81	0.00	0.95	-	High	-	High

Dorso-ventral axis formation | hsa04320	0.01	0.01	0.04	High	High	High	High
VEGF signaling pathway | hsa04370	0.27	0.04	0.02	-	High	High	High
Osteoclast differentiation | hsa04380	0.88	0.21	0.08	-	High	High	High
Focal adhesion | hsa04510	0.77	0.12	0.00	-	High	High	High
Adherens junction | hsa04520	0.20	0.01	0.01	High	High	High	High
Platelet activation | hsa04611	0.96	0.10	0.00	-	High	High	High
Antigen processing and presentation | hsa04612	0.74	0.14	0.02	-	High	High	High
Toll-like receptor signaling pathway | hsa04620	0.85	0.17	0.55	-	High	High	High
RIG-I-like receptor signaling pathway | hsa04622	0.92	0.11	0.44	-	High	-	High
Jak-STAT signaling pathway | hsa04630	0.96	0.08	0.62	-	High	-	High
Fc epsilon RI signaling pathway | hsa04664	0.06	0.04	0.06	High	High	High	High
Fc gamma R-mediated phagocytosis | hsa04666	0.10	0.01	0.01	High	High	High	High
TNF signaling pathway | hsa04668	0.50	0.06	0.48	High	High	High	High
Leukocyte transendothelial migration | hsa04670	0.43	0.00	0.05	-	High	High	High
Synaptic vesicle cycle | hsa04721	0.78	0.97	0.11	-	-	High	High
Regulation of actin cytoskeleton | hsa04810	0.76	0.01	0.01	-	High	High	High
Insulin signaling pathway | hsa04910	0.72	0.01	0.47	-	High	High	High
GnRH signaling pathway | hsa04912	0.08	0.21	0.15	High	High	High	High
Ovarian steroidogenesis | hsa04913	0.99	0.02	0.80	-	High	-	High
Progesterone-mediated oocyte maturation | hsa04914	0.80	0.03	0.18	-	High	-	High
Prolactin signaling pathway | hsa04917	0.12	0.02	0.53	High	High	-	High
Vitamin digestion and absorption | hsa04977	0.84	0.35	0.97	-	Low	-	High
Amyotrophic lateral sclerosis (ALS) | hsa05014	0.14	0.11	0.26	-	High	High	High
Morphine addiction | hsa05032	0.20	0.28	0.02	-	High	High	High
Alcoholism | hsa05034	0.28	0.03	0.11	High	High	High	High
Bacterial invasion of epithelial cells | hsa05100	0.49	0.10	0.04	-	High	High	High
Vibrio cholerae infection | hsa05110	0.21	0.67	0.24	High	-	High	High

Epithelial cell signaling in Helicobacter pylori infection | hsa05120	0.12	0.21	0.57	High	High	High	High
Salmonella infection | hsa05132	0.07	0.55	0.38	High	-	High	High
Pertussis | hsa05133	0.98	0.50	0.39	-	-	High	High
Legionellosis | hsa05134	0.31	0.98	0.63	High	-	High	High
Chagas disease (American trypanosomiasis) | hsa05142	0.71	0.10	0.12	-	High	High	High
Amoebiasis | hsa05146	0.67	0.92	0.03	-	-	High	High
Tuberculosis | hsa05152	0.99	0.96	0.01	-	-	High	High
Hepatitis C | hsa05160	0.32	0.03	0.32	High	High	High	High
Hepatitis B | hsa05161	0.19	0.05	0.14	High	High	High	High
Pathways in cancer | hsa05200	0.67	0.01	0.01	-	High	High	High
Transcriptional misregulation in cancer | hsa05202	0.80	0.44	0.06	-	-	High	High
Chemical carcinogenesis | hsa05204	0.80	0.05	0.02	-	Low	Low	High
Proteoglycans in cancer | hsa05205	0.84	0.06	0.04	-	High	High	High
Renal cell carcinoma | hsa05211	0.60	0.04	0.08	-	High	High	High
Pancreatic cancer | hsa05212	0.45	0.01	0.28	High	High	High	High
Glioma | hsa05214	0.61	0.16	0.07	-	High	High	High
Prostate cancer | hsa05215	0.39	0.01	0.02	-	High	High	High
Melanoma | hsa05218	0.59	0.10	0.01	-	High	High	High
Bladder cancer | hsa05219	0.00	0.00	0.03	High	High	High	High
Acute myeloid leukemia | hsa05221	0.47	0.00	0.76	-	High	-	High
Non-small cell lung cancer | hsa05223	0.57	0.02	0.57	High	High	-	High
Central carbon metabolism in cancer | hsa05230	0.69	0.02	0.10	-	High	High	High
Choline metabolism in cancer | hsa05231	0.04	0.01	0.03	High	High	High	High
Primary immunodeficiency | hsa05340	0.77	0.22	0.31	-	High	High	High
Fraction of pathways associated with survival	0.14	0.52	0.42				

Supplementary Table S4: List of additional cancer data sets for machine learning-based prediction of cancer samples.

GEO_ID	Cancer	Type of tumour	Number of samples	Number of tumour samples used in analysis	Number of control samples used in analysis	Platform	Normalization
GSE103512	Breast, Colorectal, Prostate, And Non-Small Cell Lung Cancer	Solid Tumor	280	242	38	GPL13158[HT_HG-U133_Plus_PM] Affymetrix HT HG-U133+ PM Array Plate	Quantile
GSE112790	Hepatocellular Carcinoma	Solid Tumor	198	183	15	GPL570 [HG-U133_Plus_2] Affymetrix Human Genome U133 Plus 2.0 Array	Quantile
GSE32665	Lung adenocarcinoma	Solid Tumor	170	85	85	GPL6102Illumina human-6 v2.0 expression beadchip	Quantile
GSE33479	Lung squamous carcinogenesis	Solid Tumor	122	14	27	GPL6480 Agilent-014850 Whole Human Genome Microarray 4x44K G4112F (Probe Name version)	Natural log of (Cy5/Cy3)
GSE84984	Colorectal Cancer	Solid Tumor	15	9	6	GPL17586 [HTA-2_0] Affymetrix Human Transcriptome Array 2.0 [transcript (gene) version]	RMA
GSE103236	Gastric Cancer	Solid Tumor	19	9	9	GPL4133Agilent-014850 Whole Human Genome Microarray 4x44K G4112F (Feature Number version)	Lowess

Supplemental Table S5: Viral integration in TCGA samples. Results are derived from published data.

	Tang2013 [a]		**Cao2016 [b]**		**Kazemina2015 [c] ****	
	N (%)	P-value	N (%)	P-value	N (%)	P-value
Samples analysed in current manuscript	687	3.00E-04	687	1.00E-03	N.A.	4.10E-13
Overlap with published study	425 (61.9%)		533 (77.6%)		N.A.	
SLC samples	120 (28.2%)		200 (37.5%)		305	
CA samples	305 (71.8%)		333 (62.5%)		1175	
Viral integration in SLC	9 (7.5%)		60 (30%)		57 (18.7%)	
Viral integration in CA	2 (0.66 %)		58 (17.4 %)		66 (5.6%)	
					** Sample-level data are not available. Number and proportion of viral integration in SLC and CA samples are calculated from summary data provided in the publication (Table 1 of [c]).	

[a] Tang KW, Alaei-Mahabadi B, Samuelsson T, Lindh M, Larsson E. The landscape of viral expression and host gene fusion and adaptation in human cancer. Nature Communications. 2013;4:1–9.

[b] Cao S, Wendl MC, Wyczalkowski MA, Wylie K, Ye K, Jayasinghe R, et al. Divergent viral presentation among human tumors and adjacent normal tissues. Scientific Reports. 2016;6 June:1–12.

[c] Kazemian M, Ren M, Lin J-X, Liao W, Spolski R, Leonard WJ. Possible Human Papillomavirus 38 Contamination of Endometrial Cancer RNA Sequencing Samples in The Cancer Genome Atlas Database. Journal of Virology. 2015;89:8967–73.

Additional text : Functional classification of the pathways

The selected 66 pathways are divided into categories based on their functional relevance. The categories include catabolism, immune system, infection, cancer, signal transduction, ribosome biogenesis and carbohydrate metabolism. Many of these pathways are related to immune response to infection, such as, clot formation, proinflammatory effects, antiviral effects, chemotactic effects and T cell stimulation, degranulation, cytokine gene transcription and generation of eicosanoids, phagocytosis, and migration of leukocytes to the site of injury, and are consistently up-regulated in both SS and SLC group.

Catabolism

Two catabolic pathways namely, Lysosome and Phagosome, are observed to be mostly up-regulated in SS and SLC (Fig. 2, Additional File 4: Table S1). Upon network analysis, it is revealed that lysosome pathway has a very high value for betweenness centrality (680.2) (Additional File 5: Table S2), thus being essential to the structure of the network. Likewise, Phagosome, another catabolic pathway linked to lysosome, is uniformly up regulated in SS and SLC groups (Additional File 2: Figure S2).

Muscle wasting is one of the most common phenomena in both SS and cancer. Lysosome mediated protein degradation has been noted on a substantial scale in such cases. Further, transcriptome based meta-analysis conducted by Ma et al., reported up-regulation of lysosome pathway in sepsis while increased biogenesis of lysosomes has been observed in cancer cells. In this study, we observe consistent up-regulation of catabolic pathways associated with lysosome and phagosome in SS and SLC, suggesting high catabolic rate in both the groups. Besides, lysosome is now considered a hub of metabolic signalling given its key role in maintaining cellular homeostasis. It also appears as a central node in our network with high betweenness centrality.

Immune system

Both cancer and septic shock are associated with dysregulation in immune function. It is observed that immune system pathways associated with clot formation (Platelet activation), proinflammatory effects, antiviral effects, chemotactic effects and T cell stimulation (Toll-like receptor signalling pathway), degranulation, cytokine gene transcription and generation of eicosanoids (Fc epsilon RI signalling pathway), phagocytosis (Fc gamma R-mediated phagocytosis), and migration of leukocytes to the site of injury (Leukocyte transendothelial migration) are uniformly up regulated in both SS and SLC groups (Additional File 2: Figure S2).

Infection

Infection is a common theme in both septic shock (which originates as sepsis) and many cancers (known to be induced by microbial infection). Many infection-associated pathways, such as, Bacterial invasion of epithelial cells, Vibrio cholerae infection, Epithelial cell signalling in Helicobacter pylori infection, Salmonella infection, Pertussis, Legionellosis, Tuberculosis, Chagas disease (American trypanosomiasis), Amoebiasis, Hepatitis C and Hepatitis B are significantly up regulated in SS and SLC group (Additional File 2: Figure S2).

Cancer pathways

Many cancer-associated pathways, such as Transcriptional misregulation in cancer, Proteoglycans in cancer, Central carbon metabolism in cancer, Choline metabolism in cancer, Chemical carcinogenesis, Renal cell carcinoma, Pancreatic cancer, Glioma, Prostate cancer, Melanoma, Bladder cancer, Acute myeloid leukemia, Non-small cell lung cancer are up regulated in SS and SLC group (Additional File 2: Figure S2).

Signal transduction

Signal transduction pathways involved in cell proliferation, differentiation, adhesion, migration, survival, cell cycle progression, anti-apoptosis (MAPK, ErbB, Rap1, VEGF, JAK-STAT and PI3k-Akt signalling pathways) and cell cycle regulation, apoptosis, autophagy, oxidative stress response, DNA repair, immune regulation, muscle atrophy, growth arrest, leukocyte recruitment and activation, synthesis of inflammatory mediators, remodelling of extracellular matrix (HIF1, AMPK, FoxO and TNF signalling pathways) are uniformly up-regulated in SS group, and in most of the SLC group (Additional File 2: Figure S2).

Endocrine system

Five pathways associated with endocrine system viz., Insulin signalling, GnRH signalling, Progesterone-mediated oocyte maturation, Prolactin signalling pathway and Ovarian steroidogenesis are up-regulated in all SS groups as well as in SLC group (Additional File 2: Figure S2).

Carbohydrate metabolism

Carbohydrate metabolism pathways including Galactose metabolism, Glycolysis/Gluconeogenesis, and Pentose phosphate pathway are up-regulated in SS group and most of the SLC group cancers. In our study, Galactose metabolism pathway is up-regulated in SLC and SS groups. Glycolysis/Gluconeogenesis (a source of energy and metabolite precursors of other pathways) plays a central role in cell as reflected by highest betweenness centrality parameter value i.e. 1599.06 (Additional File 5: Table S2). Pentose phosphate pathway, which generates precursors for synthesis of purine, pyrimidine and histidine, is up-regulated across the SS group along with the LIHC, CHOL, ESCA and STAD of SLC group.

Gene–level heatmap for 66 pathways

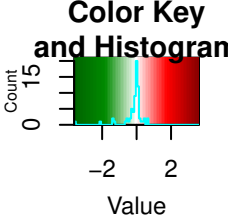

Chemical carcinogenesis
hsa05204

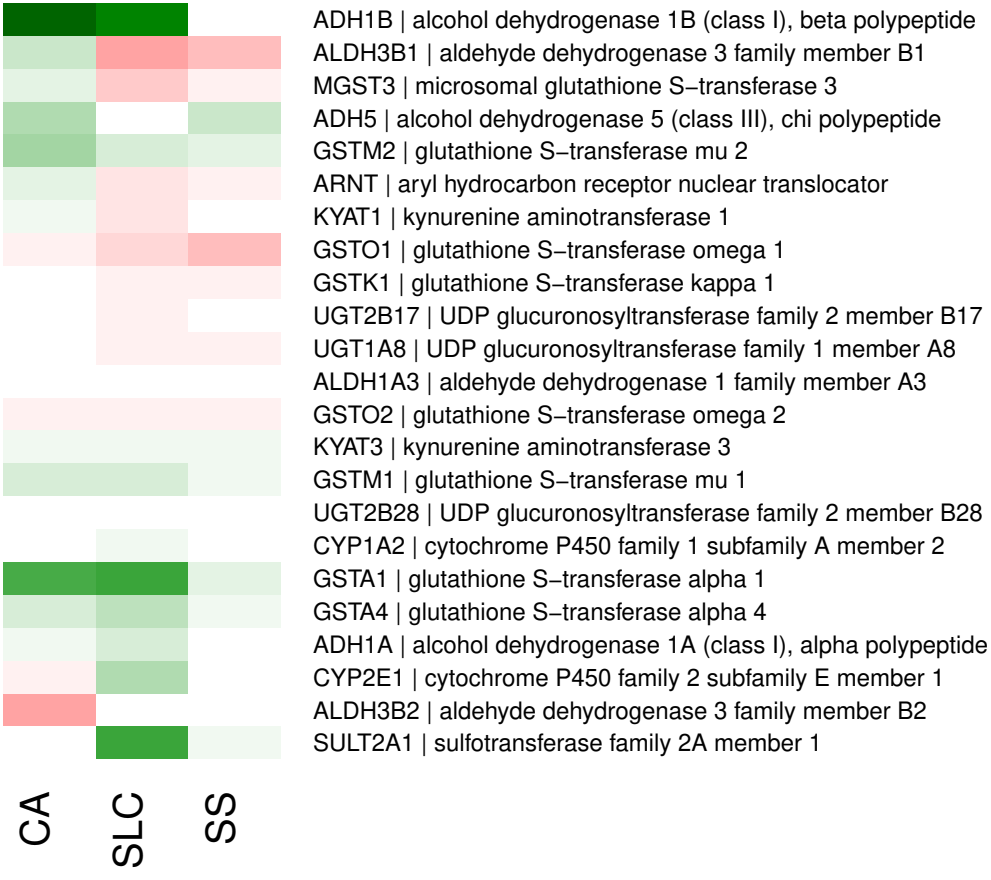

Cancer

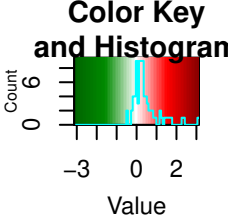

Bladder cancer
hsa05219

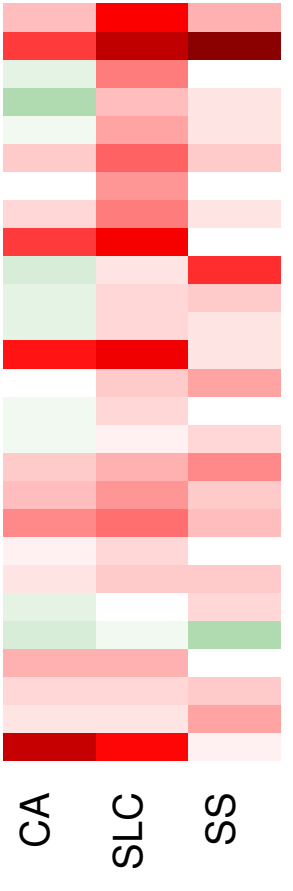

TYMP | thymidine phosphorylase
MMP9 | matrix metallopeptidase 9
MMP2 | matrix metallopeptidase 2
MAPK3 | mitogen−activated protein kinase 3
RB1 | RB transcriptional corepressor 1
VEGFA | vascular endothelial growth factor A
DAPK3 | death associated protein kinase 3
NRAS | NRAS proto−oncogene, GTPase
CDKN2A | cyclin dependent kinase inhibitor 2A
THBS1 | thrombospondin 1
EGFR | epidermal growth factor receptor
ARAF | A−Raf proto−oncogene, serine/threonine kinase
E2F1 | E2F transcription factor 1
MAPK1 | mitogen−activated protein kinase 1
FGFR3 | fibroblast growth factor receptor 3
DAPK2 | death associated protein kinase 2
MDM2 | MDM2 proto−oncogene
E2F2 | E2F transcription factor 2
E2F3 | E2F transcription factor 3
MAP2K1 | mitogen−activated protein kinase kinase 1
MAP2K2 | mitogen−activated protein kinase kinase 2
EGF | epidermal growth factor
RPS6KA5 | ribosomal protein S6 kinase A5
ERBB2 | erb−b2 receptor tyrosine kinase 2
KRAS | KRAS proto−oncogene, GTPase
BRAF | B−Raf proto−oncogene, serine/threonine kinase
MMP1 | matrix metallopeptidase 1

Cancer

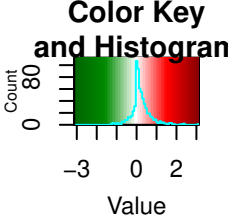

Pathways in cancer
hsa05200

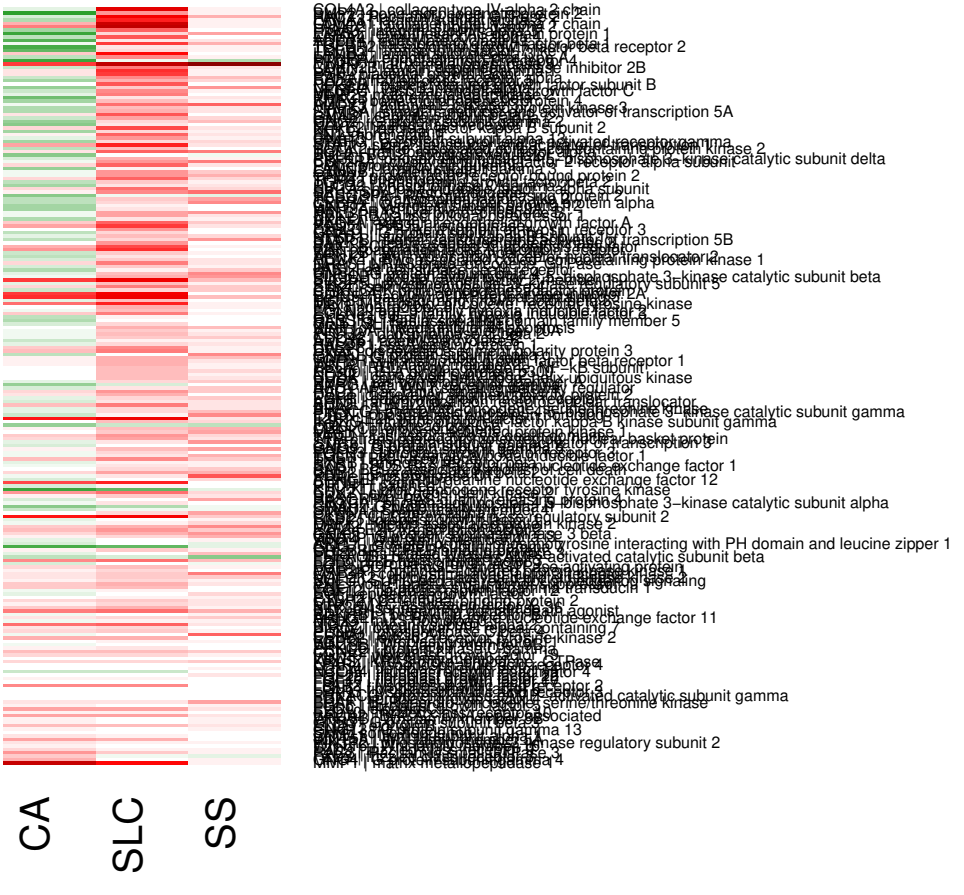

Cancer

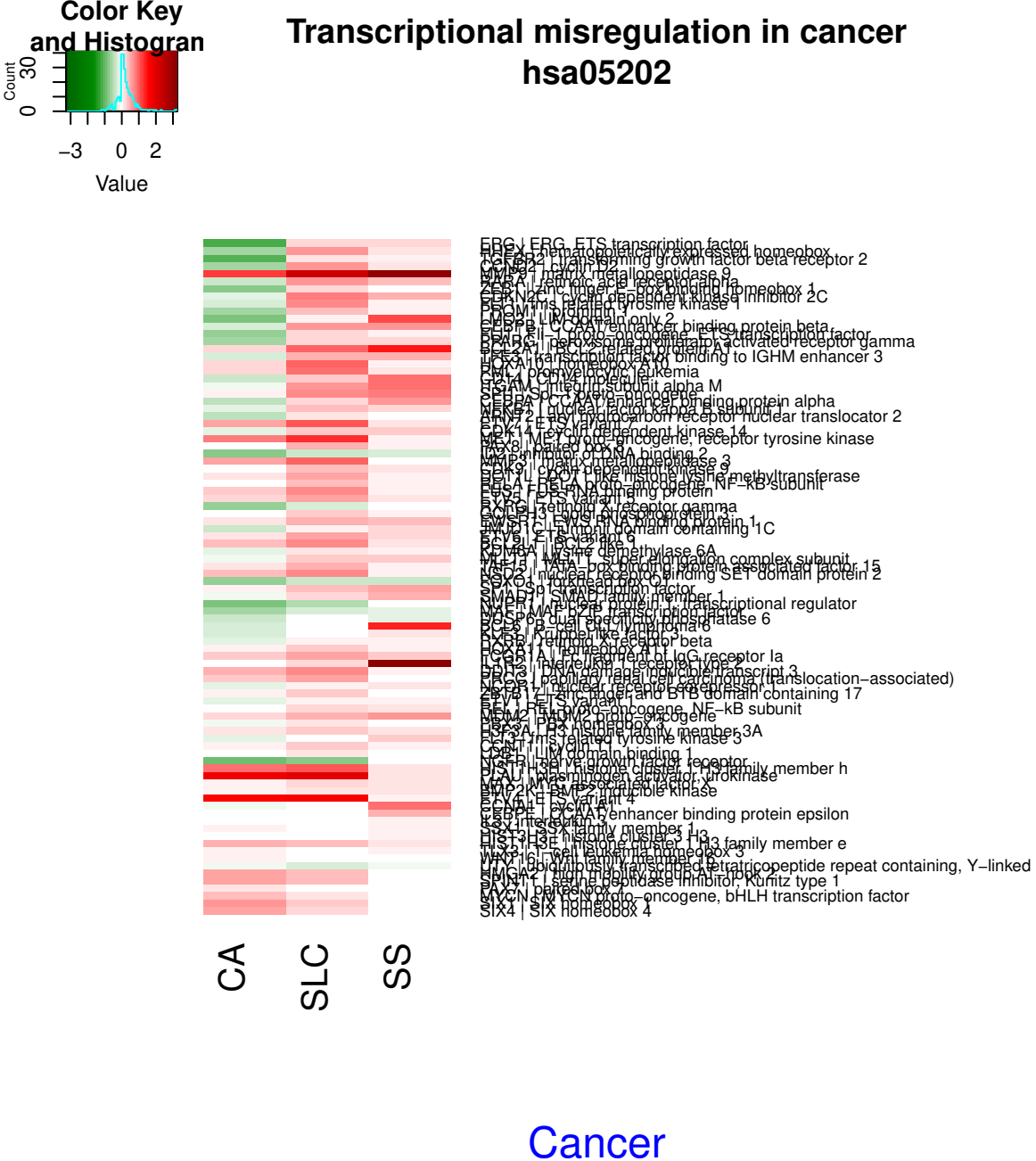
Color Key and Histogram
Count
30
0
−3
0
2
Value
Transcriptional misregulation in cancer
hsa05202
ERG | ERG, ETS transcription factor
HOXA9 | homeobox A9
CCNA2 | cyclin A2
MMP9 | matrix metallopeptidase 9
RARA | retinoic acid receptor alpha
ZEB1 | zinc finger E−box binding homeobox 1
CDKN2C | cyclin dependent kinase inhibitor 2C
PDGFRB | platelet derived growth factor receptor beta
FOS | FOS, AP−1 transcription factor
CEBPB | CCAAT/enhancer binding protein beta
PPARG | peroxisome proliferator activated receptor gamma
IGH@ | immunoglobulin heavy locus
HOXA10 | homeobox A10
RUNX1 | runx1 runt−related transcription factor 1
CDKN1A | cyclin dependent kinase inhibitor 1A
ITGAM | integrin subunit alpha M
CEBPA | CCAAT/enhancer binding protein alpha
NFKB2 | nuclear factor kappa B subunit 2
ARNT2 | aryl hydrocarbon receptor nuclear translocator 2
CDK14 | cyclin dependent kinase 14
MEF2B | MEF2, myocyte enhancer factor 2B
HOXB13 | homeobox B13
PAX8 | paired box 8
MMP2 | matrix metallopeptidase 2
MMP3 | matrix metallopeptidase 3
EZH2 | enhancer of zeste homolog 2
DOT1L | DOT1 like histone lysine methyltransferase
RELA | RELA, proto−oncogene, NF−kB subunit
EWSR1 | EWS RNA binding protein 1
FUS | FUS, RNA binding protein
CCNA1 | cyclin A1
ETV6 | ETS variant 6
KDM6A | lysine demethylase 6A
TAF15 | TATA box binding protein associated factor 15
NSD2 | nuclear receptor binding SET domain protein 2
SOX9 | SOX9, transcription factor
SMAD4 | SMAD family member 4
NUP214 | nucleoporin 214
MAFB | MAF bZIP transcriptional regulator
DUSP6 | dual specificity phosphatase 6
BCL6 | B−cell CLL/lymphoma 6
KLF4 | Kruppel−like factor 4
RXRB | retinoid X receptor beta
FOXA1 | forkhead box A1
FCGR1A | Fc fragment of IgG, receptor Ia
IL3RA | interleukin 3 receptor, alpha
PPARG | peroxisome proliferator activated receptor gamma
PRCC | papillary renal cell carcinoma (translocation−associated)
NCOA4 | nuclear receptor coactivator 4
ZBTB17 | zinc finger and BTB domain containing 17
ETV1 | ETS variant 1
MDM2 | MDM2 proto−oncogene
HOXA3 | homeobox A3
PDGFRA | platelet derived growth factor receptor alpha
CCND1 | cyclin D1
CBL | Cbl proto−oncogene, E3 ubiquitin protein ligase
NTRK3 | neurotrophic tyrosine kinase, receptor, type 3
PLAU | plasminogen activator, urokinase
MAPK14 | mitogen activated protein kinase 14
MMP2 | matrix metallopeptidase 2
ETV4 | ETS variant 4
CCNE1 | cyclin E1
CEBPE | CCAAT/enhancer binding protein epsilon
CSF1 | colony stimulating factor 1
HIST1H3A | histone cluster 1 H3 family member a
HIST1H3E | histone cluster 1 H3 family member e
MLL3 | myeloid/lymphoid or mixed lineage leukemia 3
MYH11 | myosin heavy chain 11
UTX | ubiquitously transcribed tetratricopeptide repeat containing, Y−linked
SMARCA4 | SWI/SNF related, matrix associated, actin dependent regulator of chromatin, subfamily a, member 4
SPINK1 | serine peptidase inhibitor, Kunitz type 1
PAX6 | paired box 6
MYCN | MYCN proto−oncogene, bHLH transcription factor
SIX1 | SIX homeobox 1
SIX4 | SIX homeobox 4
CA
SLC
SS
Cancer

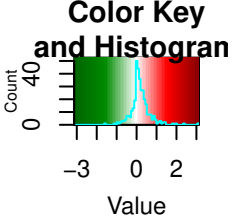

Proteoglycans in cancer
hsa05205

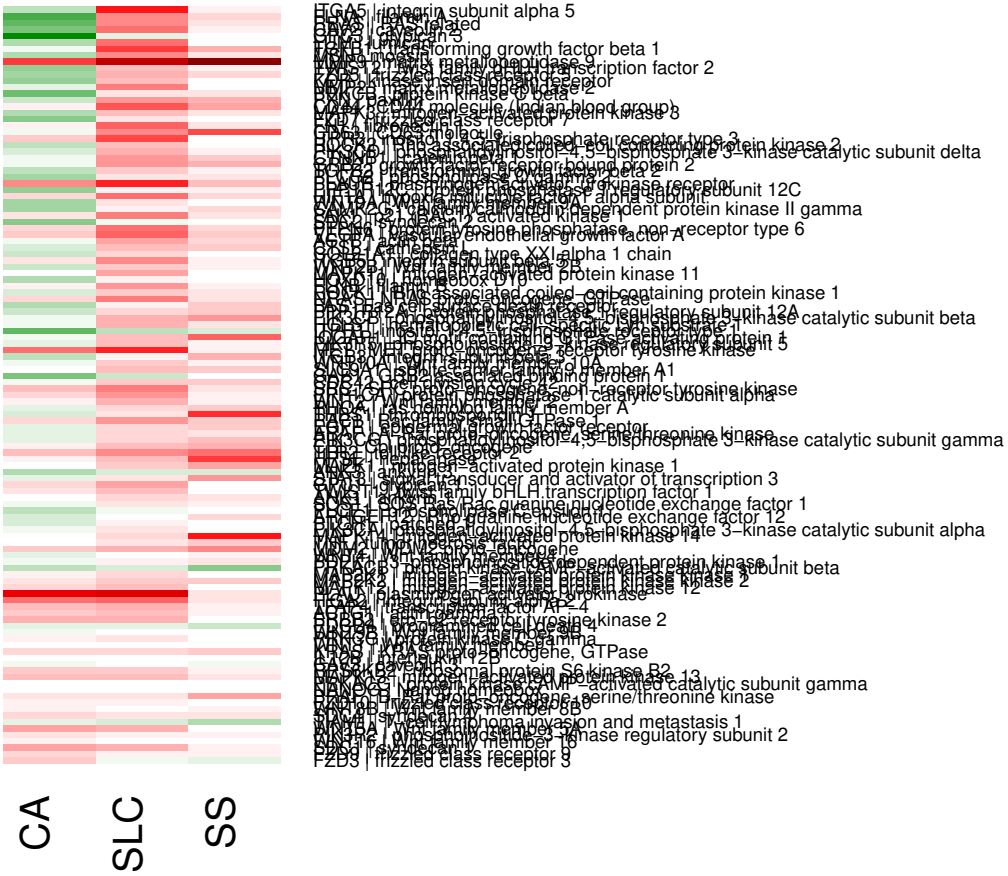

Cancer

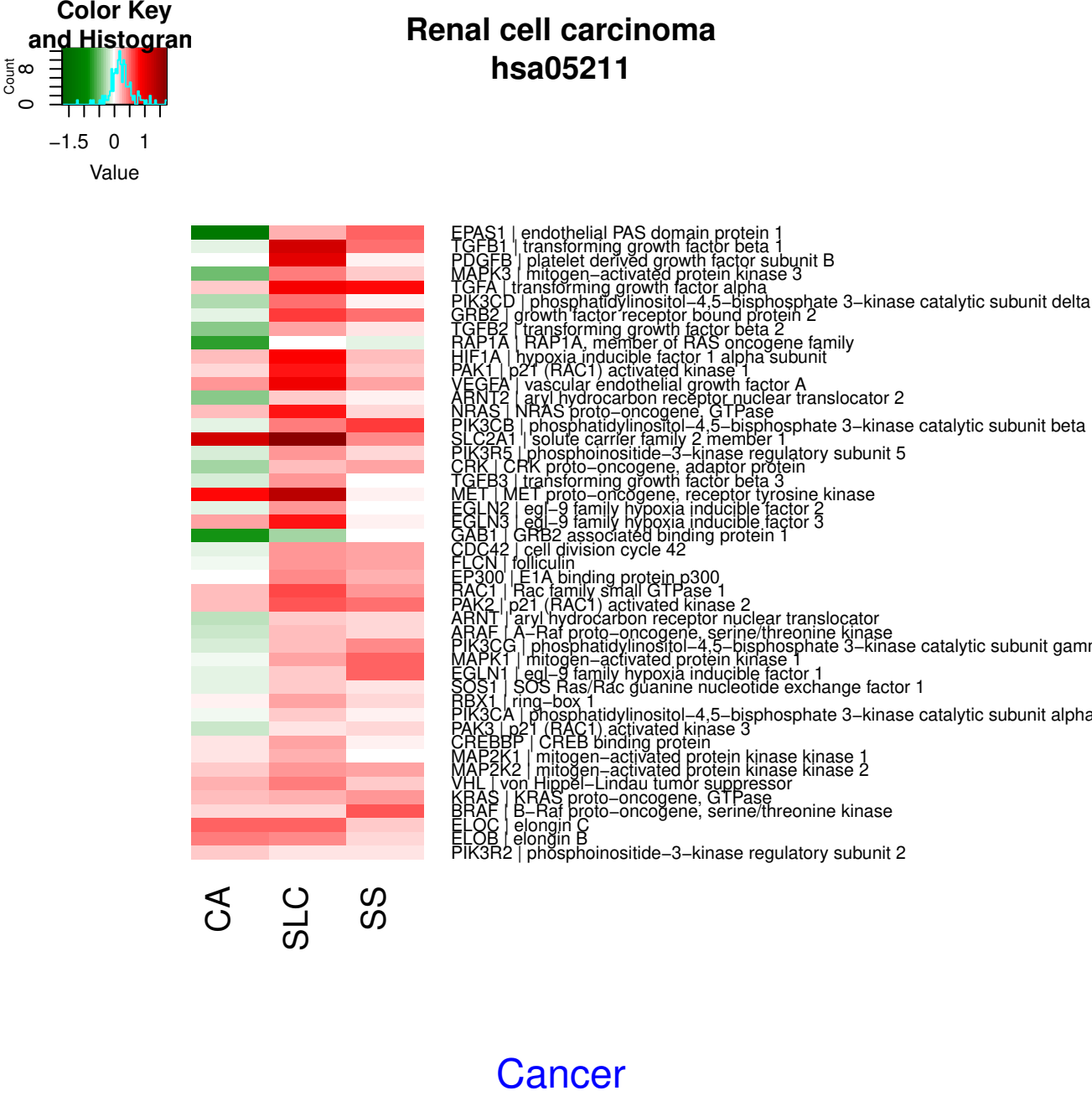
Color Key
and Histogram
Count
0
8
−1.5
0
1
Value
Renal cell carcinoma
hsa05211
EPAS1 | endothelial PAS domain protein 1
TGFB1 | transforming growth factor beta 1
PDGFB | platelet derived growth factor subunit B
MAPK3 | mitogen−activated protein kinase 3
TGFA | transforming growth factor alpha
PIK3CD | phosphatidylinositol−4,5−bisphosphate 3−kinase catalytic subunit delta
GRB2 | growth factor receptor bound protein 2
TGFB2 | transforming growth factor beta 2
RAP1A | RAP1A, member of RAS oncogene family
HIF1A | hypoxia inducible factor 1 alpha subunit
PAK1 | p21 (RAC1) activated kinase 1
VEGFA | vascular endothelial growth factor A
ARNT2 | aryl hydrocarbon receptor nuclear translocator 2
NRAS | NRAS proto−oncogene, GTPase
PIK3CB | phosphatidylinositol−4,5−bisphosphate 3−kinase catalytic subunit beta
SLC2A1 | solute carrier family 2 member 1
PIK3R5 | phosphoinositide−3−kinase regulatory subunit 5
CRK | CRK proto−oncogene, adaptor protein
TGFB3 | transforming growth factor beta 3
MET | MET proto−oncogene, receptor tyrosine kinase
EGLN2 | egl−9 family hypoxia inducible factor 2
EGLN3 | egl−9 family hypoxia inducible factor 3
GAB1 | GRB2 associated binding protein 1
CDC42 | cell division cycle 42
FLCN | folliculin
EP300 | E1A binding protein p300
RAC1 | Rac family small GTPase 1
PAK2 | p21 (RAC1) activated kinase 2
ARNT | aryl hydrocarbon receptor nuclear translocator
ARAF | A−Raf proto−oncogene, serine/threonine kinase
PIK3CG | phosphatidylinositol−4,5−bisphosphate 3−kinase catalytic subunit gamm
MAPK1 | mitogen−activated protein kinase 1
EGLN1 | egl−9 family hypoxia inducible factor 1
SOS1 | SOS Ras/Rac guanine nucleotide exchange factor 1
RBX1 | ring−box 1
PIK3CA | phosphatidylinositol−4,5−bisphosphate 3−kinase catalytic subunit alpha
PAK3 | p21 (RAC1) activated kinase 3
CREBBP | CREB binding protein
MAP2K1 | mitogen−activated protein kinase kinase 1
MAP2K2 | mitogen−activated protein kinase kinase 2
VHL | von Hippel−Lindau tumor suppressor
KRAS | KRAS proto−oncogene, GTPase
BRAF | B−Raf proto−oncogene, serine/threonine kinase
ELOC | elongin C
ELOB | elongin B
PIK3R2 | phosphoinositide−3−kinase regulatory subunit 2
CA
SLC
SS
Cancer

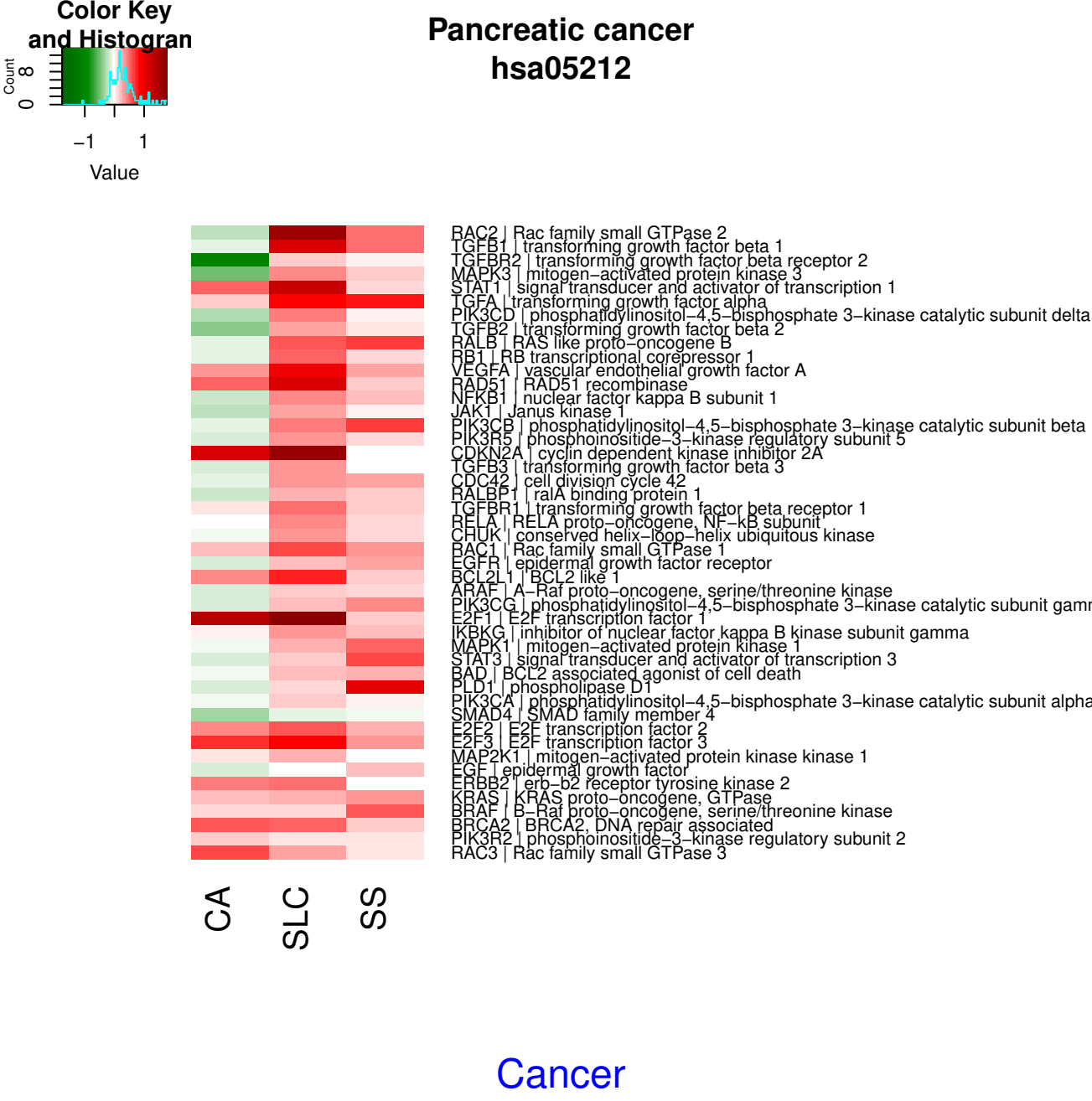
Color Key
and Histogram
Count
0
8
−1
1
Value
Pancreatic cancer
hsa05212
RAC2 | Rac family small GTPase 2
TGFB1 | transforming growth factor beta 1
TGFBR2 | transforming growth factor beta receptor 2
MAPK3 | mitogen−activated protein kinase 3
STAT1 | signal transducer and activator of transcription 1
TGFA | transforming growth factor alpha
PIK3CD | phosphatidylinositol−4,5−bisphosphate 3−kinase catalytic subunit delta
TGFB2 | transforming growth factor beta 2
RALB | RAS like proto−oncogene B
RB1 | RB transcriptional corepressor 1
VEGFA | vascular endothelial growth factor A
RAD51 | RAD51 recombinase
NFKB1 | nuclear factor kappa B subunit 1
JAK1 | Janus kinase 1
PIK3CB | phosphatidylinositol−4,5−bisphosphate 3−kinase catalytic subunit beta
PIK3R5 | phosphoinositide−3−kinase regulatory subunit 5
CDKN2A | cyclin dependent kinase inhibitor 2A
TGFB3 | transforming growth factor beta 3
CDC42 | cell division cycle 42
RALBP1 | ralA binding protein 1
TGFBR1 | transforming growth factor beta receptor 1
RELA | RELA proto−oncogene, NF−kB subunit
CHUK | conserved helix−loop−helix ubiquitous kinase
RAC1 | Rac family small GTPase 1
EGFR | epidermal growth factor receptor
BCL2L1 | BCL2 like 1
ARAF | A−Raf proto−oncogene, serine/threonine kinase
PIK3CG | phosphatidylinositol−4,5−bisphosphate 3−kinase catalytic subunit gamm
E2F1 | E2F transcription factor 1
IKBKG | inhibitor of nuclear factor kappa B kinase subunit gamma
MAPK1 | mitogen−activated protein kinase 1
STAT3 | signal transducer and activator of transcription 3
BAD | BCL2 associated agonist of cell death
PLD1 | phospholipase D1
PIK3CA | phosphatidylinositol−4,5−bisphosphate 3−kinase catalytic subunit alpha
SMAD4 | SMAD family member 4
E2F2 | E2F transcription factor 2
E2F3 | E2F transcription factor 3
MAP2K1 | mitogen−activated protein kinase kinase 1
EGF | epidermal growth factor
ERBB2 | erb−b2 receptor tyrosine kinase 2
KRAS | KRAS proto−oncogene, GTPase
BRAF | B−Raf proto−oncogene, serine/threonine kinase
BRCA2 | BRCA2, DNA repair associated
PIK3R2 | phosphoinositide−3−kinase regulatory subunit 2
RAC3 | Rac family small GTPase 3
CA
SLC
SS
Cancer

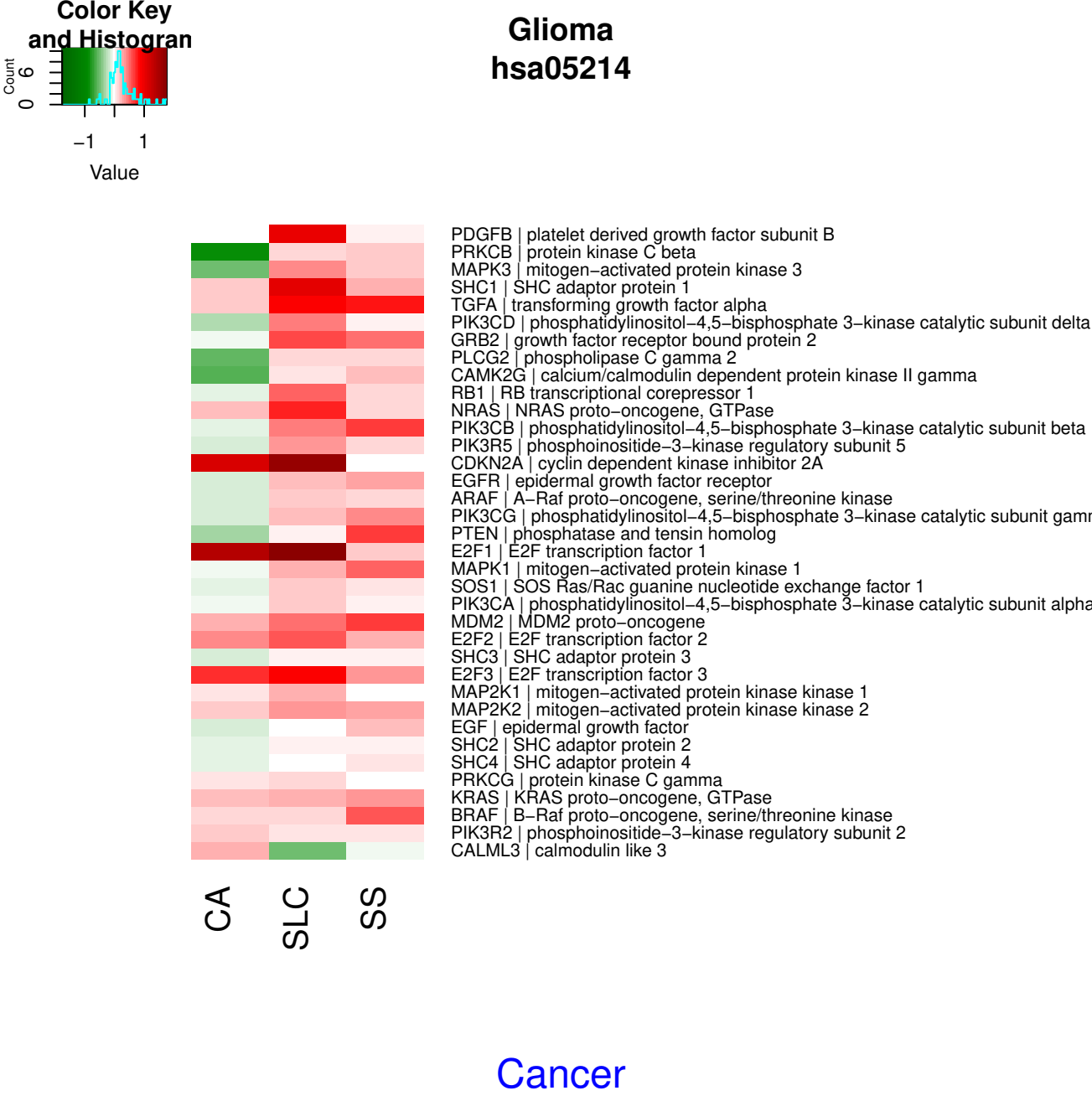
Color Key
and Histogram
Count
0
6
−1
1
Value
Glioma
hsa05214
PDGFB | platelet derived growth factor subunit B
PRKCB | protein kinase C beta
MAPK3 | mitogen−activated protein kinase 3
SHC1 | SHC adaptor protein 1
TGFA | transforming growth factor alpha
PIK3CD | phosphatidylinositol−4,5−bisphosphate 3−kinase catalytic subunit delta
GRB2 | growth factor receptor bound protein 2
PLCG2 | phospholipase C gamma 2
CAMK2G | calcium/calmodulin dependent protein kinase II gamma
RB1 | RB transcriptional corepressor 1
NRAS | NRAS proto−oncogene, GTPase
PIK3CB | phosphatidylinositol−4,5−bisphosphate 3−kinase catalytic subunit beta
PIK3R5 | phosphoinositide−3−kinase regulatory subunit 5
CDKN2A | cyclin dependent kinase inhibitor 2A
EGFR | epidermal growth factor receptor
ARAF | A−Raf proto−oncogene, serine/threonine kinase
PIK3CG | phosphatidylinositol−4,5−bisphosphate 3−kinase catalytic subunit gamm
PTEN | phosphatase and tensin homolog
E2F1 | E2F transcription factor 1
MAPK1 | mitogen−activated protein kinase 1
SOS1 | SOS Ras/Rac guanine nucleotide exchange factor 1
PIK3CA | phosphatidylinositol−4,5−bisphosphate 3−kinase catalytic subunit alpha
MDM2 | MDM2 proto−oncogene
E2F2 | E2F transcription factor 2
SHC3 | SHC adaptor protein 3
E2F3 | E2F transcription factor 3
MAP2K1 | mitogen−activated protein kinase kinase 1
MAP2K2 | mitogen−activated protein kinase kinase 2
EGF | epidermal growth factor
SHC2 | SHC adaptor protein 2
SHC4 | SHC adaptor protein 4
PRKCG | protein kinase C gamma
KRAS | KRAS proto−oncogene, GTPase
BRAF | B−Raf proto−oncogene, serine/threonine kinase
PIK3R2 | phosphoinositide−3−kinase regulatory subunit 2
CALML3 | calmodulin like 3
CA
SLC
SS
Cancer

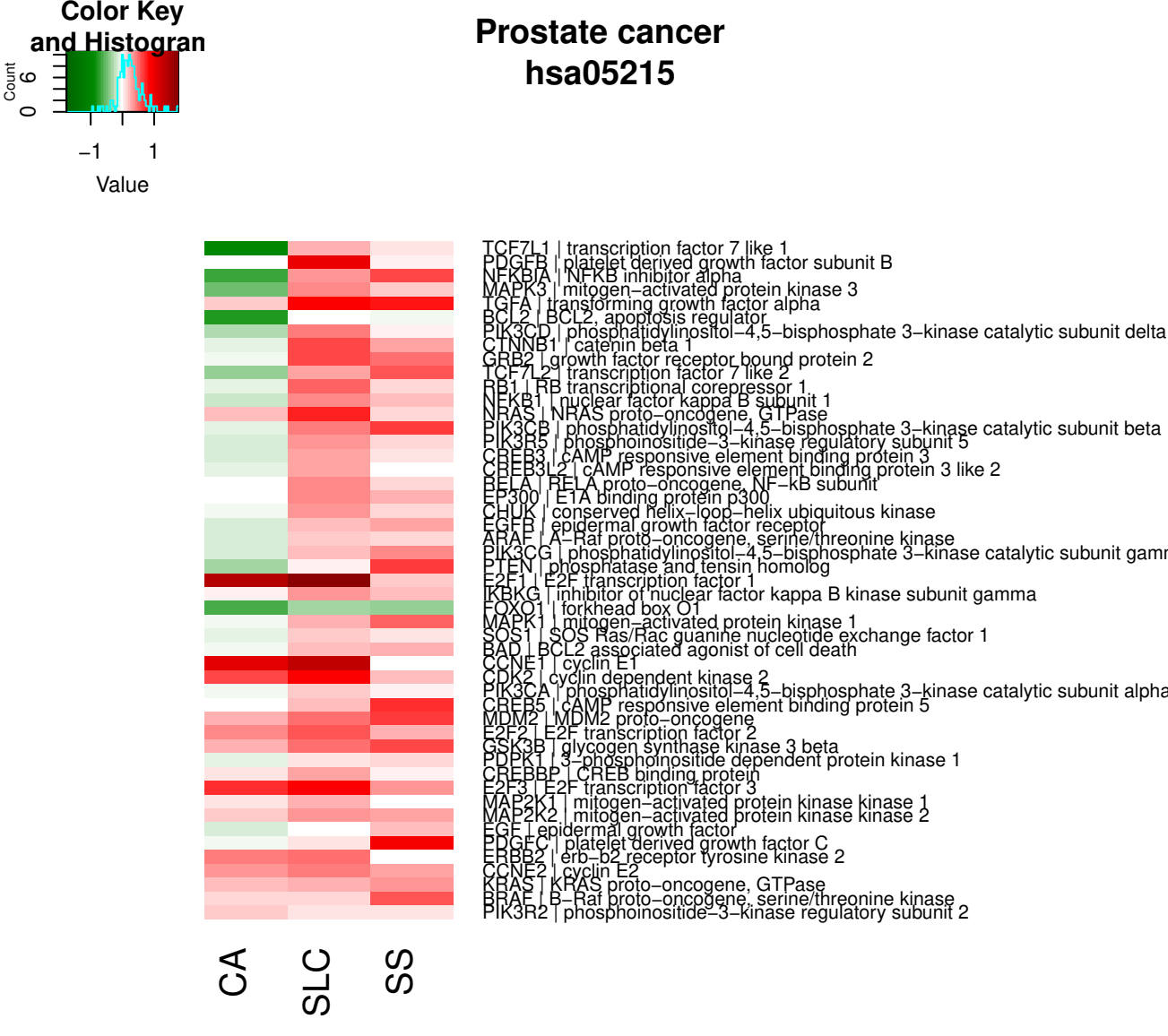
Color Key
and Histogram
Count
0
6
−1
1
Value
Prostate cancer
hsa05215
TCF7L1 | transcription factor 7 like 1
PDGFB | platelet derived growth factor subunit B
NFKBIA | NFKB inhibitor alpha
MAPK3 | mitogen−activated protein kinase 3
TGFA | transforming growth factor alpha
BCL2 | BCL2, apoptosis regulator
PIK3CD | phosphatidylinositol−4,5−bisphosphate 3−kinase catalytic subunit delta
CTNNB1 | catenin beta 1
GRB2 | growth factor receptor bound protein 2
TCF7L2 | transcription factor 7 like 2
RB1 | RB transcriptional corepressor 1
NFKB1 | nuclear factor kappa B subunit 1
NRAS | NRAS proto−oncogene, GTPase
PIK3CB | phosphatidylinositol−4,5−bisphosphate 3−kinase catalytic subunit beta
PIK3R5 | phosphoinositide−3−kinase regulatory subunit 5
CREB3 | cAMP responsive element binding protein 3
CREB3L2 | cAMP responsive element binding protein 3 like 2
RELA | RELA proto−oncogene, NF−kB subunit
EP300 | E1A binding protein p300
CHUK | conserved helix−loop−helix ubiquitous kinase
EGFR | epidermal growth factor receptor
ARAF | A−Raf proto−oncogene, serine/threonine kinase
PIK3CG | phosphatidylinositol−4,5−bisphosphate 3−kinase catalytic subunit gamm
PTEN | phosphatase and tensin homolog
E2F1 | E2F transcription factor 1
IKBKG | inhibitor of nuclear factor kappa B kinase subunit gamma
FOXO1 | forkhead box O1
MAPK1 | mitogen−activated protein kinase 1
SOS1 | SOS Ras/Rac guanine nucleotide exchange factor 1
BAD | BCL2 associated agonist of cell death
CCNE1 | cyclin E1
CDK2 | cyclin dependent kinase 2
PIK3CA | phosphatidylinositol−4,5−bisphosphate 3−kinase catalytic subunit alpha
CREB5 | cAMP responsive element binding protein 5
MDM2 | MDM2 proto−oncogene
E2F2 | E2F transcription factor 2
GSK3B | glycogen synthase kinase 3 beta
PDPK1 | 3−phosphoinositide dependent protein kinase 1
CREBBP | CREB binding protein
E2F3 | E2F transcription factor 3
MAP2K1 | mitogen−activated protein kinase kinase 1
MAP2K2 | mitogen−activated protein kinase kinase 2
EGF | epidermal growth factor
PDGFC | platelet derived growth factor C
ERBB2 | erb−b2 receptor tyrosine kinase 2
CCNE2 | cyclin E2
KRAS | KRAS proto−oncogene, GTPase
BRAF | B−Raf proto−oncogene, serine/threonine kinase
PIK3R2 | phosphoinositide−3−kinase regulatory subunit 2
CA
SLC
SS
Cancer

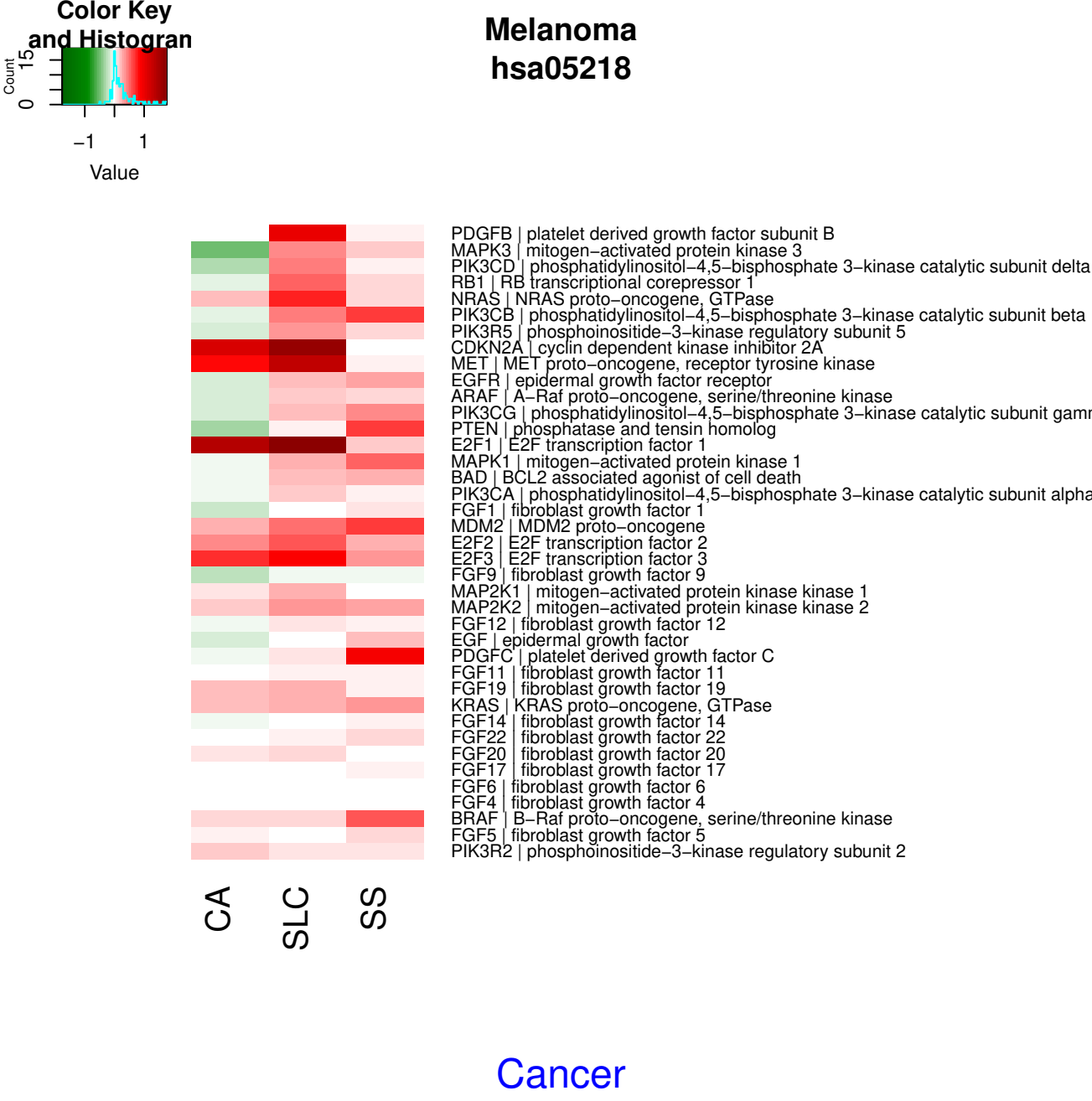
Color Key
and Histogram
Count
15
0
−1
1
Value
Melanoma
hsa05218
PDGFB | platelet derived growth factor subunit B
MAPK3 | mitogen−activated protein kinase 3
PIK3CD | phosphatidylinositol−4,5−bisphosphate 3−kinase catalytic subunit delta
RB1 | RB transcriptional corepressor 1
NRAS | NRAS proto−oncogene, GTPase
PIK3CB | phosphatidylinositol−4,5−bisphosphate 3−kinase catalytic subunit beta
PIK3R5 | phosphoinositide−3−kinase regulatory subunit 5
CDKN2A | cyclin dependent kinase inhibitor 2A
MET | MET proto−oncogene, receptor tyrosine kinase
EGFR | epidermal growth factor receptor
ARAF | A−Raf proto−oncogene, serine/threonine kinase
PIK3CG | phosphatidylinositol−4,5−bisphosphate 3−kinase catalytic subunit gamm
PTEN | phosphatase and tensin homolog
E2F1 | E2F transcription factor 1
MAPK1 | mitogen−activated protein kinase 1
BAD | BCL2 associated agonist of cell death
PIK3CA | phosphatidylinositol−4,5−bisphosphate 3−kinase catalytic subunit alpha
FGF1 | fibroblast growth factor 1
MDM2 | MDM2 proto−oncogene
E2F2 | E2F transcription factor 2
E2F3 | E2F transcription factor 3
FGF9 | fibroblast growth factor 9
MAP2K1 | mitogen−activated protein kinase kinase 1
MAP2K2 | mitogen−activated protein kinase kinase 2
FGF12 | fibroblast growth factor 12
EGF | epidermal growth factor
PDGFC | platelet derived growth factor C
FGF11 | fibroblast growth factor 11
FGF19 | fibroblast growth factor 19
KRAS | KRAS proto−oncogene, GTPase
FGF14 | fibroblast growth factor 14
FGF22 | fibroblast growth factor 22
FGF20 | fibroblast growth factor 20
FGF17 | fibroblast growth factor 17
FGF6 | fibroblast growth factor 6
FGF4 | fibroblast growth factor 4
BRAF | B−Raf proto−oncogene, serine/threonine kinase
FGF5 | fibroblast growth factor 5
PIK3R2 | phosphoinositide−3−kinase regulatory subunit 2
CA
SLC
SS
Cancer

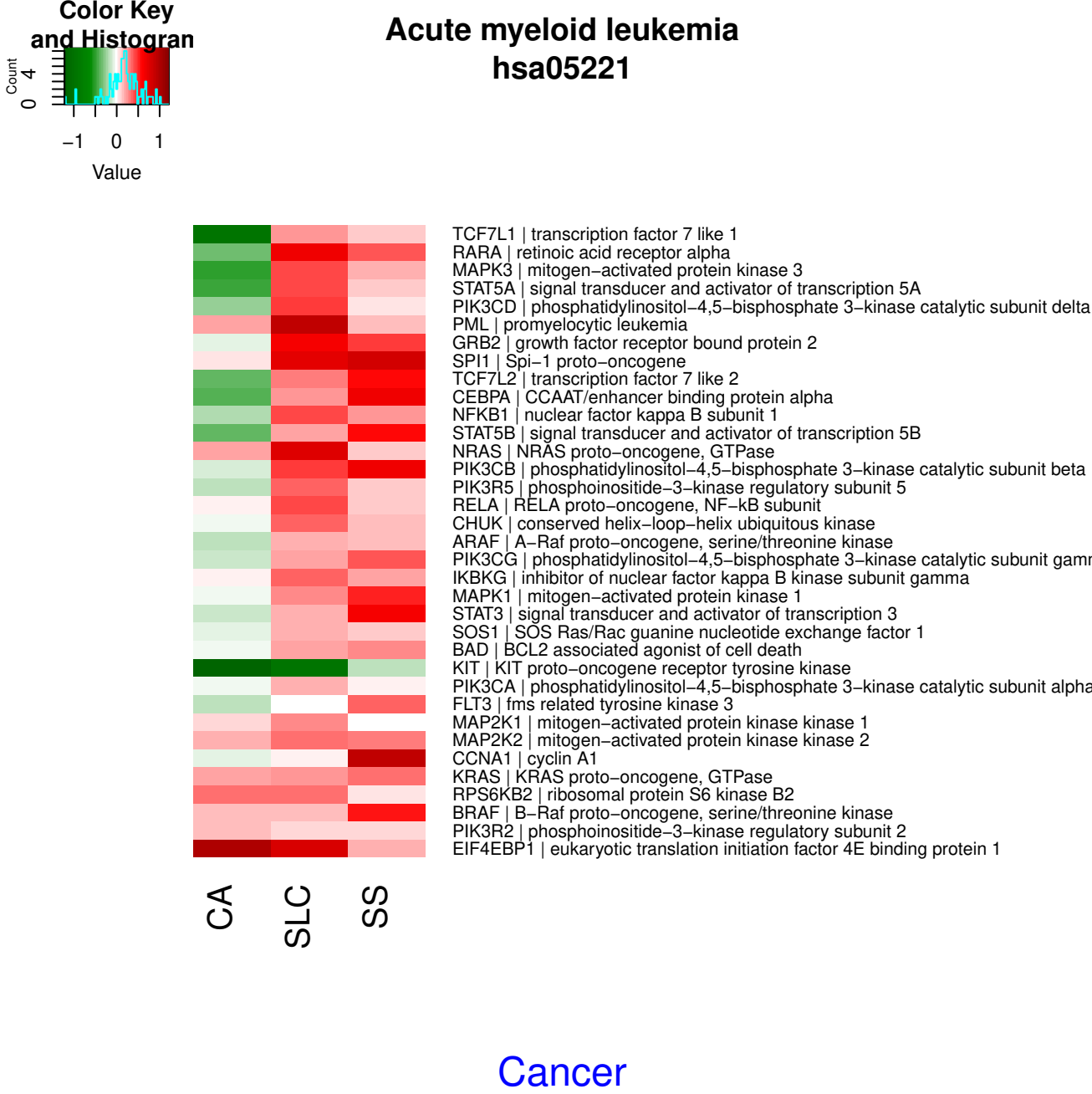
Color Key
and Histogram
Count
0
4
−1
0
1
Value
Acute myeloid leukemia
hsa05221
TCF7L1 | transcription factor 7 like 1
RARA | retinoic acid receptor alpha
MAPK3 | mitogen−activated protein kinase 3
STAT5A | signal transducer and activator of transcription 5A
PIK3CD | phosphatidylinositol−4,5−bisphosphate 3−kinase catalytic subunit delta
PML | promyelocytic leukemia
GRB2 | growth factor receptor bound protein 2
SPI1 | Spi−1 proto−oncogene
TCF7L2 | transcription factor 7 like 2
CEBPA | CCAAT/enhancer binding protein alpha
NFKB1 | nuclear factor kappa B subunit 1
STAT5B | signal transducer and activator of transcription 5B
NRAS | NRAS proto−oncogene, GTPase
PIK3CB | phosphatidylinositol−4,5−bisphosphate 3−kinase catalytic subunit beta
PIK3R5 | phosphoinositide−3−kinase regulatory subunit 5
RELA | RELA proto−oncogene, NF−kB subunit
CHUK | conserved helix−loop−helix ubiquitous kinase
ARAF | A−Raf proto−oncogene, serine/threonine kinase
PIK3CG | phosphatidylinositol−4,5−bisphosphate 3−kinase catalytic subunit gamm
IKBKG | inhibitor of nuclear factor kappa B kinase subunit gamma
MAPK1 | mitogen−activated protein kinase 1
STAT3 | signal transducer and activator of transcription 3
SOS1 | SOS Ras/Rac guanine nucleotide exchange factor 1
BAD | BCL2 associated agonist of cell death
KIT | KIT proto−oncogene receptor tyrosine kinase
PIK3CA | phosphatidylinositol−4,5−bisphosphate 3−kinase catalytic subunit alpha
FLT3 | fms related tyrosine kinase 3
MAP2K1 | mitogen−activated protein kinase kinase 1
MAP2K2 | mitogen−activated protein kinase kinase 2
CCNA1 | cyclin A1
KRAS | KRAS proto−oncogene, GTPase
RPS6KB2 | ribosomal protein S6 kinase B2
BRAF | B−Raf proto−oncogene, serine/threonine kinase
PIK3R2 | phosphoinositide−3−kinase regulatory subunit 2
EIF4EBP1 | eukaryotic translation initiation factor 4E binding protein 1
CA
SLC
SS
Cancer

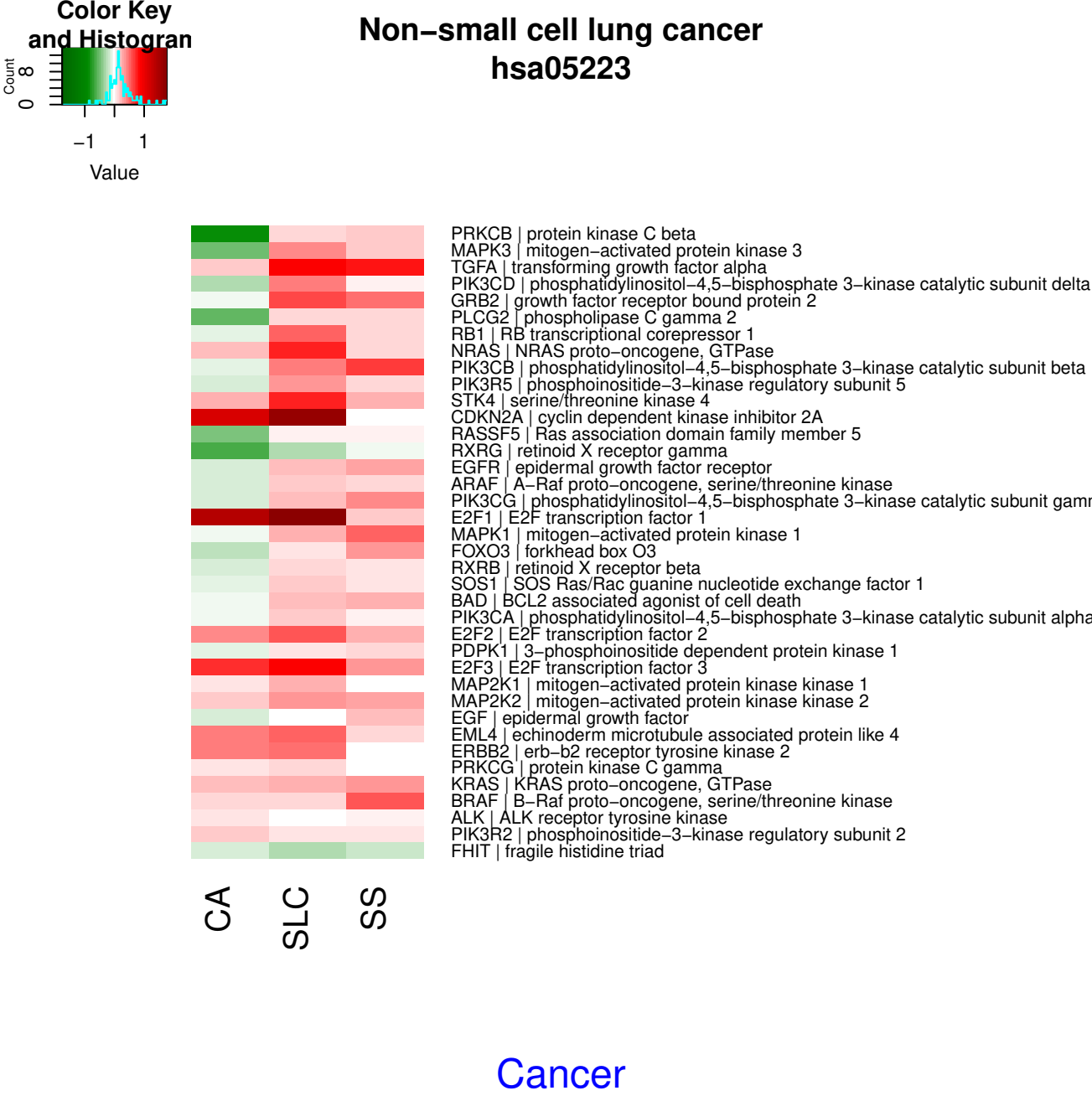
Color Key
and Histogram
Count
0
8
−1
1
Value
Non−small cell lung cancer
hsa05223
PRKCB | protein kinase C beta
MAPK3 | mitogen−activated protein kinase 3
TGFA | transforming growth factor alpha
PIK3CD | phosphatidylinositol−4,5−bisphosphate 3−kinase catalytic subunit delta
GRB2 | growth factor receptor bound protein 2
PLCG2 | phospholipase C gamma 2
RB1 | RB transcriptional corepressor 1
NRAS | NRAS proto−oncogene, GTPase
PIK3CB | phosphatidylinositol−4,5−bisphosphate 3−kinase catalytic subunit beta
PIK3R5 | phosphoinositide−3−kinase regulatory subunit 5
STK4 | serine/threonine kinase 4
CDKN2A | cyclin dependent kinase inhibitor 2A
RASSF5 | Ras association domain family member 5
RXRG | retinoid X receptor gamma
EGFR | epidermal growth factor receptor
ARAF | A−Raf proto−oncogene, serine/threonine kinase
PIK3CG | phosphatidylinositol−4,5−bisphosphate 3−kinase catalytic subunit gamm
E2F1 | E2F transcription factor 1
MAPK1 | mitogen−activated protein kinase 1
FOXO3 | forkhead box O3
RXRB | retinoid X receptor beta
SOS1 | SOS Ras/Rac guanine nucleotide exchange factor 1
BAD | BCL2 associated agonist of cell death
PIK3CA | phosphatidylinositol−4,5−bisphosphate 3−kinase catalytic subunit alpha
E2F2 | E2F transcription factor 2
PDPK1 | 3−phosphoinositide dependent protein kinase 1
E2F3 | E2F transcription factor 3
MAP2K1 | mitogen−activated protein kinase kinase 1
MAP2K2 | mitogen−activated protein kinase kinase 2
EGF | epidermal growth factor
EML4 | echinoderm microtubule associated protein like 4
ERBB2 | erb−b2 receptor tyrosine kinase 2
PRKCG | protein kinase C gamma
KRAS | KRAS proto−oncogene, GTPase
BRAF | B−Raf proto−oncogene, serine/threonine kinase
ALK | ALK receptor tyrosine kinase
PIK3R2 | phosphoinositide−3−kinase regulatory subunit 2
FHIT | fragile histidine triad
CA
SLC
SS
Cancer

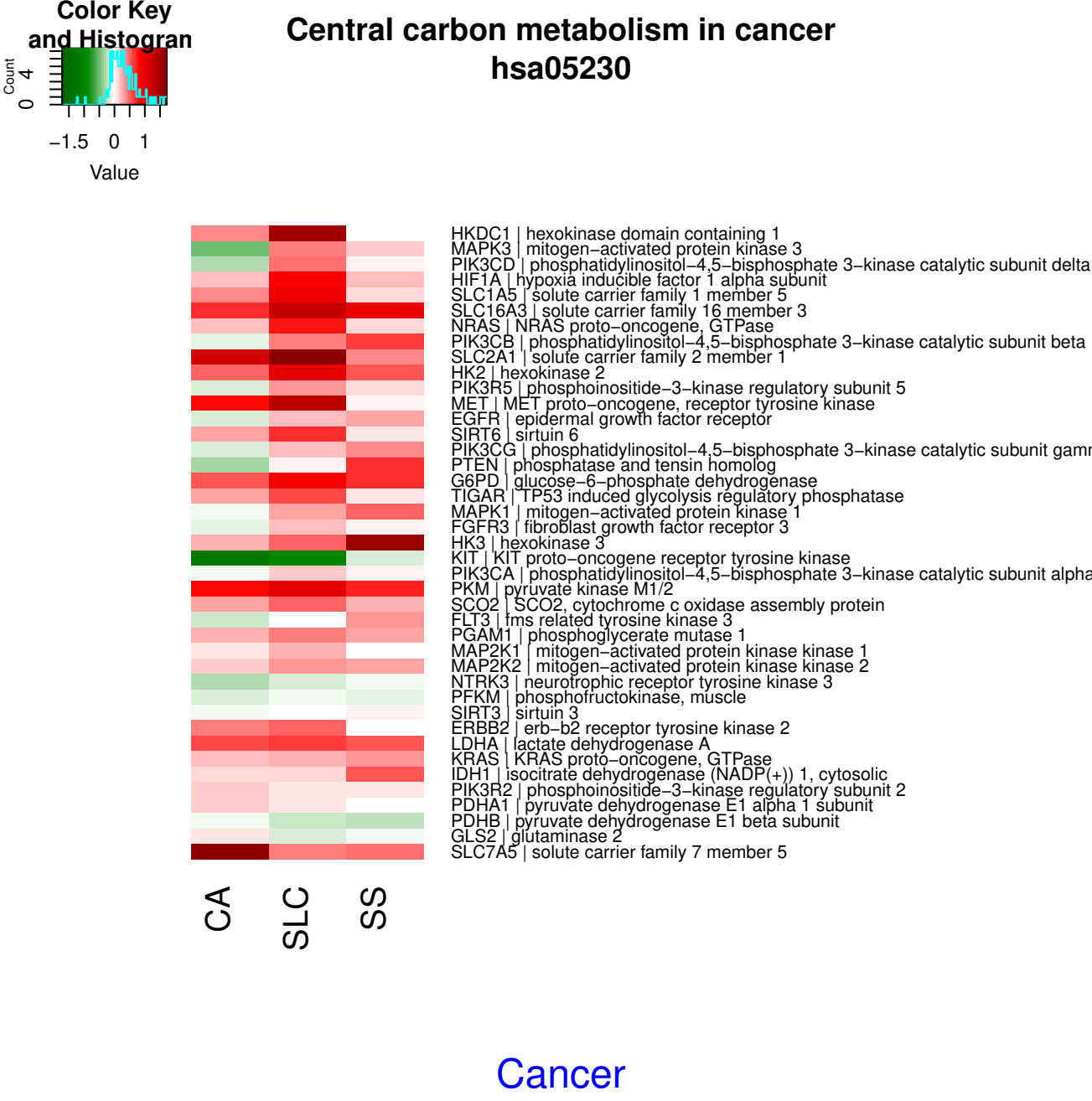
Color Key
and Histogram
Count
0
4
−1.5
0
1
Value
Central carbon metabolism in cancer
hsa05230
HKDC1 | hexokinase domain containing 1
MAPK3 | mitogen−activated protein kinase 3
PIK3CD | phosphatidylinositol−4,5−bisphosphate 3−kinase catalytic subunit delta
HIF1A | hypoxia inducible factor 1 alpha subunit
SLC1A5 | solute carrier family 1 member 5
SLC16A3 | solute carrier family 16 member 3
NRAS | NRAS proto−oncogene, GTPase
PIK3CB | phosphatidylinositol−4,5−bisphosphate 3−kinase catalytic subunit beta
SLC2A1 | solute carrier family 2 member 1
HK2 | hexokinase 2
PIK3R5 | phosphoinositide−3−kinase regulatory subunit 5
MET | MET proto−oncogene, receptor tyrosine kinase
EGFR | epidermal growth factor receptor
SIRT6 | sirtuin 6
PIK3CG | phosphatidylinositol−4,5−bisphosphate 3−kinase catalytic subunit gamm
PTEN | phosphatase and tensin homolog
G6PD | glucose−6−phosphate dehydrogenase
TIGAR | TP53 induced glycolysis regulatory phosphatase
MAPK1 | mitogen−activated protein kinase 1
FGFR3 | fibroblast growth factor receptor 3
HK3 | hexokinase 3
KIT | KIT proto−oncogene receptor tyrosine kinase
PIK3CA | phosphatidylinositol−4,5−bisphosphate 3−kinase catalytic subunit alpha
PKM | pyruvate kinase M1/2
SCO2 | SCO2, cytochrome c oxidase assembly protein
FLT3 | fms related tyrosine kinase 3
PGAM1 | phosphoglycerate mutase 1
MAP2K1 | mitogen−activated protein kinase kinase 1
MAP2K2 | mitogen−activated protein kinase kinase 2
NTRK3 | neurotrophic receptor tyrosine kinase 3
PFKM | phosphofructokinase, muscle
SIRT3 | sirtuin 3
ERBB2 | erb−b2 receptor tyrosine kinase 2
LDHA | lactate dehydrogenase A
KRAS | KRAS proto−oncogene, GTPase
IDH1 | isocitrate dehydrogenase (NADP(+)) 1, cytosolic
PIK3R2 | phosphoinositide−3−kinase regulatory subunit 2
PDHA1 | pyruvate dehydrogenase E1 alpha 1 subunit
PDHB | pyruvate dehydrogenase E1 beta subunit
GLS2 | glutaminase 2
SLC7A5 | solute carrier family 7 member 5
CA
SLC
SS
Cancer

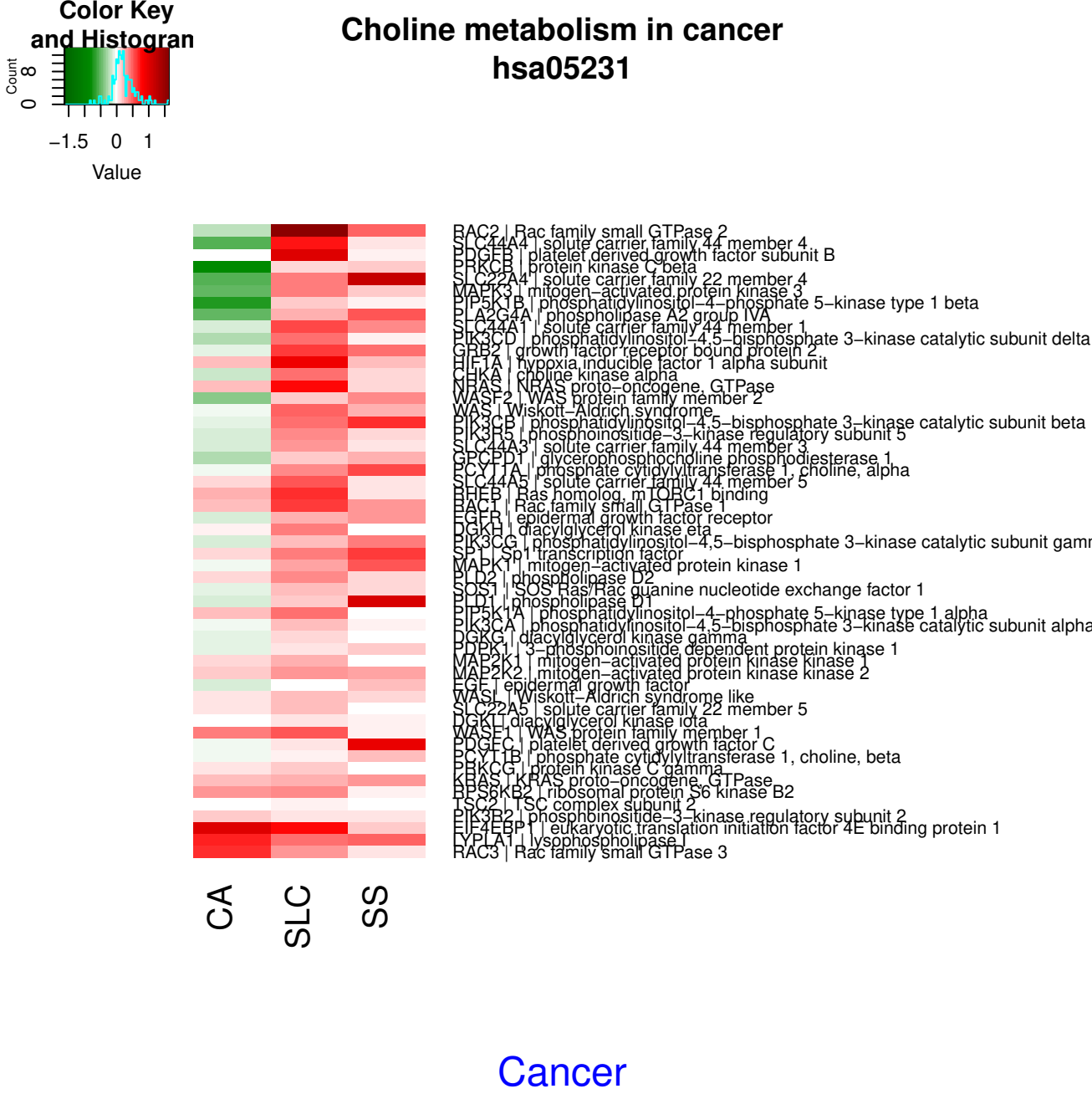
Color Key
and Histogram
Count
0
8
−1.5
0
1
Value
Choline metabolism in cancer
hsa05231
RAC2 | Rac family small GTPase 2
SLC44A4 | solute carrier family 44 member 4
PDGFB | platelet derived growth factor subunit B
PRKCB | protein kinase C beta
SLC22A4 | solute carrier family 22 member 4
MAPK3 | mitogen−activated protein kinase 3
PIP5K1B | phosphatidylinositol−4−phosphate 5−kinase type 1 beta
PLA2G4A | phospholipase A2 group IVA
SLC44A1 | solute carrier family 44 member 1
PIK3CD | phosphatidylinositol−4,5−bisphosphate 3−kinase catalytic subunit delta
GRB2 | growth factor receptor bound protein 2
HIF1A | hypoxia inducible factor 1 alpha subunit
CHKA | choline kinase alpha
NRAS | NRAS proto−oncogene, GTPase
WASF2 | WAS protein family member 2
WAS | Wiskott−Aldrich syndrome
PIK3CB | phosphatidylinositol−4,5−bisphosphate 3−kinase catalytic subunit beta
PIK3R5 | phosphoinositide−3−kinase regulatory subunit 5
SLC44A3 | solute carrier family 44 member 3
GPCPD1 | glycerophosphocholine phosphodiesterase 1
PCYT1A | phosphate cytidylyltransferase 1, choline, alpha
SLC44A5 | solute carrier family 44 member 5
RHEB | Ras homolog, mTORC1 binding
RAC1 | Rac family small GTPase 1
EGFR | epidermal growth factor receptor
DGKH | diacylglycerol kinase eta
PIK3CG | phosphatidylinositol−4,5−bisphosphate 3−kinase catalytic subunit gamm
SP1 | Sp1 transcription factor
MAPK1 | mitogen−activated protein kinase 1
PLD2 | phospholipase D2
SOS1 | SOS Ras/Rac guanine nucleotide exchange factor 1
PLD1 | phospholipase D1
PIP5K1A | phosphatidylinositol−4−phosphate 5−kinase type 1 alpha
PIK3CA | phosphatidylinositol−4,5−bisphosphate 3−kinase catalytic subunit alpha
DGKG | diacylglycerol kinase gamma
PDPK1 | 3−phosphoinositide dependent protein kinase 1
MAP2K1 | mitogen−activated protein kinase kinase 1
MAP2K2 | mitogen−activated protein kinase kinase 2
EGF | epidermal growth factor
WASL | Wiskott−Aldrich syndrome like
SLC22A5 | solute carrier family 22 member 5
DGKI | diacylglycerol kinase iota
WASF1 | WAS protein family member 1
PDGFC | platelet derived growth factor C
PCYT1B | phosphate cytidylyltransferase 1, choline, beta
PRKCG | protein kinase C gamma
KRAS | KRAS proto−oncogene, GTPase
RPS6KB2 | ribosomal protein S6 kinase B2
TSC2 | TSC complex subunit 2
PIK3R2 | phosphoinositide−3−kinase regulatory subunit 2
EIF4EBP1 | eukaryotic translation initiation factor 4E binding protein 1
LYPLA1 | lysophospholipase I
RAC3 | Rac family small GTPase 3
CA
SLC
SS
Cancer

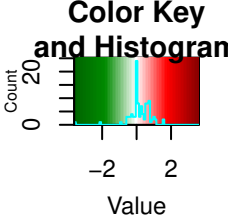

Glycolysis / Gluconeogenesis
hsa00010

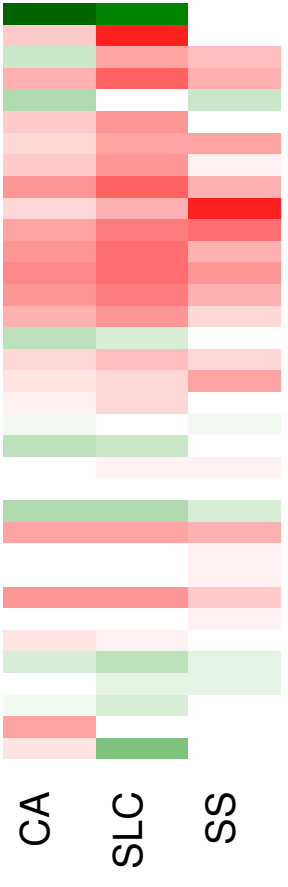

ADH1B | alcohol dehydrogenase 1B (class I), beta polypeptide
HKDC1 | hexokinase domain containing 1
ALDH3B1 | aldehyde dehydrogenase 3 family member B1
HK2 | hexokinase 2
ADH5 | alcohol dehydrogenase 5 (class III), chi polypeptide
G6PC3 | glucose−6−phosphatase catalytic subunit 3
BPGM | bisphosphoglycerate mutase
ADPGK | ADP dependent glucokinase
GAPDH | glyceraldehyde−3−phosphate dehydrogenase
HK3 | hexokinase 3
ENO1 | enolase 1
ALDOA | aldolase, fructose−bisphosphate A
PKM | pyruvate kinase M1/2
PGK1 | phosphoglycerate kinase 1
TPI1 | triosephosphate isomerase 1
ALDOC | aldolase, fructose−bisphosphate C
PGAM1 | phosphoglycerate mutase 1
PGM2 | phosphoglucomutase 2
ACSS1 | acyl−CoA synthetase short chain family member 1
PFKM | phosphofructokinase, muscle
ALDH7A1 | aldehyde dehydrogenase 7 family member A1
LDHAL6B | lactate dehydrogenase A like 6B
ALDH1A3 | aldehyde dehydrogenase 1 family member A3
ALDH3A2 | aldehyde dehydrogenase 3 family member A2
LDHA | lactate dehydrogenase A
LDHAL6A | lactate dehydrogenase A like 6A
PGK2 | phosphoglycerate kinase 2
GPI | glucose−6−phosphate isomerase
GAPDHS | glyceraldehyde−3−phosphate dehydrogenase, spermatogenic
PDHA1 | pyruvate dehydrogenase E1 alpha 1 subunit
ALDH9A1 | aldehyde dehydrogenase 9 family member A1
PDHB | pyruvate dehydrogenase E1 beta subunit
ADH1A | alcohol dehydrogenase 1A (class I), alpha polypeptide
ALDH3B2 | aldehyde dehydrogenase 3 family member B2
ENO3 | enolase 3

Carbohydrate metabolism

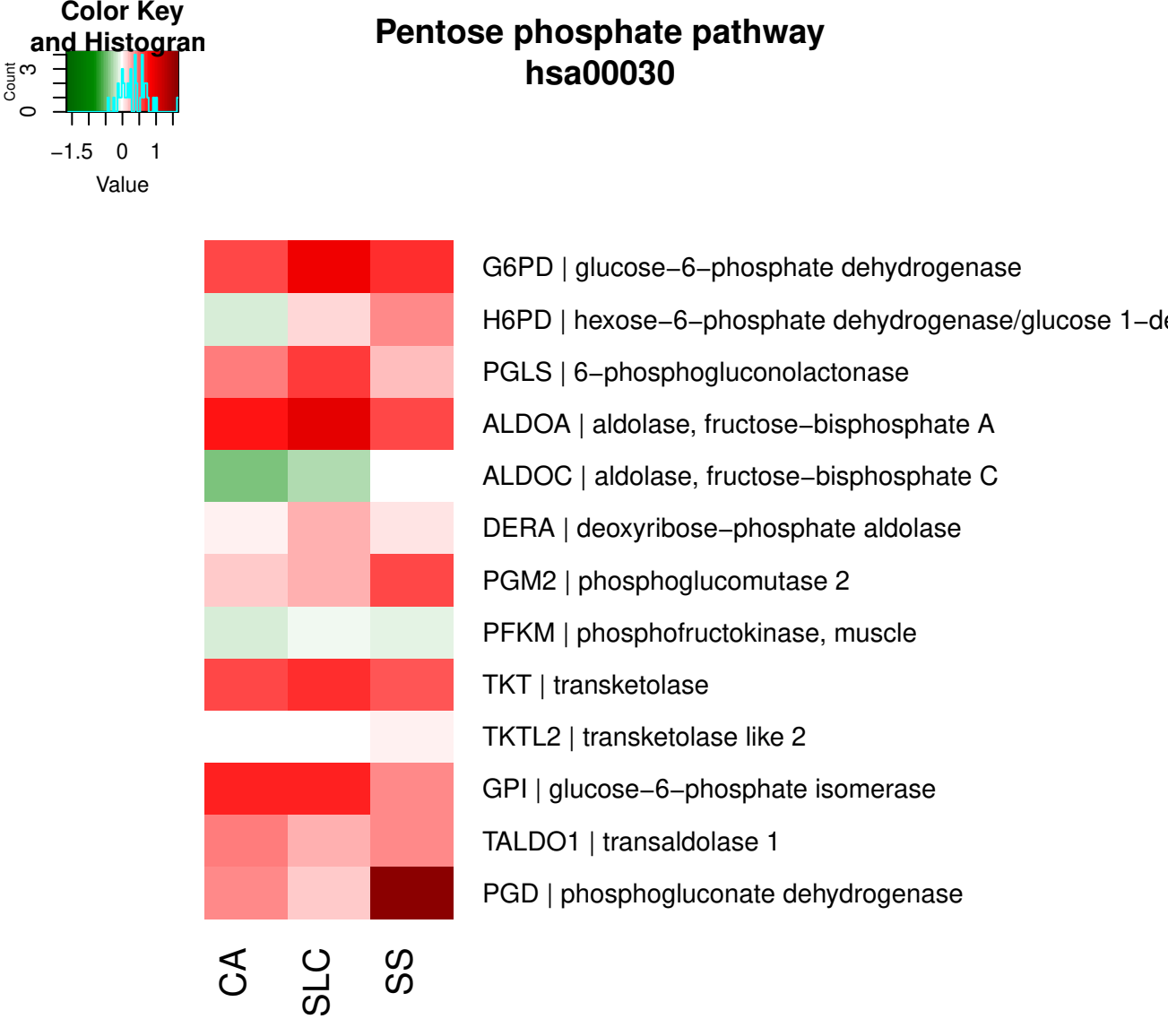

Carbohydrate metabolism

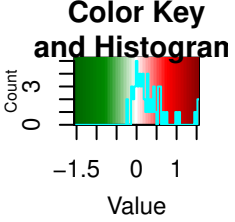

Galactose metabolism
hsa00052

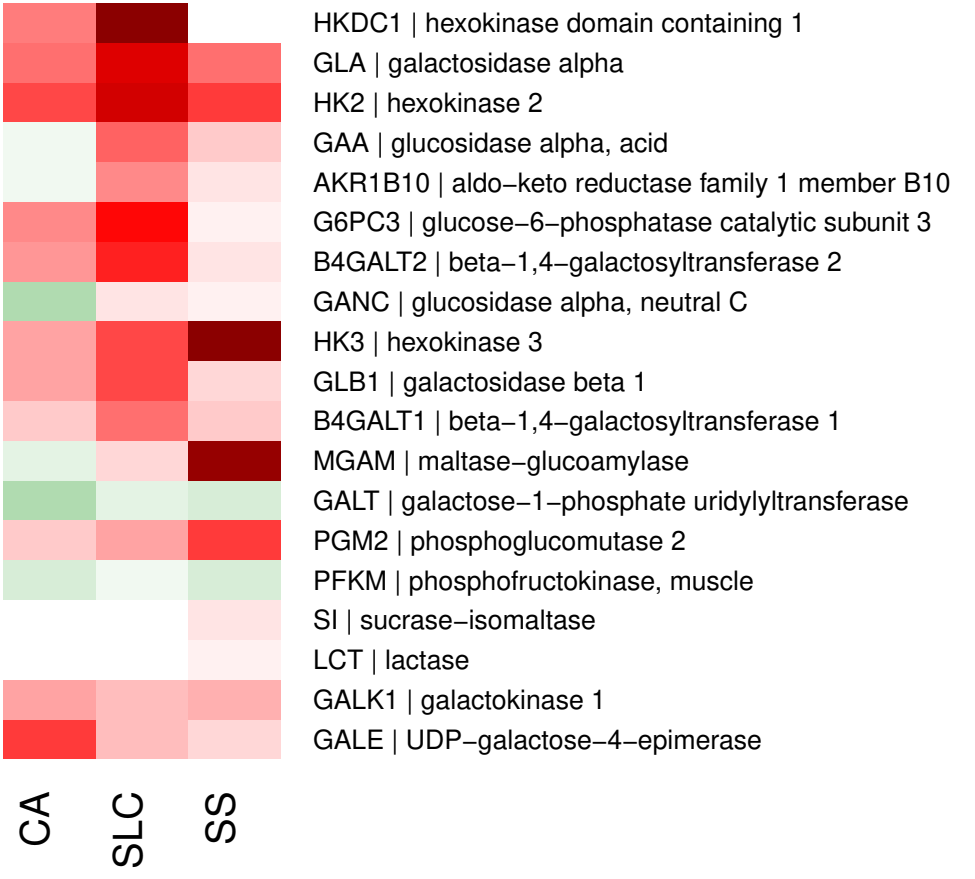

Carbohydrate metabolism

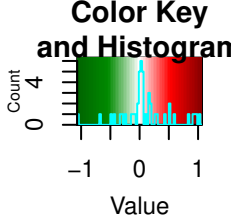

Ovarian steroidogenesis
hsa04913

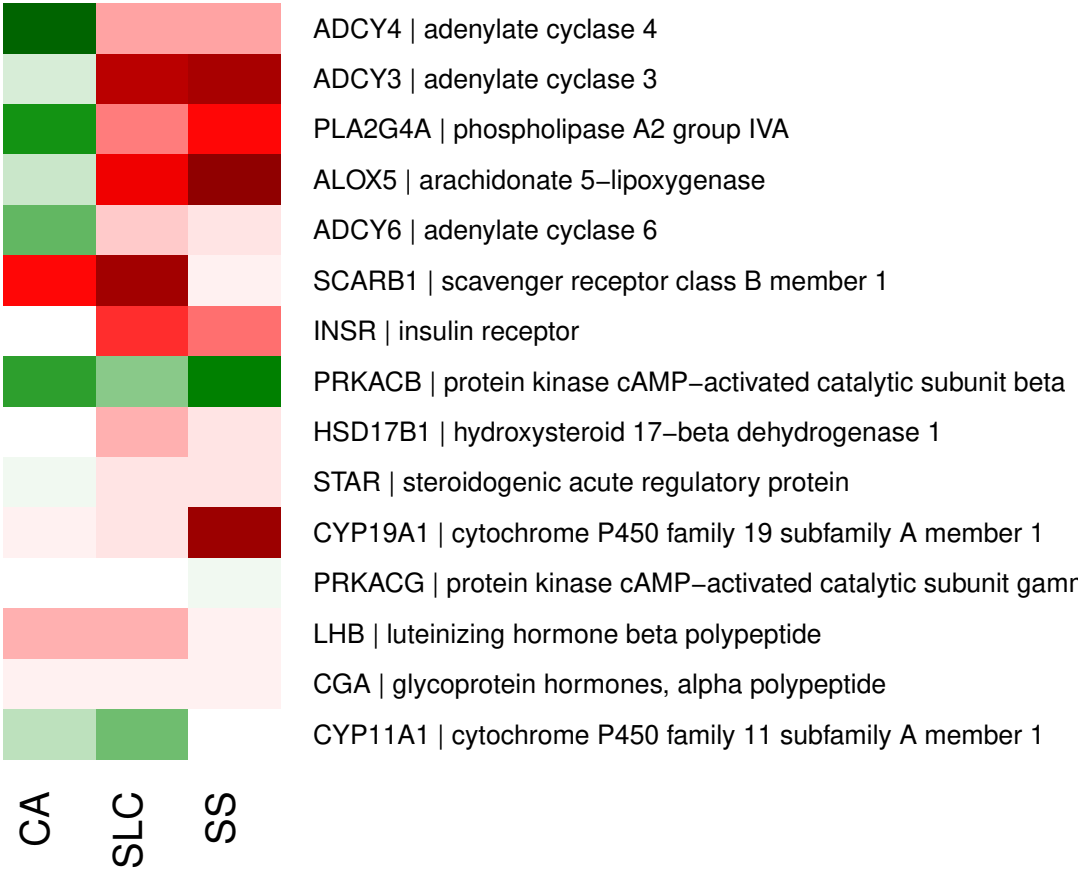

Endocrine system

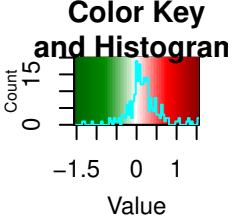

Insulin signaling pathway
hsa04910

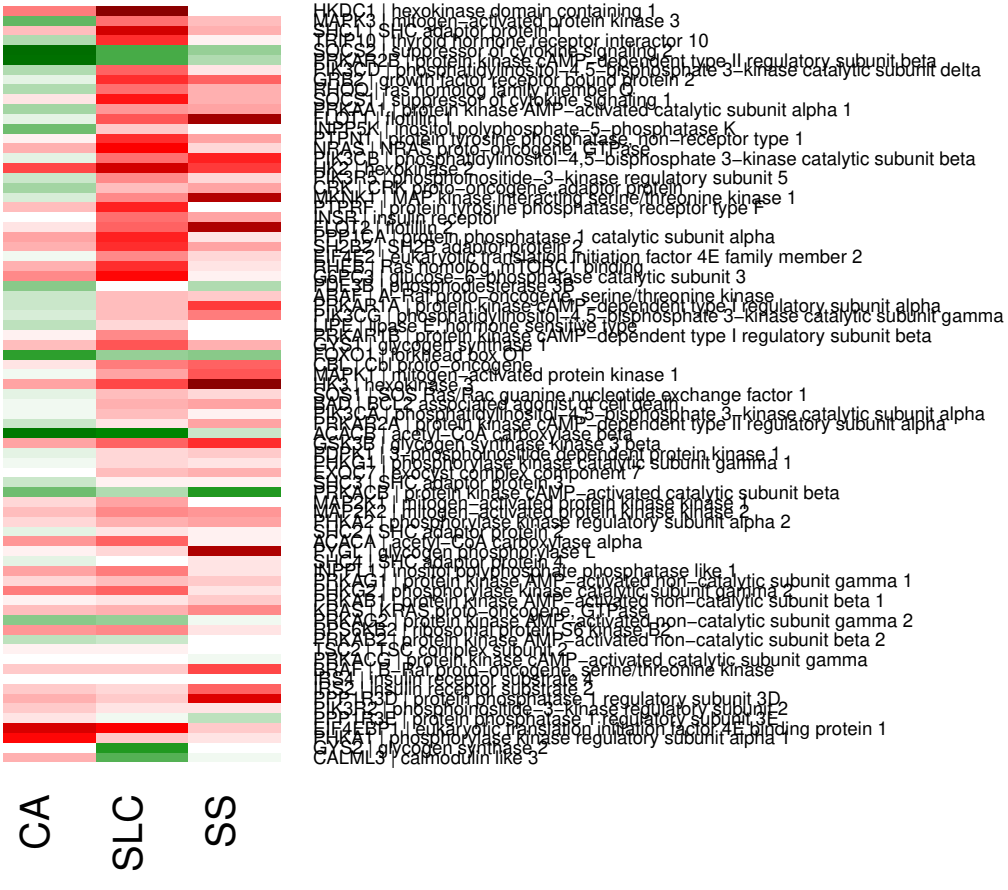

Endocrine system

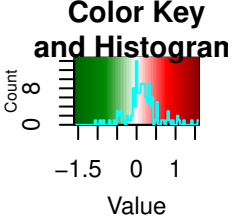

GnRH signaling pathway
hsa04912

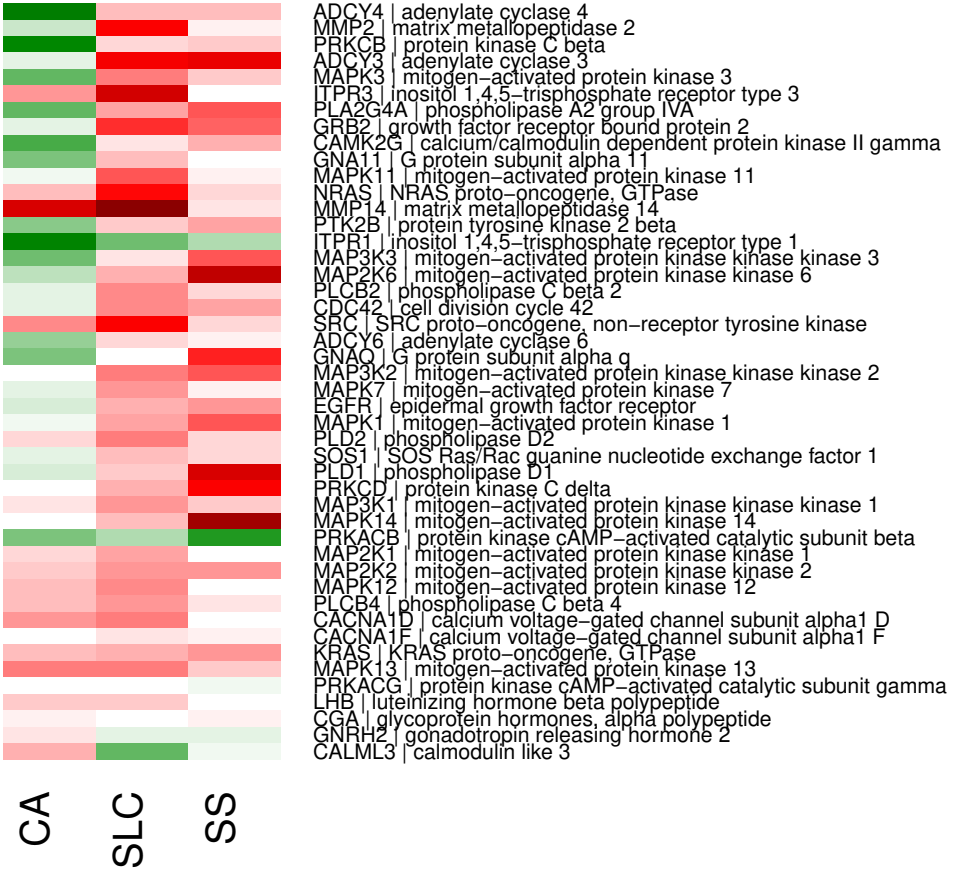

Endocrine system

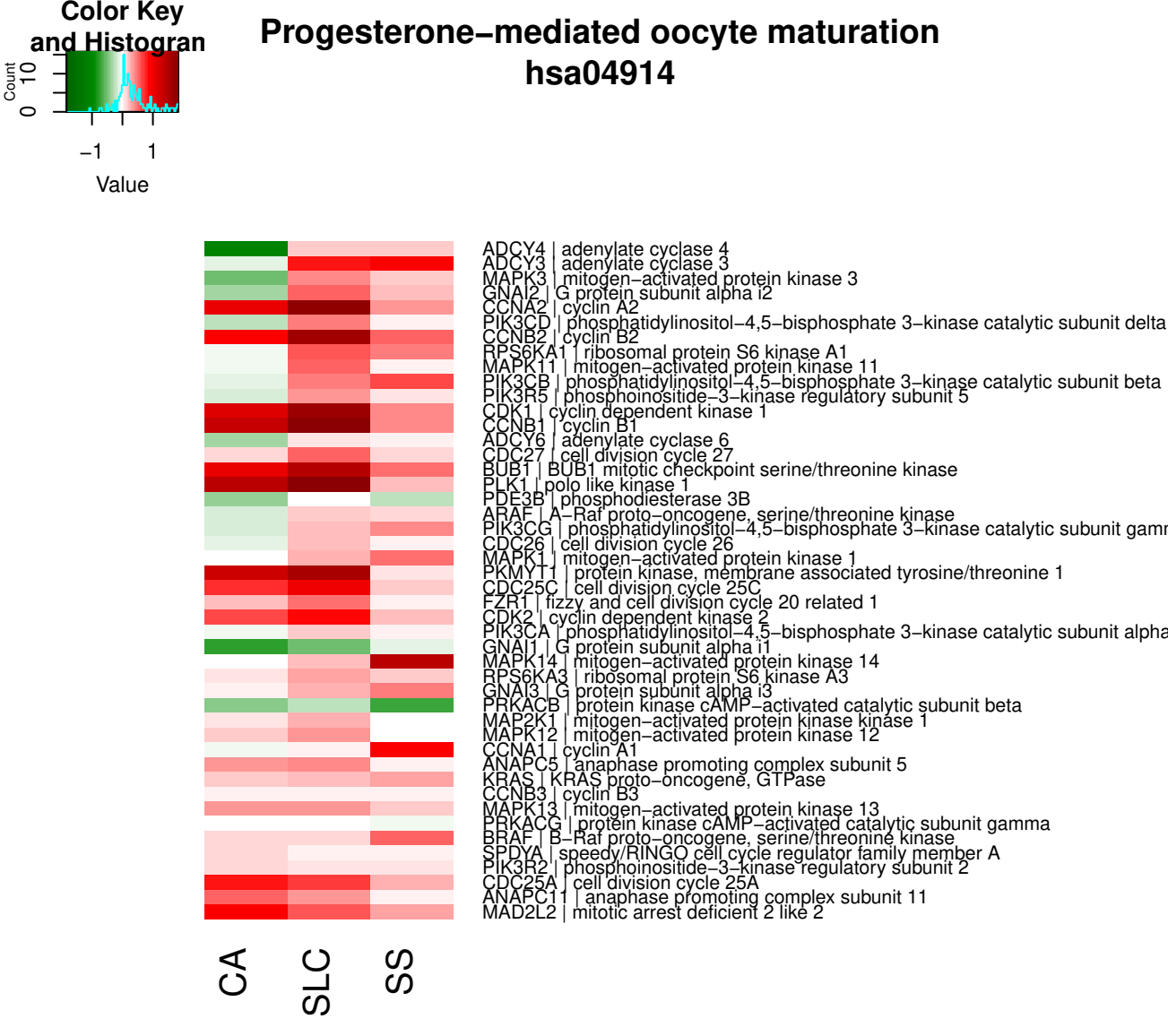

Endocrine system

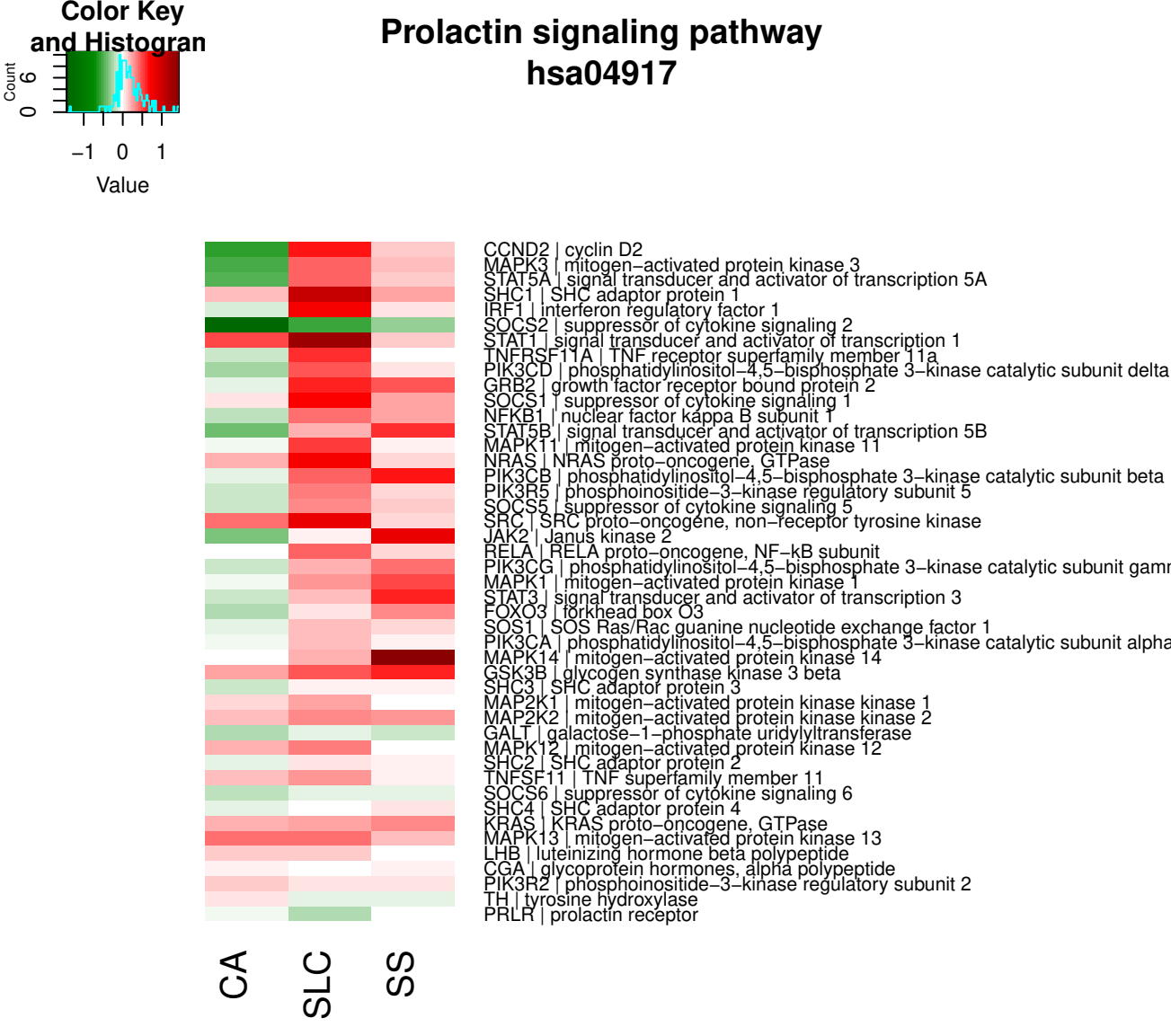
Color Key
and Histogram
Count
0
6
−1
0
1
Value
Prolactin signaling pathway
hsa04917
CCND2 | cyclin D2
MAPK3 | mitogen−activated protein kinase 3
STAT5A | signal transducer and activator of transcription 5A
SHC1 | SHC adaptor protein 1
IRF1 | interferon regulatory factor 1
SOCS2 | suppressor of cytokine signaling 2
STAT1 | signal transducer and activator of transcription 1
TNFRSF11A | TNF receptor superfamily member 11a
PIK3CD | phosphatidylinositol−4,5−bisphosphate 3−kinase catalytic subunit delta
GRB2 | growth factor receptor bound protein 2
SOCS1 | suppressor of cytokine signaling 1
NFKB1 | nuclear factor kappa B subunit 1
STAT5B | signal transducer and activator of transcription 5B
MAPK11 | mitogen−activated protein kinase 11
NRAS | NRAS proto−oncogene, GTPase
PIK3CB | phosphatidylinositol−4,5−bisphosphate 3−kinase catalytic subunit beta
PIK3R5 | phosphoinositide−3−kinase regulatory subunit 5
SOCS5 | suppressor of cytokine signaling 5
SRC | SRC proto−oncogene, non−receptor tyrosine kinase
JAK2 | Janus kinase 2
RELA | RELA proto−oncogene, NF−kB subunit
PIK3CG | phosphatidylinositol−4,5−bisphosphate 3−kinase catalytic subunit gamm
MAPK1 | mitogen−activated protein kinase 1
STAT3 | signal transducer and activator of transcription 3
FOXO3 | forkhead box O3
SOS1 | SOS Ras/Rac guanine nucleotide exchange factor 1
PIK3CA | phosphatidylinositol−4,5−bisphosphate 3−kinase catalytic subunit alpha
MAPK14 | mitogen−activated protein kinase 14
GSK3B | glycogen synthase kinase 3 beta
SHC3 | SHC adaptor protein 3
MAP2K1 | mitogen−activated protein kinase kinase 1
MAP2K2 | mitogen−activated protein kinase kinase 2
GALT | galactose−1−phosphate uridylyltransferase
MAPK12 | mitogen−activated protein kinase 12
SHC2 | SHC adaptor protein 2
TNFSF11 | TNF superfamily member 11
SOCS6 | suppressor of cytokine signaling 6
SHC4 | SHC adaptor protein 4
KRAS | KRAS proto−oncogene, GTPase
MAPK13 | mitogen−activated protein kinase 13
LHB | luteinizing hormone beta polypeptide
CGA | glycoprotein hormones, alpha polypeptide
PIK3R2 | phosphoinositide−3−kinase regulatory subunit 2
TH | tyrosine hydroxylase
PRLR | prolactin receptor
CA
SLC
SS
Endocrine system

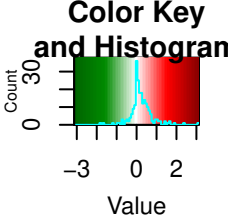

Leukocyte transendothelial migration
hsa04670

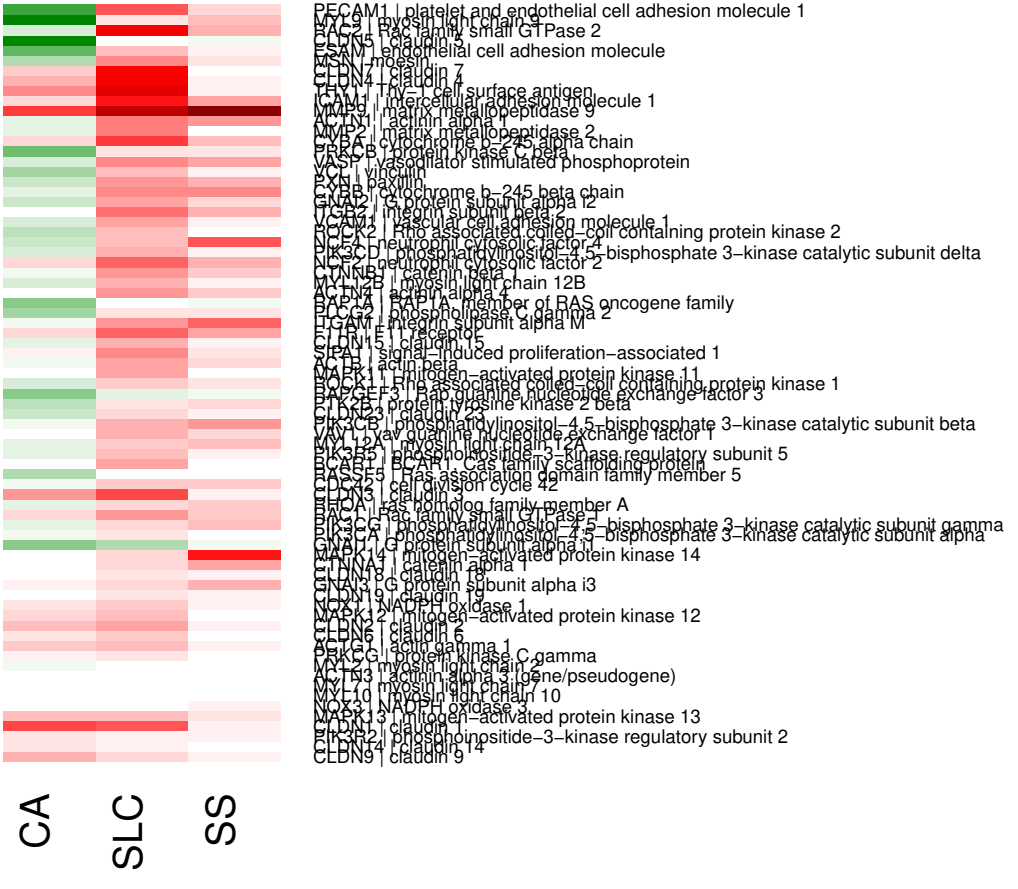

Immune system

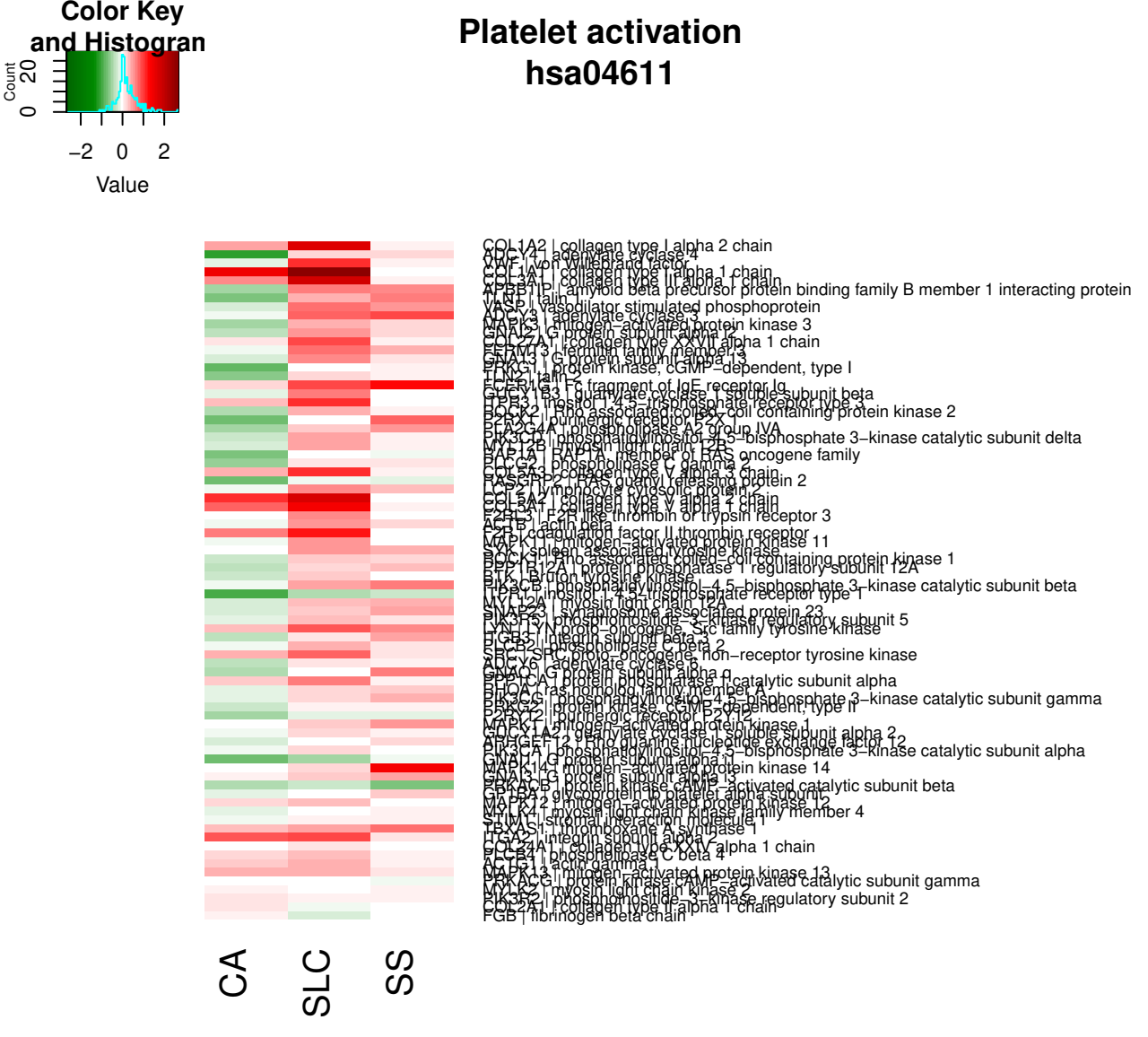
Color Key
and Histogran
Count
0
20
−2
0
2
Value
Platelet activation
hsa04611
COL1A2 | collagen type I alpha 2 chain
ADCY4 | adenylate cyclase 4
CVF1 | von willebrand factor
COL3A1 | collagen type III alpha 1 chain
APBB1P | amyloid beta precursor protein binding family B member 1 interacting protein
VAS1 | vasodilator stimulated phosphoprotein
ADCY3 | adenylate cyclase 3
MAPK3 | mitogen−activated protein kinase 3
GNAI2 | G protein subunit alpha 2
CDC2A1 | collagen type XXVII alpha 1 chain
FERM3 | fermitin family member 3
GNAI3 | G protein subunit alpha 3
PRKG1 | protein kinase, cGMP−dependent, type I
FCER1 | fain−2
FCER1G | fc fragment of IgE receptor Ig
GCEV1B3 | guanylate cyclase 1 soluble subunit beta
PTPR3 | inositol−4,5−trisphosphate receptor type 3
BCKK2 | Rho associated coiled−coil containing protein kinase 2
P2RX1 | purinergic receptor P2X 1
PLA2G4A | phospholipase A2 group IVA
PIK3D2 | phosphatidylinositol−4,5−bisphosphate 3−kinase catalytic subunit delta
MYL12B | myosin light chain 12B
RAP1A | RAP1A, member of RAS oncogene family
PLCG2 | phospholipase C gamma 2
CDC3A3 | collagen type V alpha 3 chain
RASGRP2 | RAS guanyl releasing protein 2
PLCB2 | phospholipase C beta 2
COL5A2 | collagen type V alpha 2 chain
COL3A1 | collagen type V alpha 1 chain
F2RL3 | F2R like thrombin or trypsin receptor 3
ACTB | actin beta
F2R1 | coagulation factor II thrombin receptor
MAPK1 | mitogen−activated protein kinase 11
SYK | spleen associated tyrosine kinase
BCKK1 | Rho associated coiled−coil containing protein kinase 1
PEP1B12A | protein phosphatase 1 regulatory subunit 12A
PTK1B | tyrosine kinase
PIK3CB | phosphatidylinositol−4,5−bisphosphate 3−kinase catalytic subunit beta
PTPR3 | inositol−4,5−trisphosphate receptor type I
MYL12A | myosin light chain 12A
PIKAP3 | synaptosome associated protein 23
PIK3R5 | phosphoinositide−3−kinase regulatory subunit 5
LYN3 | Lyn proto−oncogene, Src family tyrosine kinase
ITGB3 | integrin subunit beta 3
PLCB2 | phospholipase C beta 2
SRCY1 | SRC proto−oncogene, non−receptor tyrosine kinase
ADCY6 | adenylate cyclase 6
PPP1CA | protein subunit alpha g
PTPRC | ras homology family member A
PIK3CG | phosphatidylinositol−4,5−bisphosphate 3−kinase catalytic subunit gamma
PRKG2 | protein kinase, cGMP−dependent, type II
P2RY2 | purinergic receptor P2Y 12
MAPK1 | mitogen−activated protein kinase 1
GCEV1A2 | guanylate cyclase 1 soluble subunit alpha 2
ARHGEF1 | Rho guanine nucleotide exchange factor 12
PIK3CA | phosphatidylinositol−4,5−bisphosphate 3−kinase catalytic subunit alpha
GNAI1 | G protein subunit alpha 1
MAPK14 | mitogen−activated protein kinase 14
GNAI3 | G protein subunit alpha 13
PRKACB | protein kinase cAMP−activated catalytic subunit beta
GPIBA2 | glycoprotein Ib platelet alpha subunit
MAPK12 | mitogen−activated protein kinase 12
MYLK4 | myosin light chain kinase family member 4
STIM1 | stromal interaction molecule 1
TBXAS1 | thromboxane A synthase 1
ITGA2 | integrin subunit alpha 2
COL24A1 | collagen type XXIV alpha 1 chain
PLCB4 | phospholipase C beta 4
ACTG1 | actin gamma 1
MAPK13 | mitogen−activated protein kinase 13
PRKACG | protein kinase cAMP−activated catalytic subunit gamma
MYLK2 | myosin light chain kinase 2
PIK3R2 | phosphoinositide−3−kinase regulatory subunit 2
COL2A1 | collagen type II alpha 1 chain
FGB | fibrinogen beta chain
CA
SLC
SS
Immune system

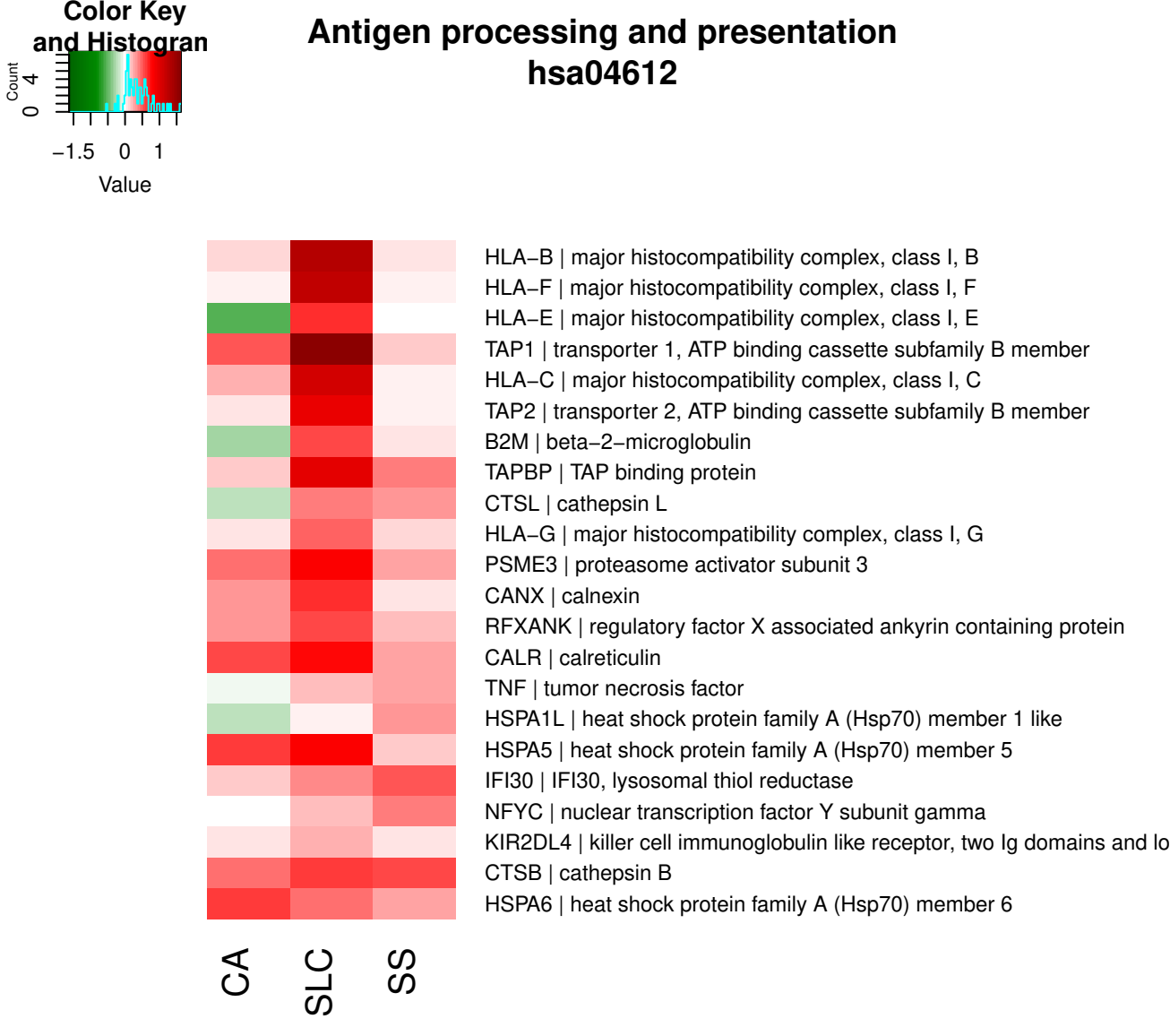

Immune system

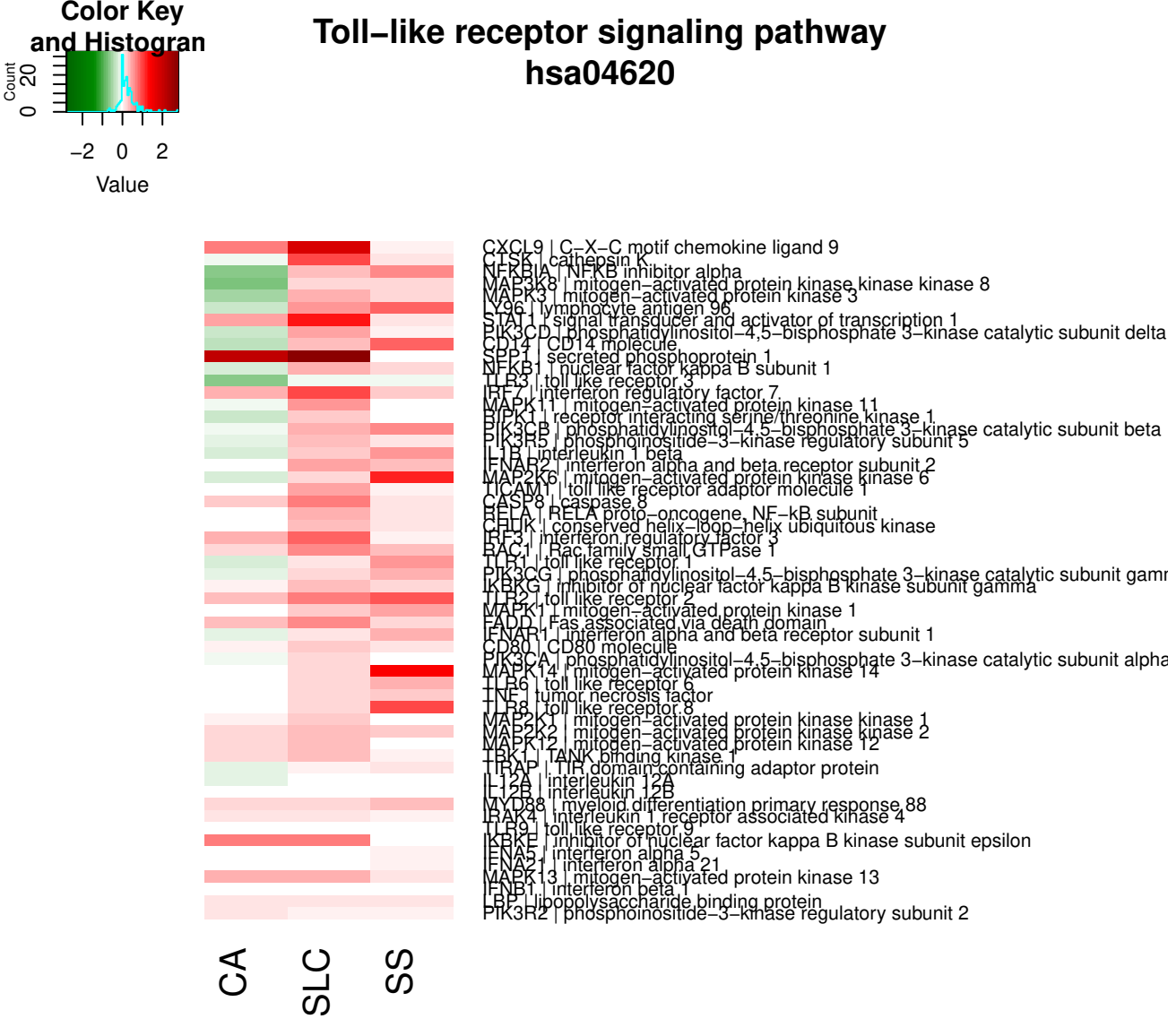
Color Key
and Histogram
Count
0
20
−2
0
2
Value
Toll−like receptor signaling pathway
hsa04620
CXCL9 | C−X−C motif chemokine ligand 9
CTSK | cathepsin K
NFKBIA | NFKB inhibitor alpha
MAP3K8 | mitogen−activated protein kinase kinase kinase 8
MAPK3 | mitogen−activated protein kinase 3
LY96 | lymphocyte antigen 96
STAT1 | signal transducer and activator of transcription 1
PIK3CD | phosphatidylinositol−4,5−bisphosphate 3−kinase catalytic subunit delta
CD14 | CD14 molecule
SPP1 | secreted phosphoprotein 1
NFKB1 | nuclear factor kappa B subunit 1
TLR3 | toll like receptor 3
IRF7 | interferon regulatory factor 7
MAPK11 | mitogen−activated protein kinase 11
RIPK1 | receptor interacting serine/threonine kinase 1
PIK3CB | phosphatidylinositol−4,5−bisphosphate 3−kinase catalytic subunit beta
PIK3R5 | phosphoinositide−3−kinase regulatory subunit 5
IL1B | interleukin 1 beta
IFNAR2 | interferon alpha and beta receptor subunit 2
MAP2K6 | mitogen−activated protein kinase kinase 6
TICAM1 | toll like receptor adaptor molecule 1
CASP8 | caspase 8
RELA | RELA proto−oncogene, NF−kB subunit
CHUK | conserved helix−loop−helix ubiquitous kinase
IRF3 | interferon regulatory factor 3
RAC1 | Rac family small GTPase 1
TLR1 | toll like receptor 1
PIK3CG | phosphatidylinositol−4,5−bisphosphate 3−kinase catalytic subunit gamma
IKBKG | inhibitor of nuclear factor kappa B kinase subunit gamma
TLR2 | toll like receptor 2
MAPK1 | mitogen−activated protein kinase 1
FADD | Fas associated via death domain
IFNAR1 | interferon alpha and beta receptor subunit 1
CD80 | CD80 molecule
PIK3CA | phosphatidylinositol−4,5−bisphosphate 3−kinase catalytic subunit alpha
MAPK14 | mitogen−activated protein kinase 14
TLR6 | toll like receptor 6
TNF | tumor necrosis factor
TLR8 | toll like receptor 8
MAP2K1 | mitogen−activated protein kinase kinase 1
MAP2K2 | mitogen−activated protein kinase kinase 2
MAPK12 | mitogen−activated protein kinase 12
TBK1 | TANK binding kinase 1
TIRAP | TIR domain−containing adaptor protein
IL12A | interleukin 12A
IL12B | interleukin 12B
MYD88 | myeloid differentiation primary response 88
IRAK4 | interleukin 1 receptor associated kinase 4
TLR9 | toll like receptor 9
IKBKE | inhibitor of nuclear factor kappa B kinase subunit epsilon
IFNA5 | interferon alpha 5
IFNA21 | interferon alpha 21
MAPK13 | mitogen−activated protein kinase 13
IFNB1 | interferon beta 1
LBP | lipopolysaccharide binding protein
PIK3R2 | phosphoinositide−3−kinase regulatory subunit 2
CA
SLC
SS
Immune system

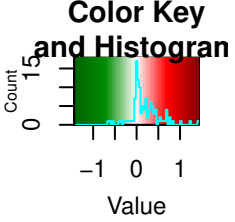

RIG−I−like receptor signaling pathway
hsa04622

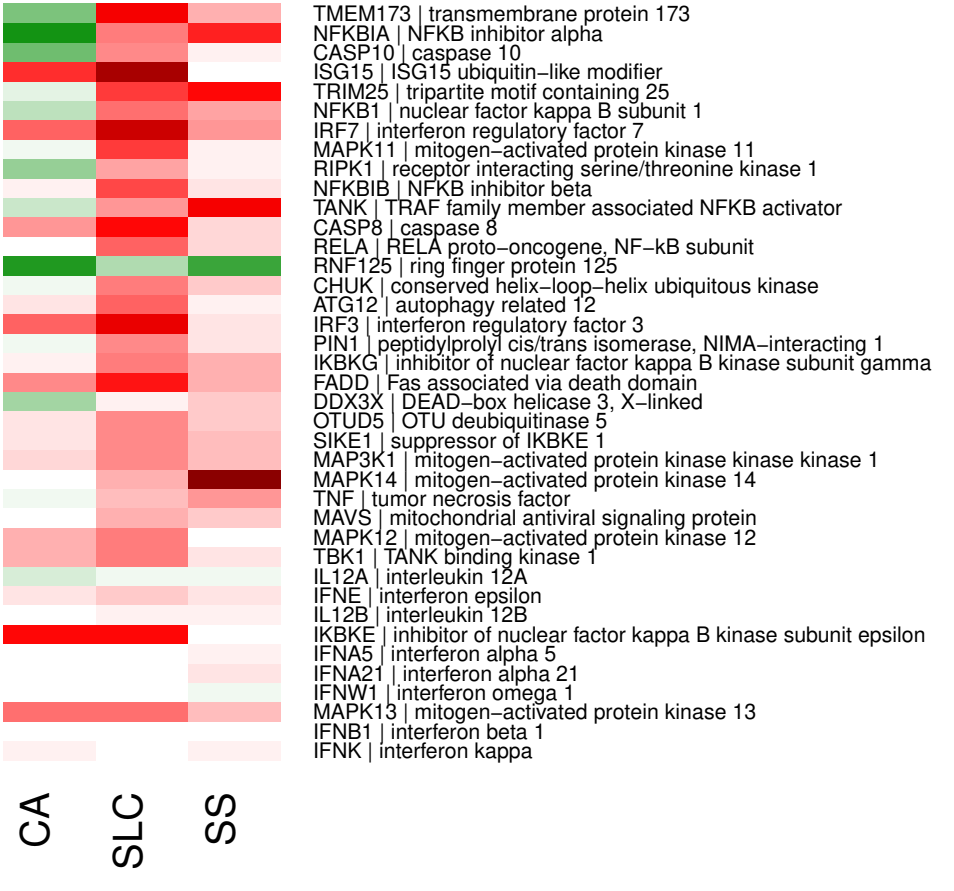

Immune system

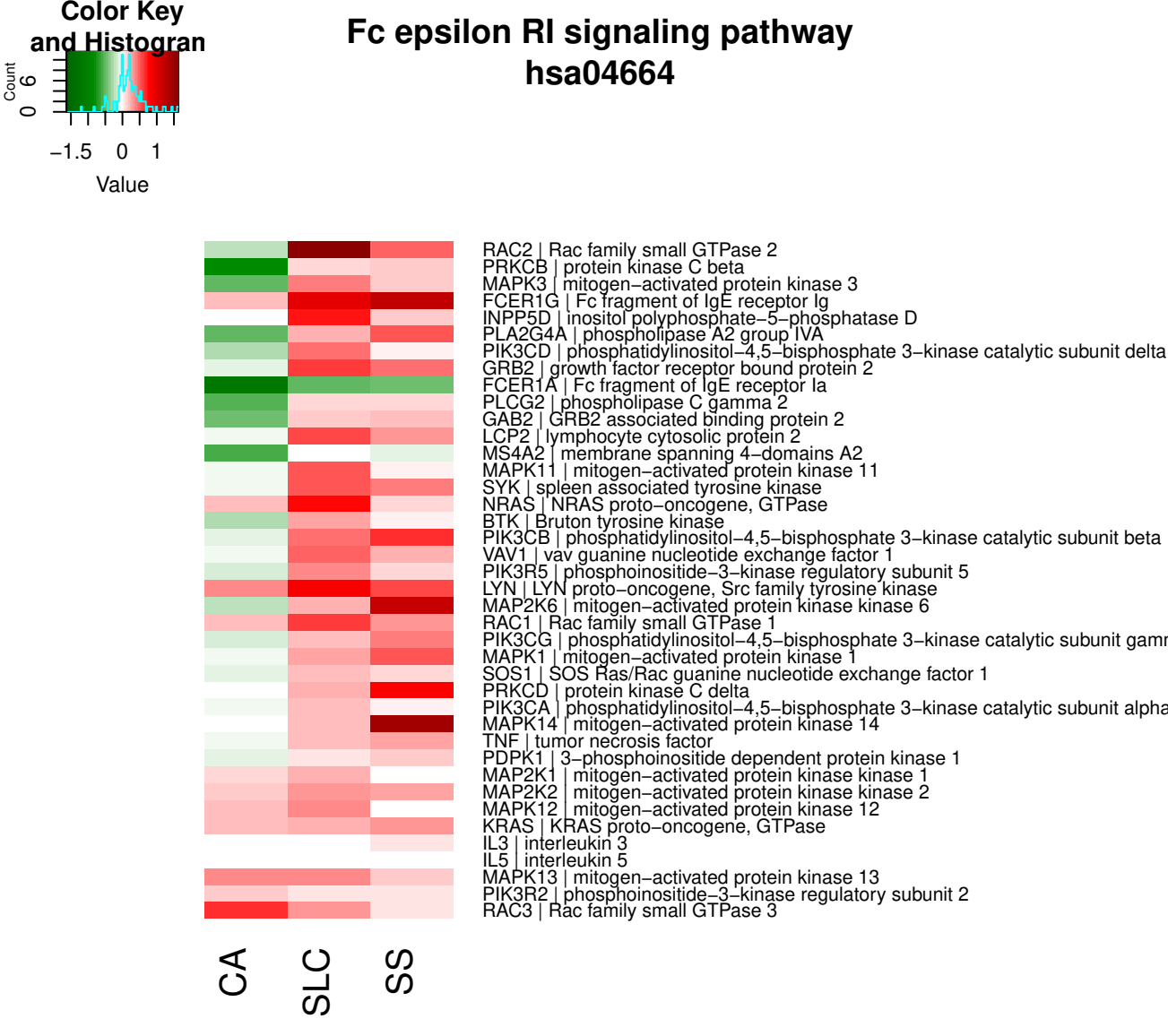

Immune system

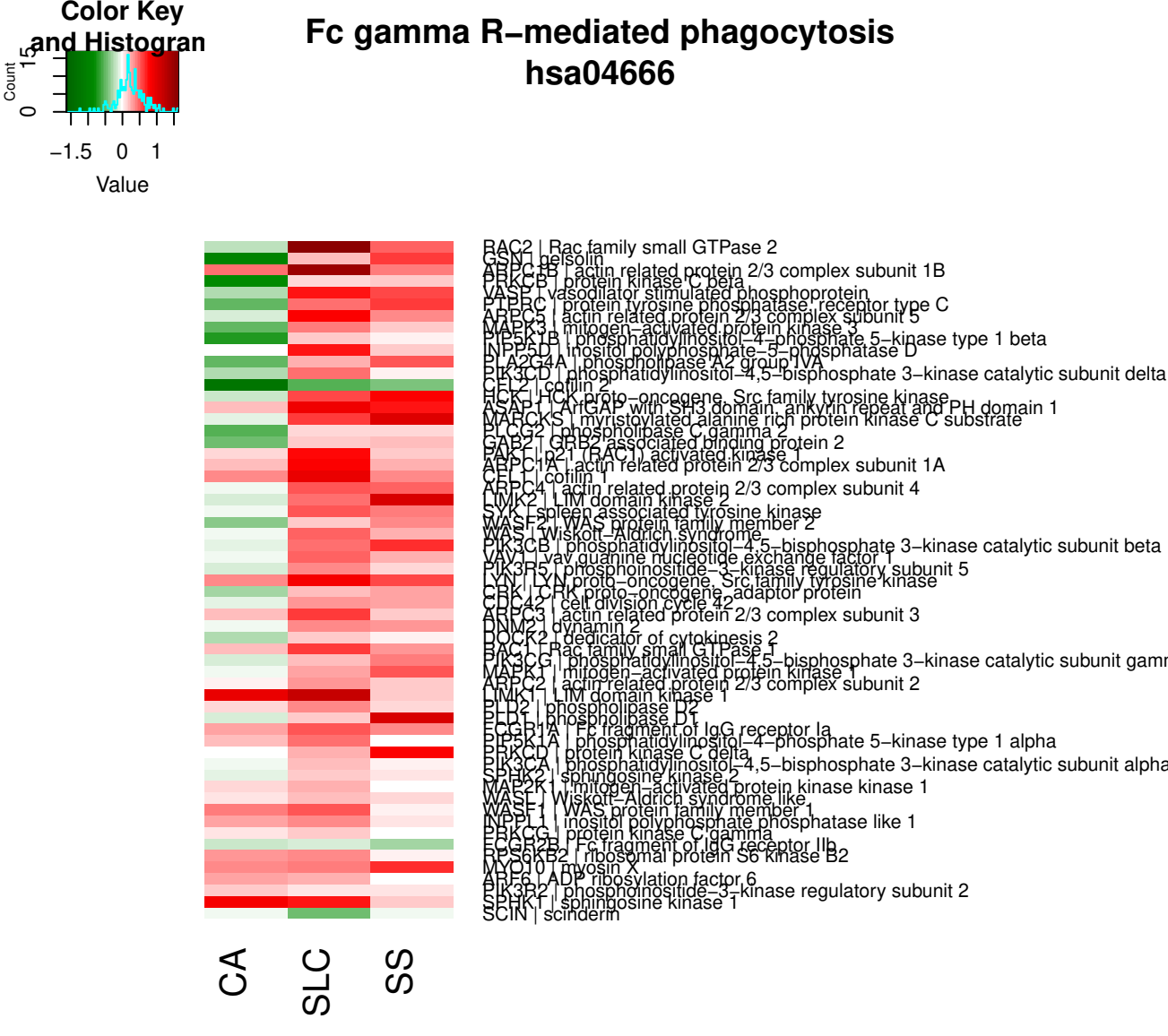

Immune system

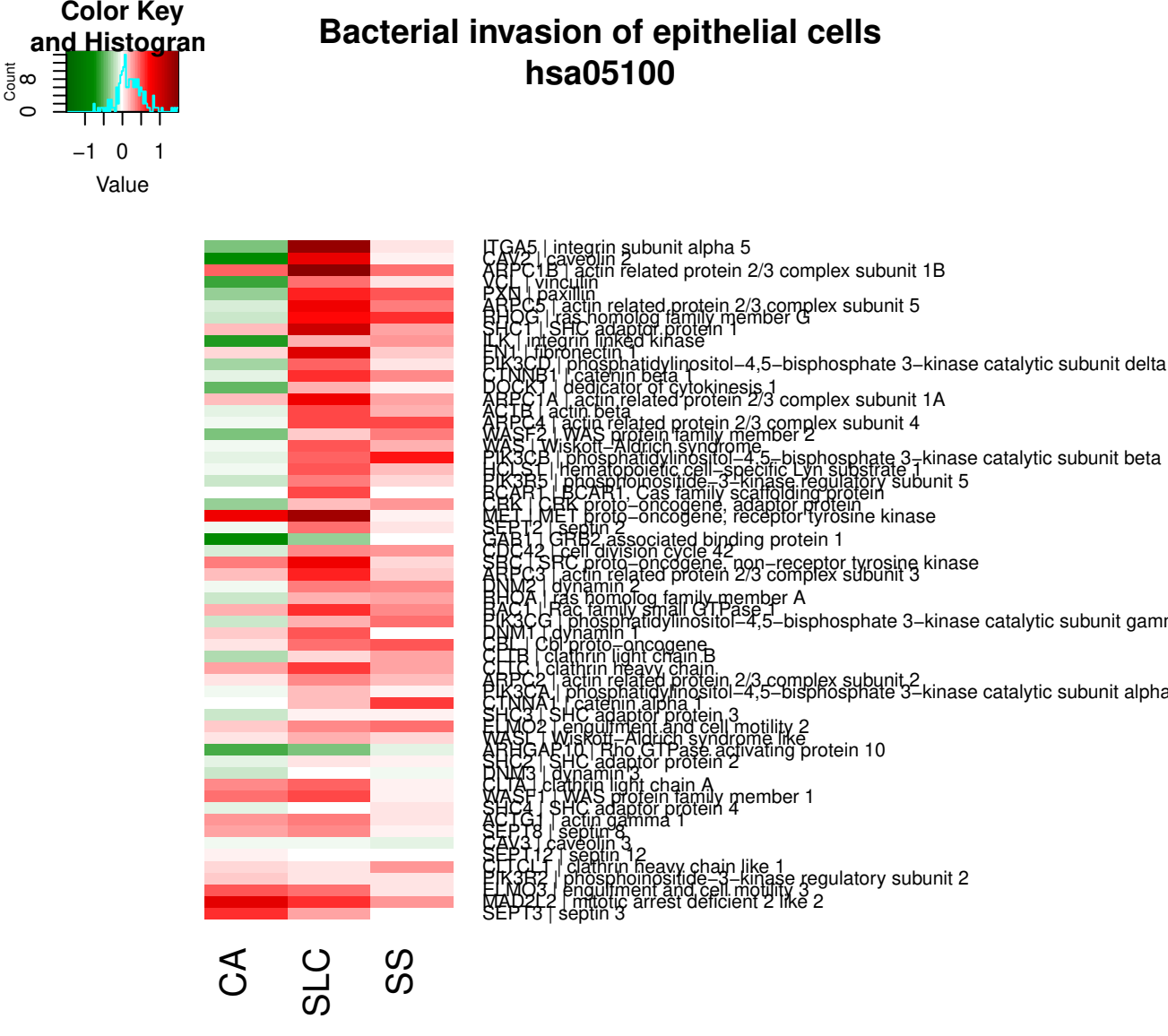
Color Key
and Histogram
Count
0
8
−1
0
1
Value
Bacterial invasion of epithelial cells
hsa05100
ITGA5 | integrin subunit alpha 5
CAV2 | caveolin 2
ARPC1B | actin related protein 2/3 complex subunit 1B
VCL | vinculin
PXN | paxillin
ARPC5 | actin related protein 2/3 complex subunit 5
RHOG | ras homolog family member G
SHC1 | SHC adaptor protein 1
ILK | integrin linked kinase
FN1 | fibronectin 1
PIK3CD | phosphatidylinositol−4,5−bisphosphate 3−kinase catalytic subunit delta
CTNNB1 | catenin beta 1
DOCK1 | dedicator of cytokinesis 1
ARPC1A | actin related protein 2/3 complex subunit 1A
ACTB | actin beta
ARPC4 | actin related protein 2/3 complex subunit 4
WASF2 | WAS protein family member 2
WAS | Wiskott−Aldrich syndrome
PIK3CB | phosphatidylinositol−4,5−bisphosphate 3−kinase catalytic subunit beta
HCLS1 | hematopoietic cell−specific Lyn substrate 1
PIK3R5 | phosphoinositide−3−kinase regulatory subunit 5
BCAR1 | BCAR1, Cas family scaffolding protein
CRK | CRK proto−oncogene, adaptor protein
MET | MET proto−oncogene, receptor tyrosine kinase
SEPT2 | septin 2
GAB1 | GRB2 associated binding protein 1
CDC42 | cell division cycle 42
SRC | SRC proto−oncogene, non−receptor tyrosine kinase
ARPC3 | actin related protein 2/3 complex subunit 3
DNM2 | dynamin 2
RHOA | ras homolog family member A
RAC1 | Rac family small GTPase 1
PIK3CG | phosphatidylinositol−4,5−bisphosphate 3−kinase catalytic subunit gamma
DNM1 | dynamin 1
CBL | Cbl proto−oncogene
CLTB | clathrin light chain B
CLTC | clathrin heavy chain
ARPC2 | actin related protein 2/3 complex subunit 2
PIK3CA | phosphatidylinositol−4,5−bisphosphate 3−kinase catalytic subunit alpha
CTNNA1 | catenin alpha 1
SHC3 | SHC adaptor protein 3
ELMO2 | engulfment and cell motility 2
WASL | Wiskott−Aldrich syndrome like
ARHGAP10 | Rho GTPase activating protein 10
SHC2 | SHC adaptor protein 2
DNM3 | dynamin 3
CLTA | clathrin light chain A
WASF1 | WAS protein family member 1
SHC4 | SHC adaptor protein 4
ACTG1 | actin gamma 1
SEPT8 | septin 8
CAV3 | caveolin 3
SEPT12 | septin 12
CLTCL1 | clathrin heavy chain like 1
PIK3R2 | phosphoinositide−3−kinase regulatory subunit 2
ELMO3 | engulfment and cell motility 3
MAD2L2 | mitotic arrest deficient 2 like 2
SEPT3 | septin 3
CA
SLC
SS
Infectious disease

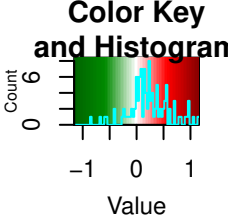

Vibrio cholerae infection
hsa05110

PRKCB | protein kinase C beta
ADCY3 | adenylate cyclase 3
KCNQ1 | potassium voltage−gated channel subfamily Q member 1
PLCG2 | phospholipase C gamma 2
ACTB | actin beta
TCIRG1 | T−cell immune regulator 1, ATPase H+ transporting V0 subunit a3
ATP6V1C1 | ATPase H+ transporting V1 subunit C1
SEC61G | Sec61 translocon gamma subunit
ATP6V1E1 | ATPase H+ transporting V1 subunit E1
KDELR1 | KDEL endoplasmic reticulum protein retention receptor 1
CFTR | cystic fibrosis transmembrane conductance regulator
ATP6V0A1 | ATPase H+ transporting V0 subunit a1
ATP6V0B | ATPase H+ transporting V0 subunit b
ATP6V0E1 | ATPase H+ transporting V0 subunit e1
TJP2 | tight junction protein 2
ATP6V1B2 | ATPase H+ transporting V1 subunit B2
ATP6V0D1 | ATPase H+ transporting V0 subunit d1
ATP6AP1 | ATPase H+ transporting accessory protein 1
ATP6V0C | ATPase H+ transporting V0 subunit c
ARF1 | ADP ribosylation factor 1
KDELR3 | KDEL endoplasmic reticulum protein retention receptor 3
PRKACB | protein kinase cAMP−activated catalytic subunit beta
KDELR2 | KDEL endoplasmic reticulum protein retention receptor 2
SEC61A1 | Sec61 translocon alpha 1 subunit
ATP6V1A | ATPase H+ transporting V1 subunit A
ATP6V1H | ATPase H+ transporting V1 subunit H
ACTG1 | actin gamma 1
PRKCG | protein kinase C gamma
ATP6V1B1 | ATPase H+ transporting V1 subunit B1
PRKACG | protein kinase cAMP−activated catalytic subunit gamma
ATP6V1F | ATPase H+ transporting V1 subunit F
SEC61A2 | Sec61 translocon alpha 2 subunit
ERO1A | endoplasmic reticulum oxidoreductase 1 alpha
ATP6V1C2 | ATPase H+ transporting V1 subunit C2
ATP6V0E2 | ATPase H+ transporting V0 subunit e2

Infectious disease

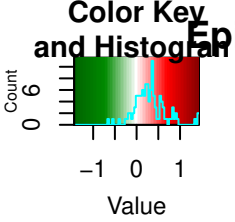

Epithelial cell signaling in Helicobacter pylori infection
hsa05120

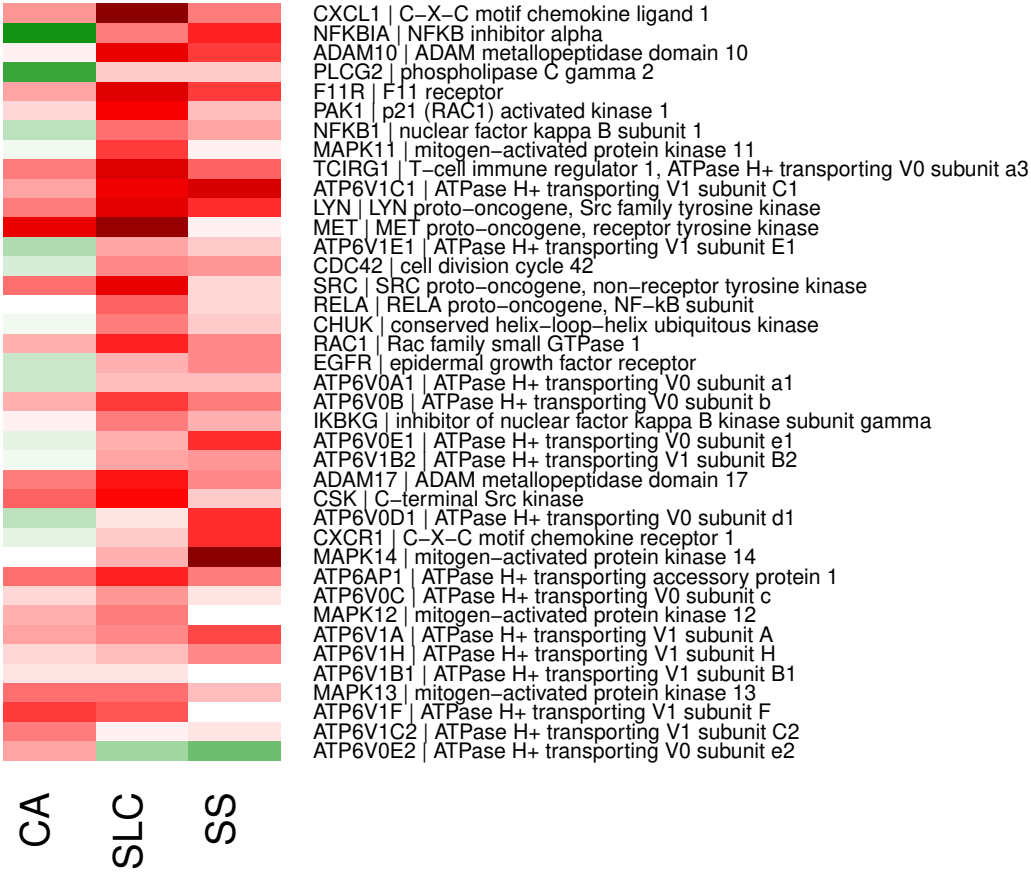

Infectious disease

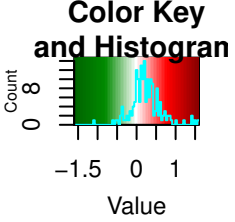

Salmonella infection
hsa05132

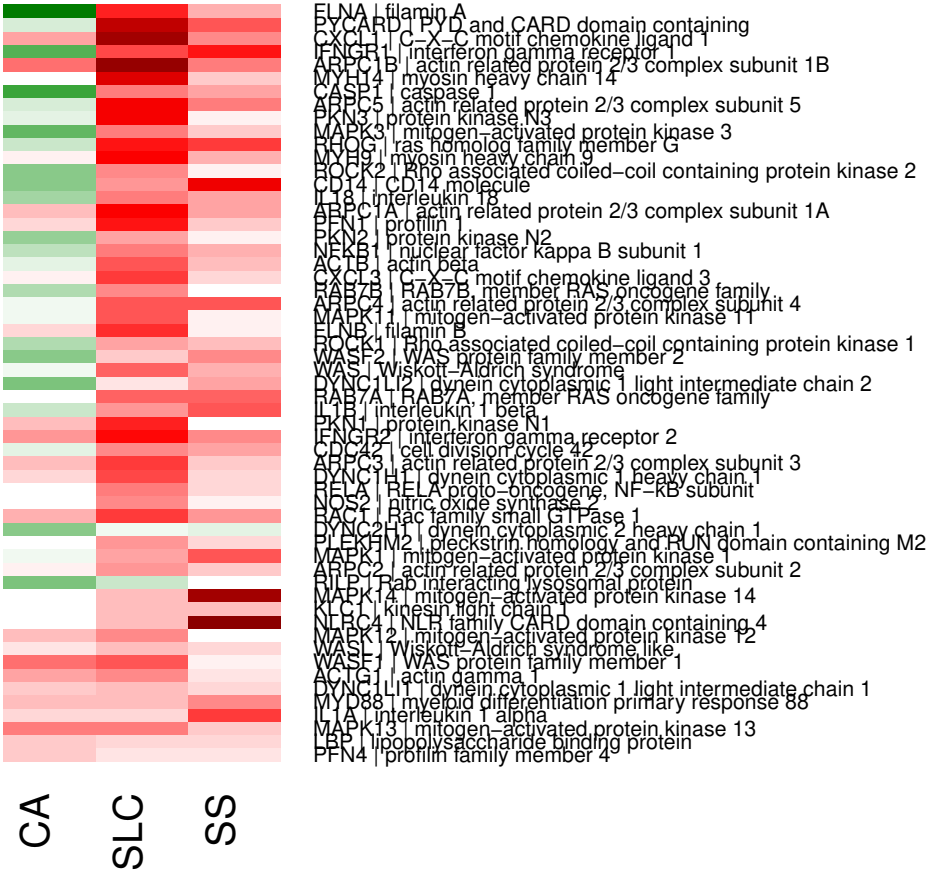

Infectious disease

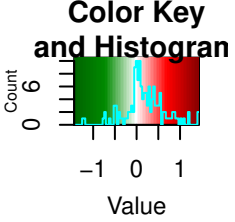

Pertussis
hsa05133

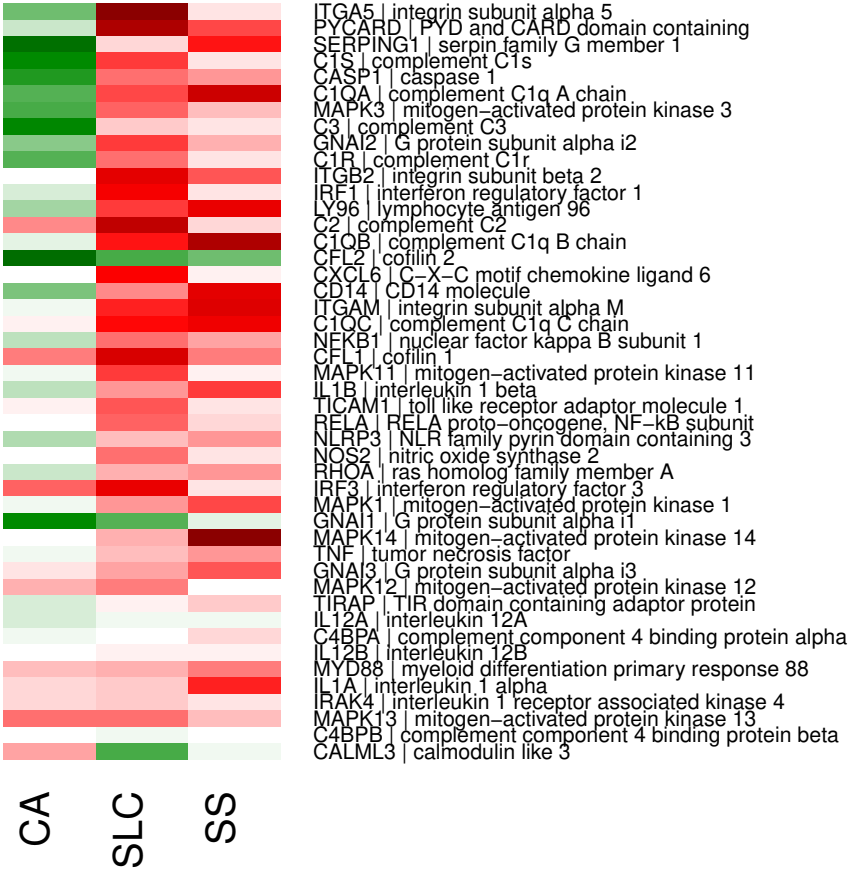

Infectious disease

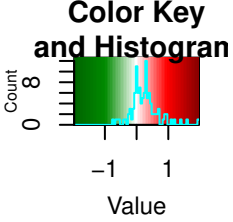

Legionellosis
hsa05134

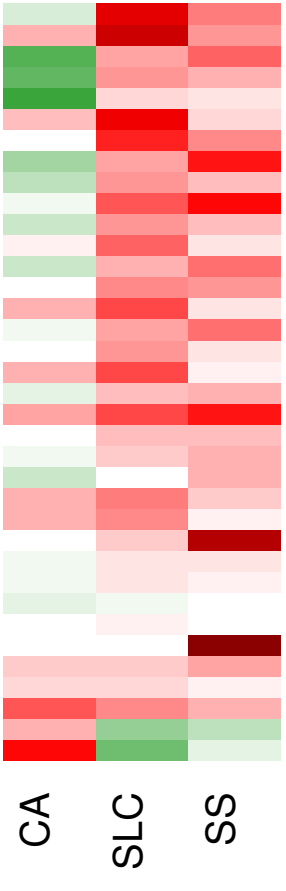

PYCARD | PYD and CARD domain containing
CXCL1 | C−X−C motif chemokine ligand 1
NFKBIA | NFKB inhibitor alpha
CASP1 | caspase 1
C3 | complement C3
NFKB2 | nuclear factor kappa B subunit 2
ITGB2 | integrin subunit beta 2
CD14 | CD14 molecule
IL18 | interleukin 18
ITGAM | integrin subunit alpha M
NFKB1 | nuclear factor kappa B subunit 1
CXCL3 | C−X−C motif chemokine ligand 3
IL1B | interleukin 1 beta
APAF1 | apoptotic peptidase activating factor 1
CASP8 | caspase 8
RAB1A | RAB1A, member RAS oncogene family
RELA | RELA proto−oncogene, NF−kB subunit
HSF1 | heat shock transcription factor 1
SAR1A | secretion associated Ras related GTPase 1A
TLR2 | toll like receptor 2
RAB1B | RAB1B, member RAS oncogene family
TNF | tumor necrosis factor
HSPA1L | heat shock protein family A (Hsp70) member 1 like
VCP | valosin containing protein
ARF1 | ADP ribosylation factor 1
NLRC4 | NLR family CARD domain containing 4
SEC22B | SEC22 homolog B, vesicle trafficking protein (gene/pseudogene)
BCL2L13 | BCL2 like 13
IL12A | interleukin 12A
IL12B | interleukin 12B
NAIP | NLR family apoptosis inhibitory protein
MYD88 | myeloid differentiation primary response 88
HBS1L | HBS1 like translational GTPase
HSPA6 | heat shock protein family A (Hsp70) member 6
BNIP3 | BCL2 interacting protein 3
EEF1A2 | eukaryotic translation elongation factor 1 alpha 2

Infectious disease

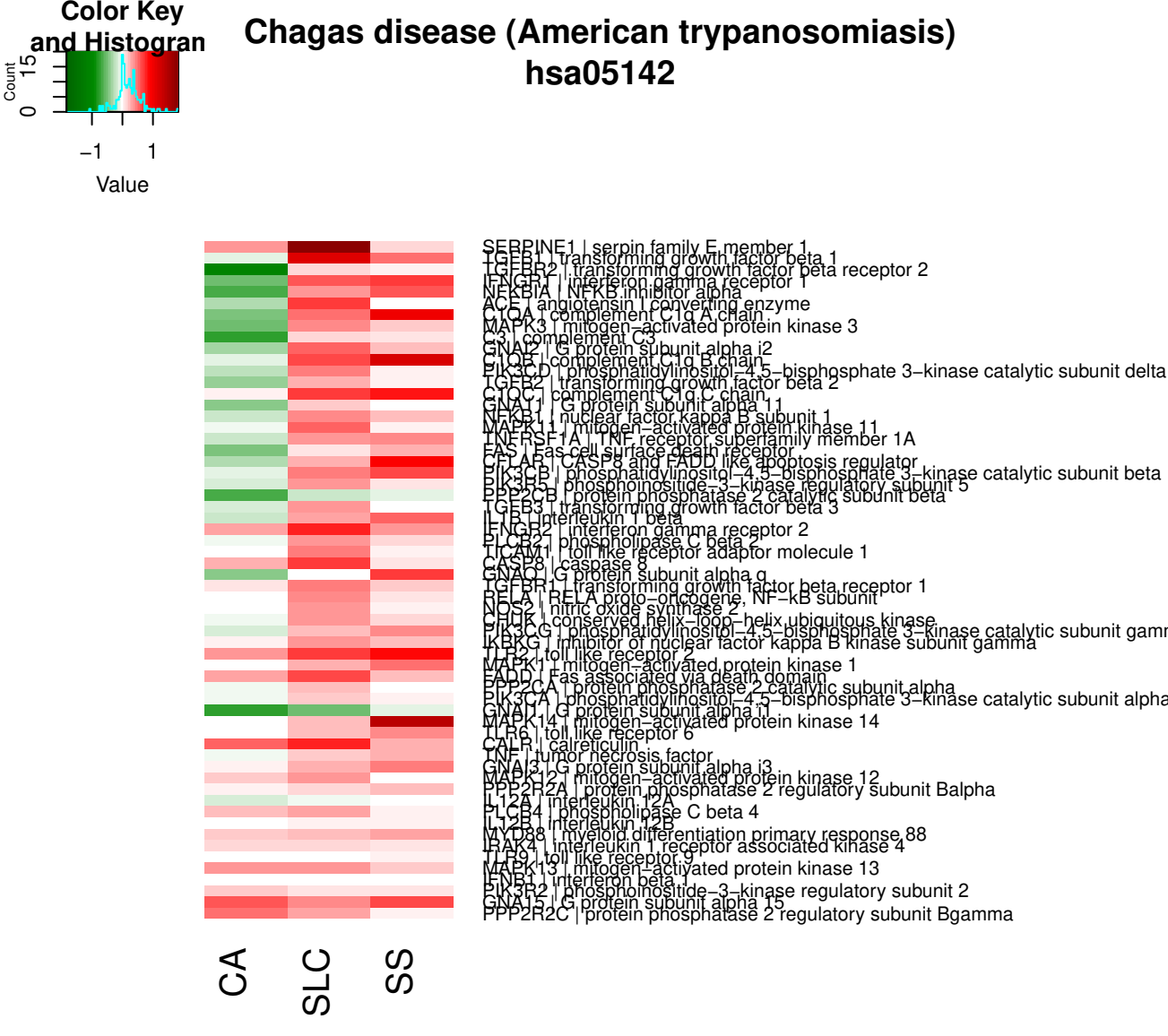
Color Key and Histogram
Count
15
0
−1
1
Value
Chagas disease (American trypanosomiasis)
hsa05142
SERPINE1 | serpin family E member 1
TGFB1 | transforming growth factor beta 1
TGFBR2 | transforming growth factor beta receptor 2
IFNGR1 | interferon gamma receptor 1
NFKBIA | NFKB inhibitor alpha
ACE | angiotensin I converting enzyme
C1QA | complement C1q A chain
MAPK3 | mitogen−activated protein kinase 3
C3 | complement C3
GNAI2 | G protein subunit alpha i2
C1QB | complement C1q B chain
PIK3CD | phosphatidylinositol−4,5−bisphosphate 3−kinase catalytic subunit delta
TGFB2 | transforming growth factor beta 2
C1QC | complement C1q C chain
GNAI1 | G protein subunit alpha i1
NFKB1 | nuclear factor kappa B subunit 1
MAPK11 | mitogen−activated protein kinase 11
TNFRSF1A | TNF receptor superfamily member 1A
FAS | Fas cell surface death receptor
CFLAR | CASP8 and FADD like apoptosis regulator
PIK3CB | phosphatidylinositol−4,5−bisphosphate 3−kinase catalytic subunit beta
PIK3R5 | phosphoinositide−3−kinase regulatory subunit 5
PPP2CB | protein phosphatase 2 catalytic subunit beta
TGFB3 | transforming growth factor beta 3
IL1B | interleukin 1 beta
IFNGR2 | interferon gamma receptor 2
PLCB2 | phospholipase C beta 2
TICAM1 | toll like receptor adaptor molecule 1
CASP8 | caspase 8
GNAQ | G protein subunit alpha q
TGFBR1 | transforming growth factor beta receptor 1
RELA | RELA proto−oncogene, NF−kB subunit
NOS2 | nitric oxide synthase 2
CHUK | conserved helix−loop−helix ubiquitous kinase
PIK3CG | phosphatidylinositol−4,5−bisphosphate 3−kinase catalytic subunit gamma
IKBKG | inhibitor of nuclear factor kappa B kinase subunit gamma
TLR2 | toll like receptor 2
MAPK1 | mitogen−activated protein kinase 1
FADD | Fas associated via death domain
PPP2CA | protein phosphatase 2 catalytic subunit alpha
PIK3CA | phosphatidylinositol−4,5−bisphosphate 3−kinase catalytic subunit alpha
GNAI1 | G protein subunit alpha i1
MAPK14 | mitogen−activated protein kinase 14
TLR6 | toll like receptor 6
CALR | calreticulin
TNF | tumor necrosis factor
GNAI3 | G protein subunit alpha i3
MAPK12 | mitogen−activated protein kinase 12
PPP2R2A | protein phosphatase 2 regulatory subunit Balpha
IL12A | interleukin 12A
PLCB4 | phospholipase C beta 4
IL12B | interleukin 12B
MYD88 | myeloid differentiation primary response 88
IRAK4 | interleukin 1 receptor associated kinase 4
TLR9 | toll like receptor 9
MAPK13 | mitogen−activated protein kinase 13
IFNB1 | interferon beta 1
PIK3R2 | phosphoinositide−3−kinase regulatory subunit 2
GNA15 | G protein subunit alpha 15
PPP2R2C | protein phosphatase 2 regulatory subunit Bgamma
CA
SLC
SS
Infectious disease

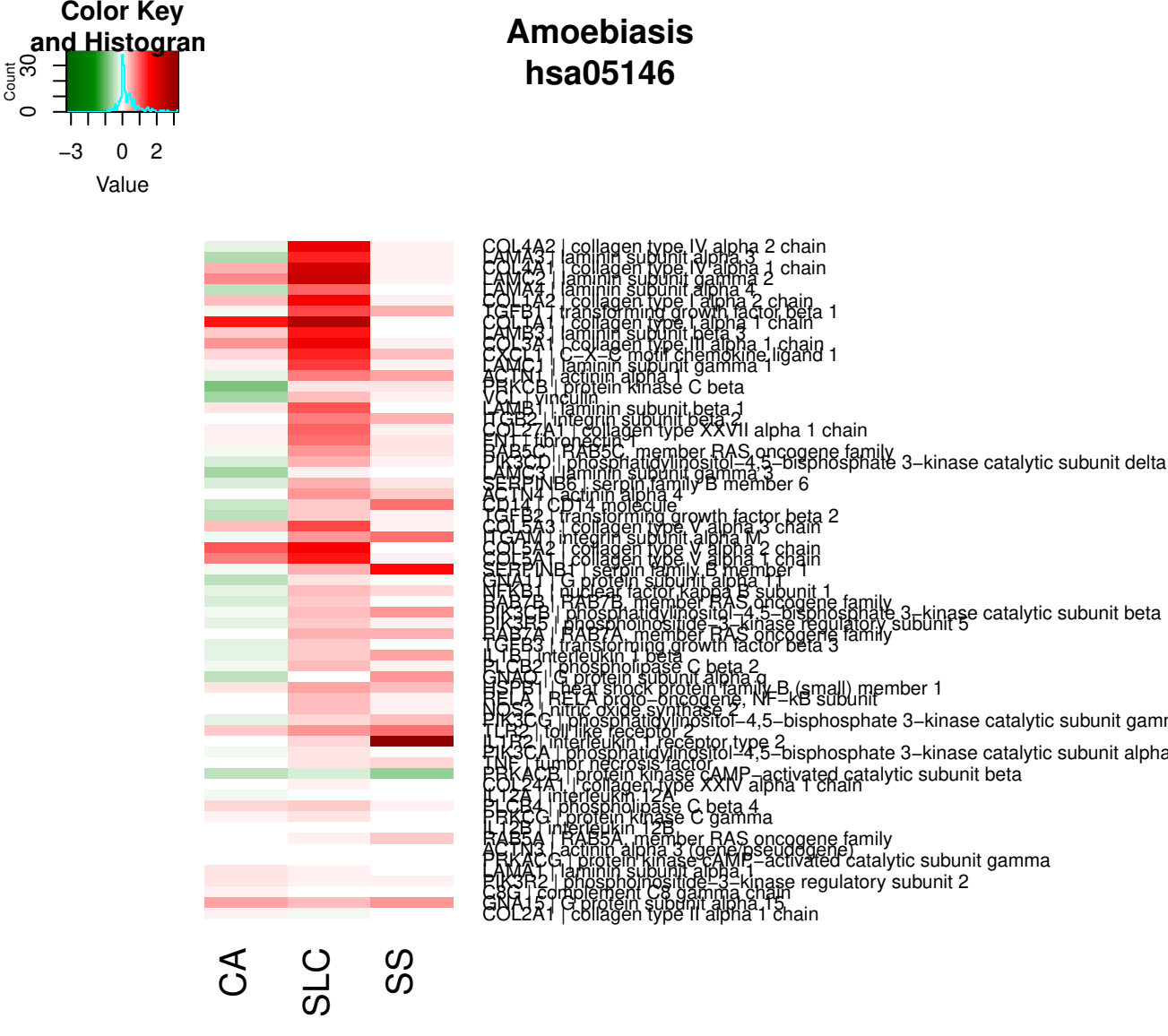

Infectious disease

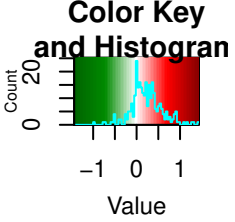

Tuberculosis
hsa05152

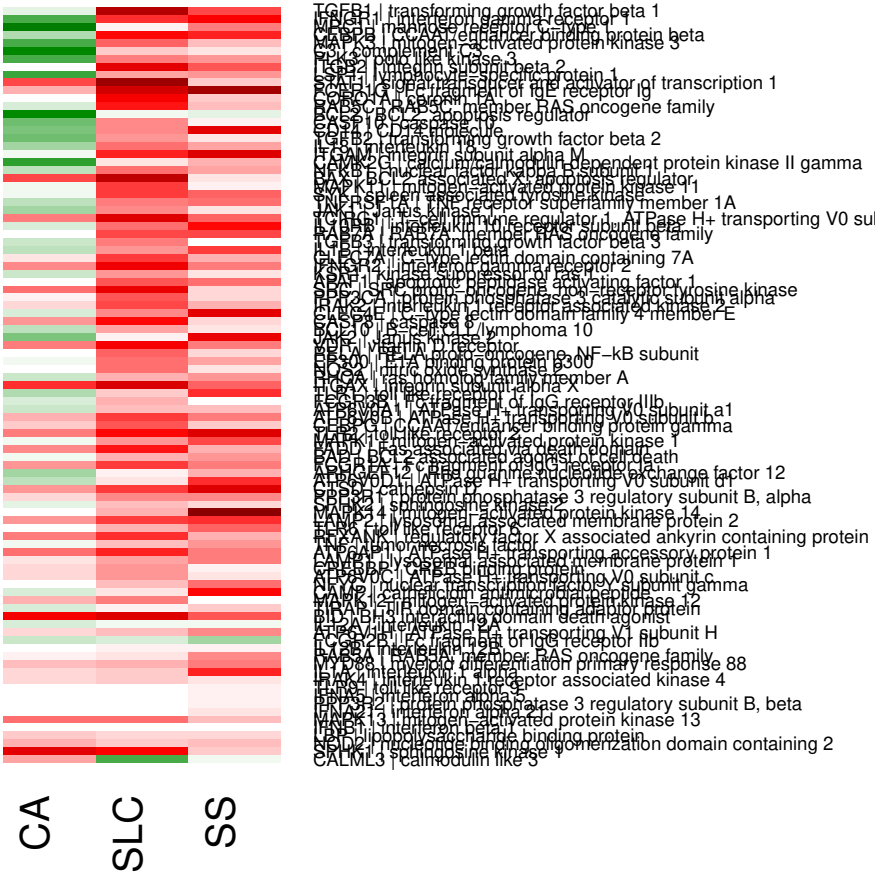

Infectious disease

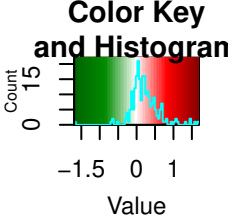

Hepatitis C
hsa05160

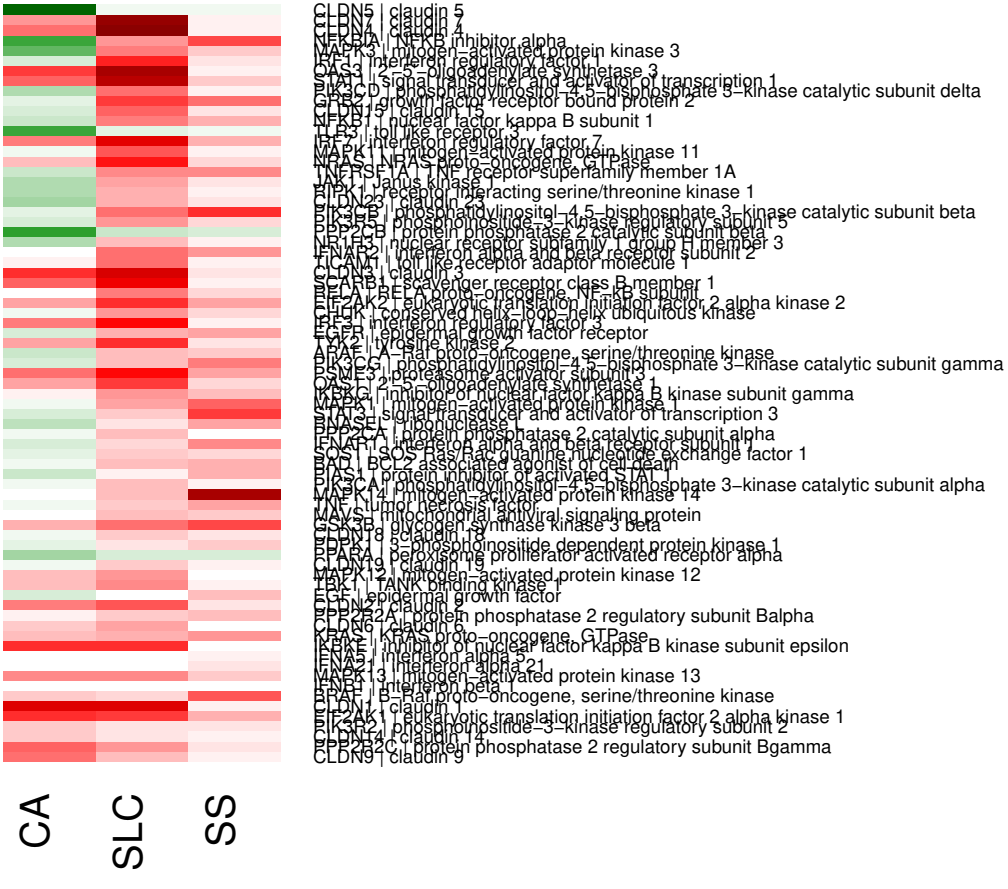

Infectious disease

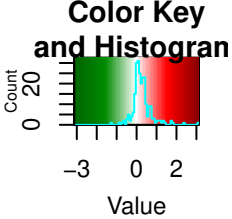

Hepatitis B
hsa05161

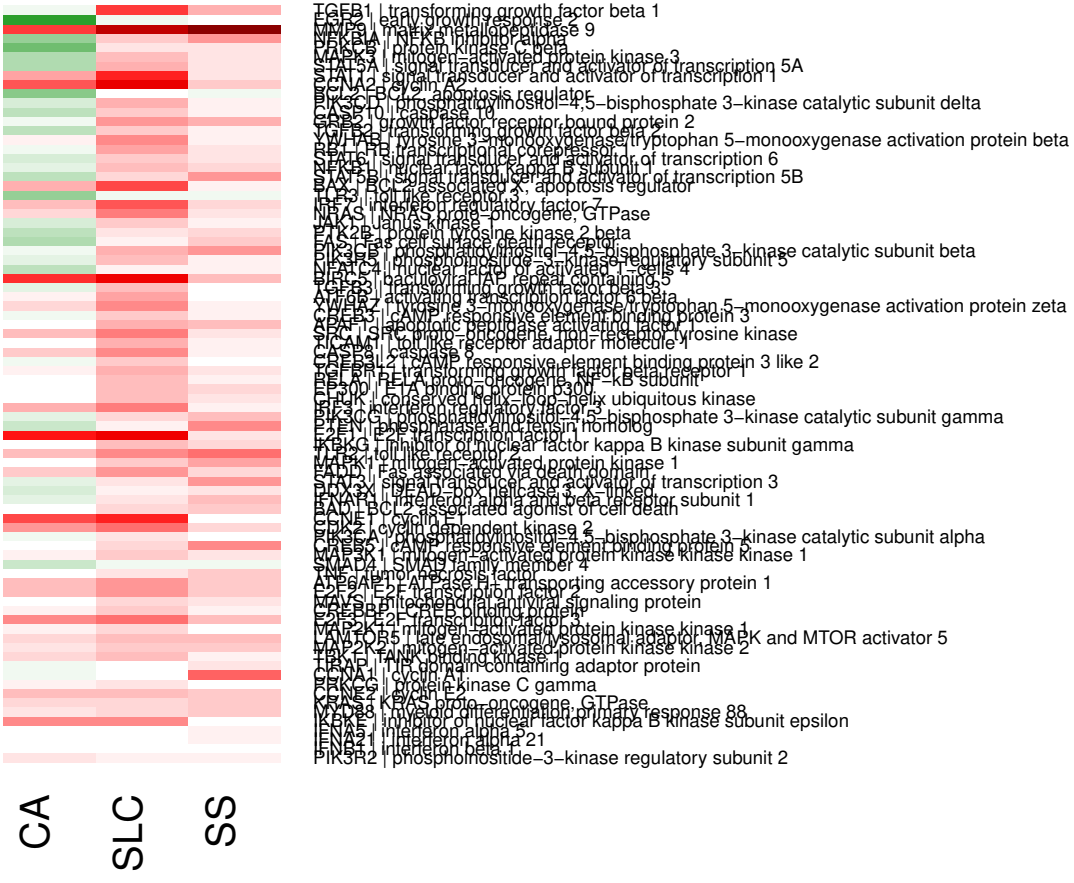

Infectious disease

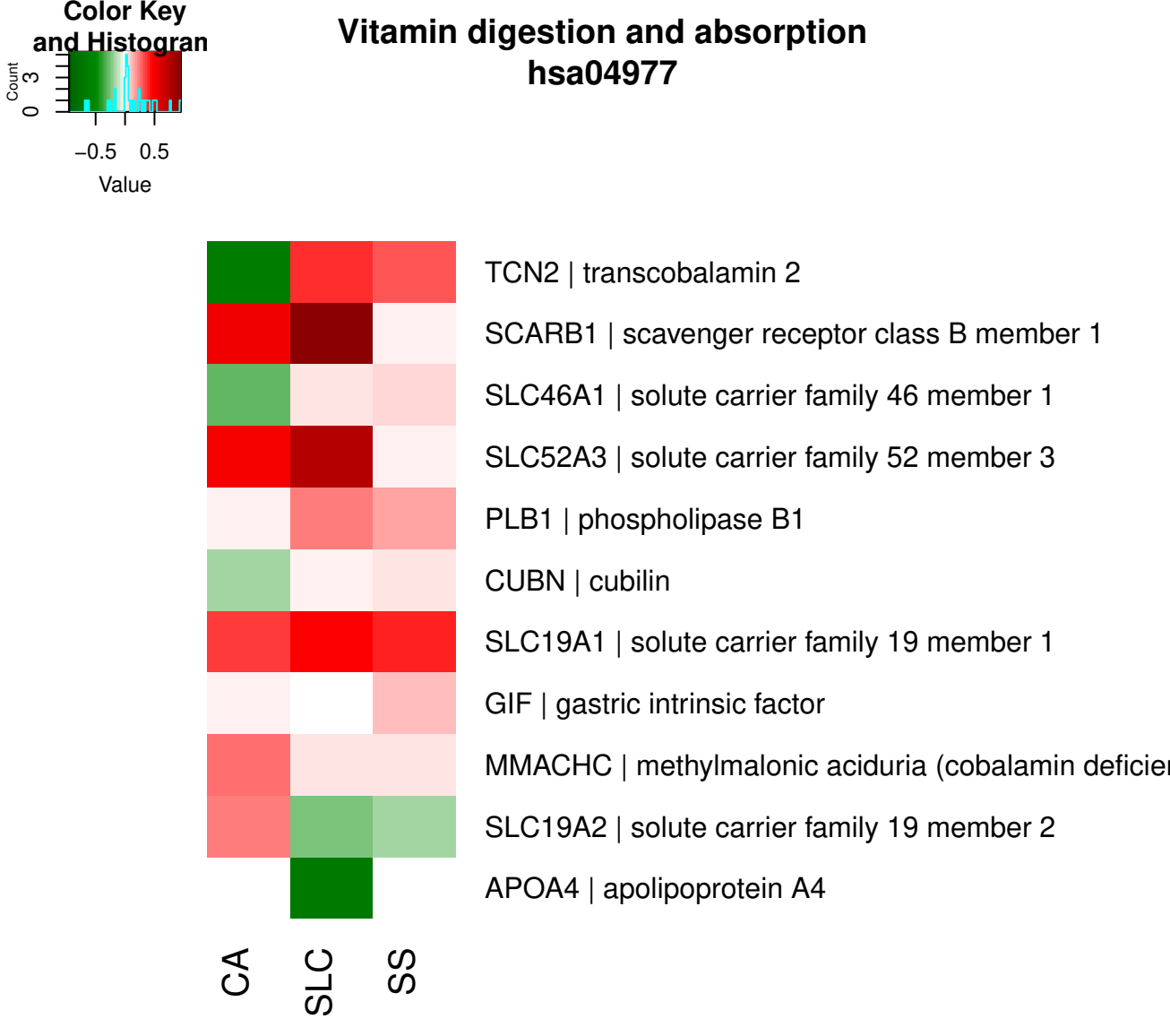
Color Key
and Histogram
Count
0
3
−0.5
0.5
Value
Vitamin digestion and absorption
hsa04977
TCN2 | transcobalamin 2
SCARB1 | scavenger receptor class B member 1
SLC46A1 | solute carrier family 46 member 1
SLC52A3 | solute carrier family 52 member 3
PLB1 | phospholipase B1
CUBN | cubilin
SLC19A1 | solute carrier family 19 member 1
GIF | gastric intrinsic factor
MMACHC | methylmalonic aciduria (cobalamin deficien
SLC19A2 | solute carrier family 19 member 2
APOA4 | apolipoprotein A4
CA
SLC
SS

Other

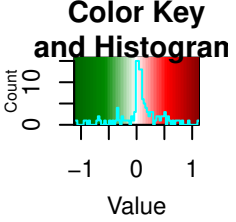

Morphine addiction
hsa05032

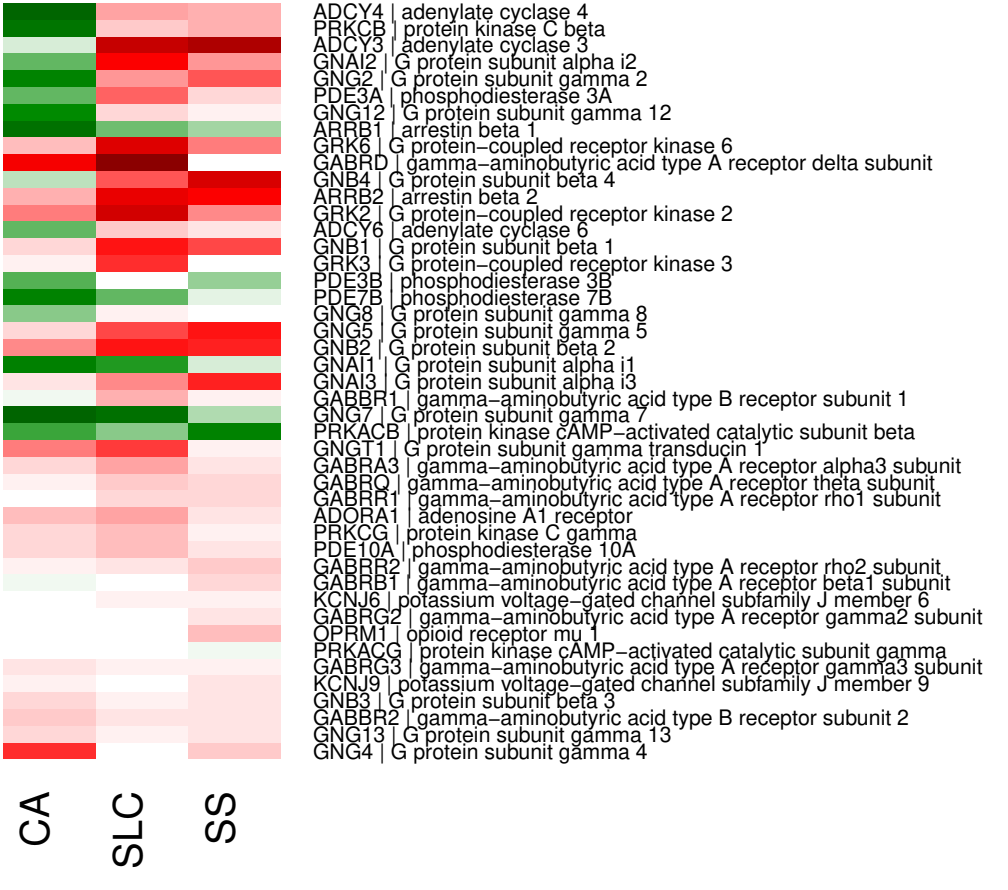

Other

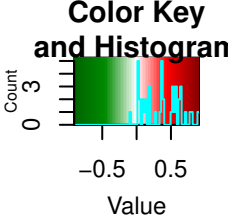

Ribosome biogenesis in eukaryotes
hsa03008

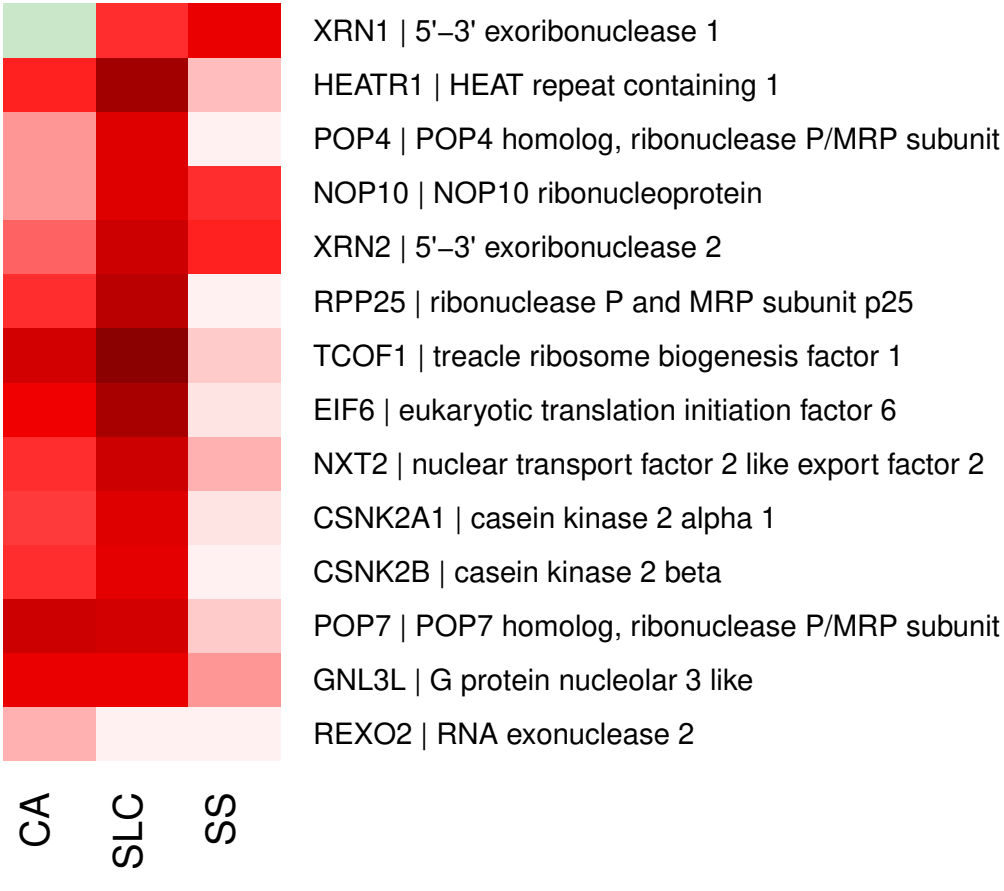

Other

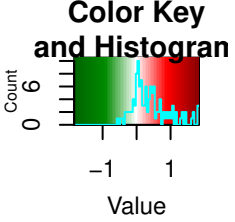

p53 signaling pathway
hsa04115

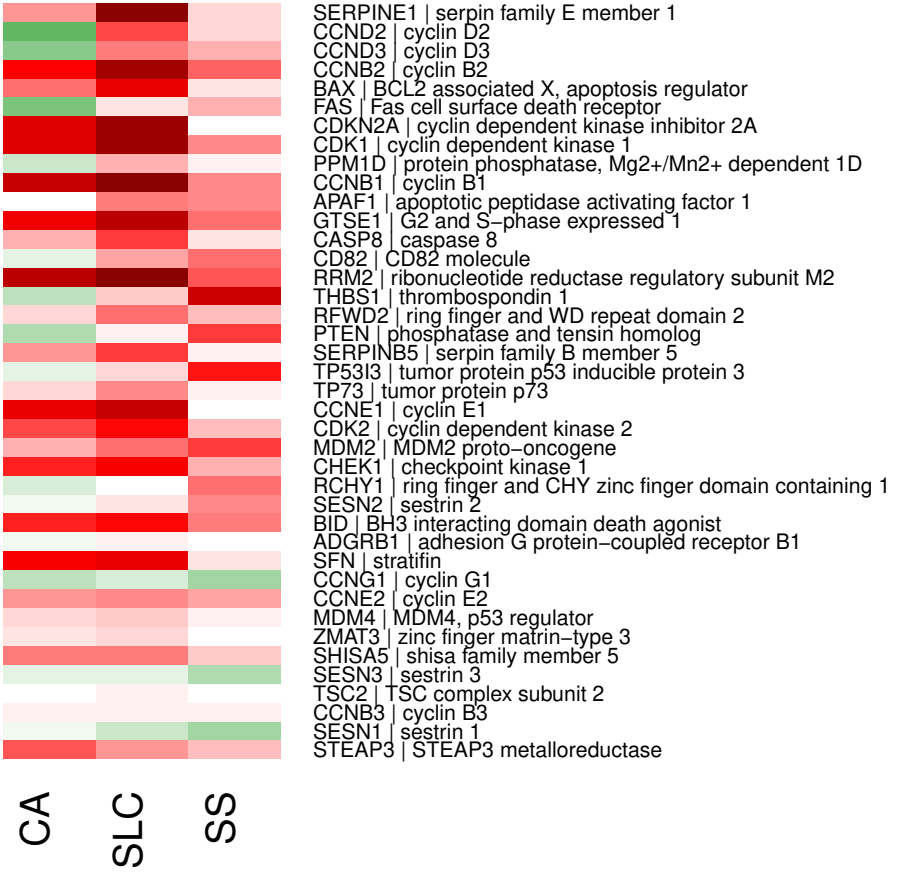

Other

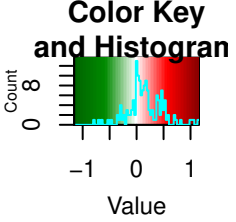

Glycerophospholipid metabolism
hsa00564

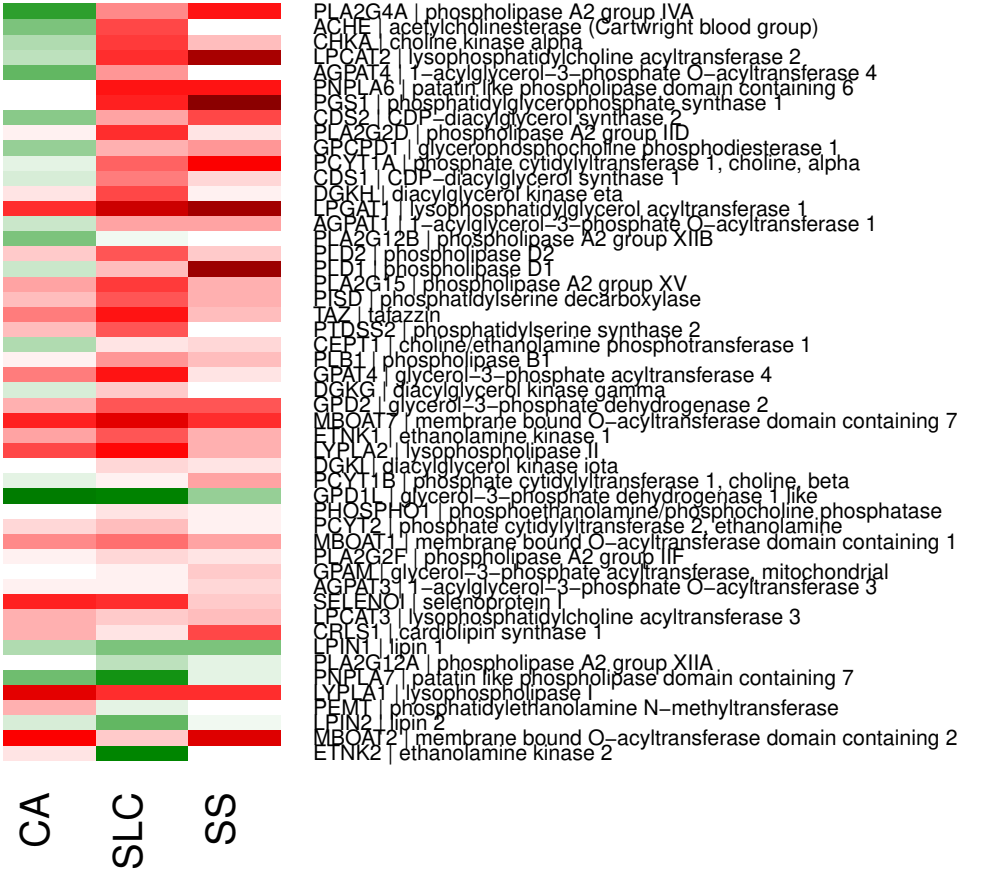

Other

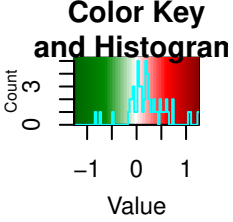

Dorso−ventral axis formation
hsa04320

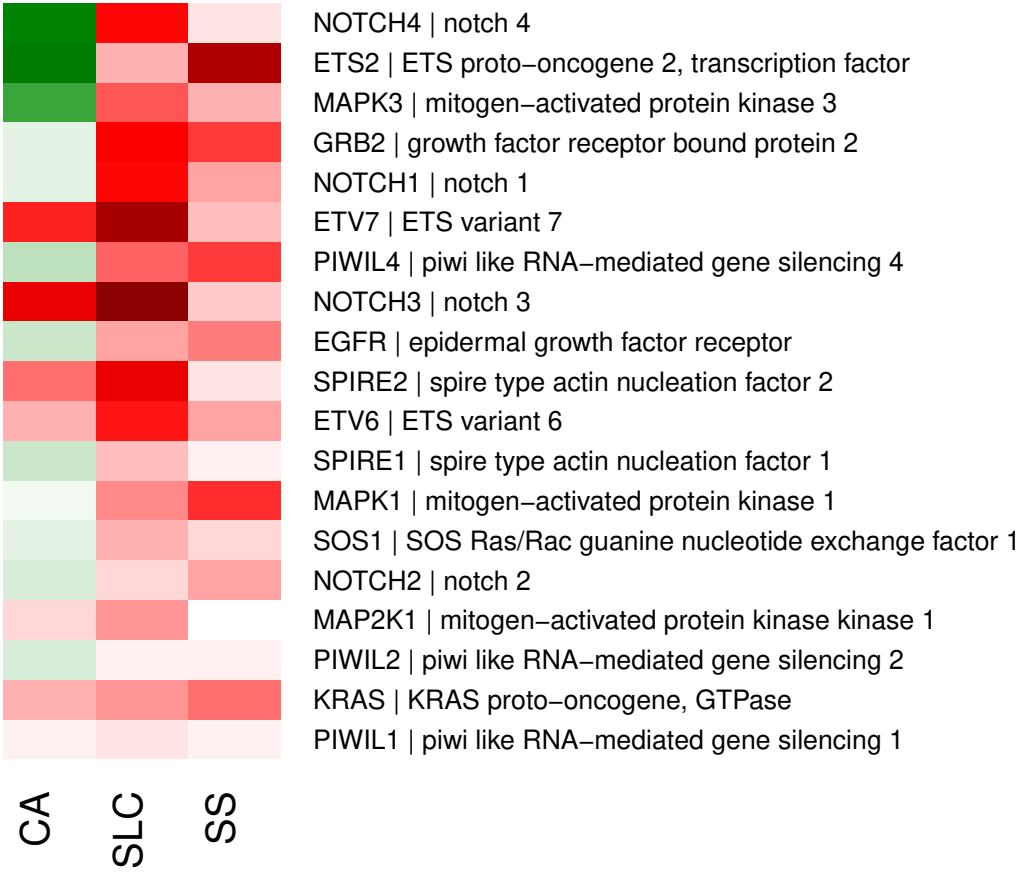

Other

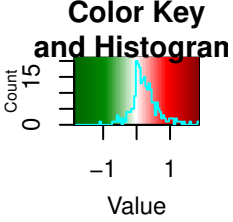

Osteoclast differentiation
hsa04380

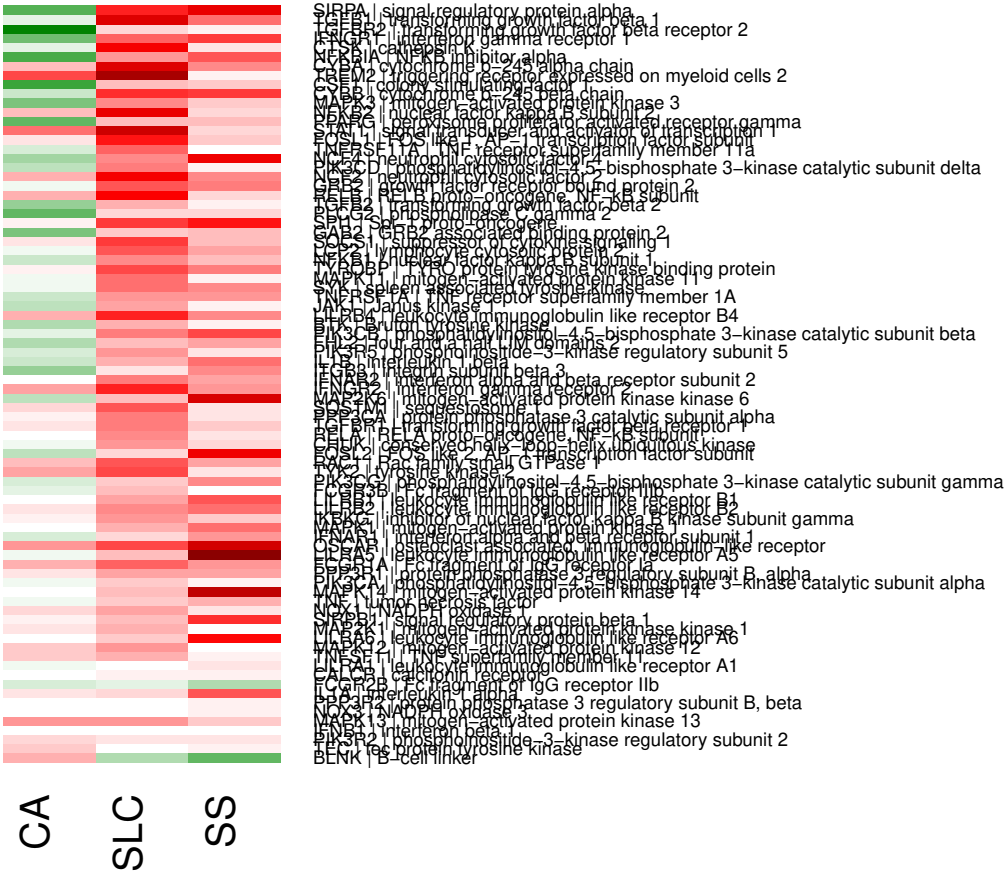

Other

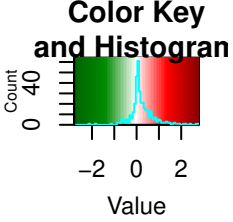

Focal adhesion
hsa04510

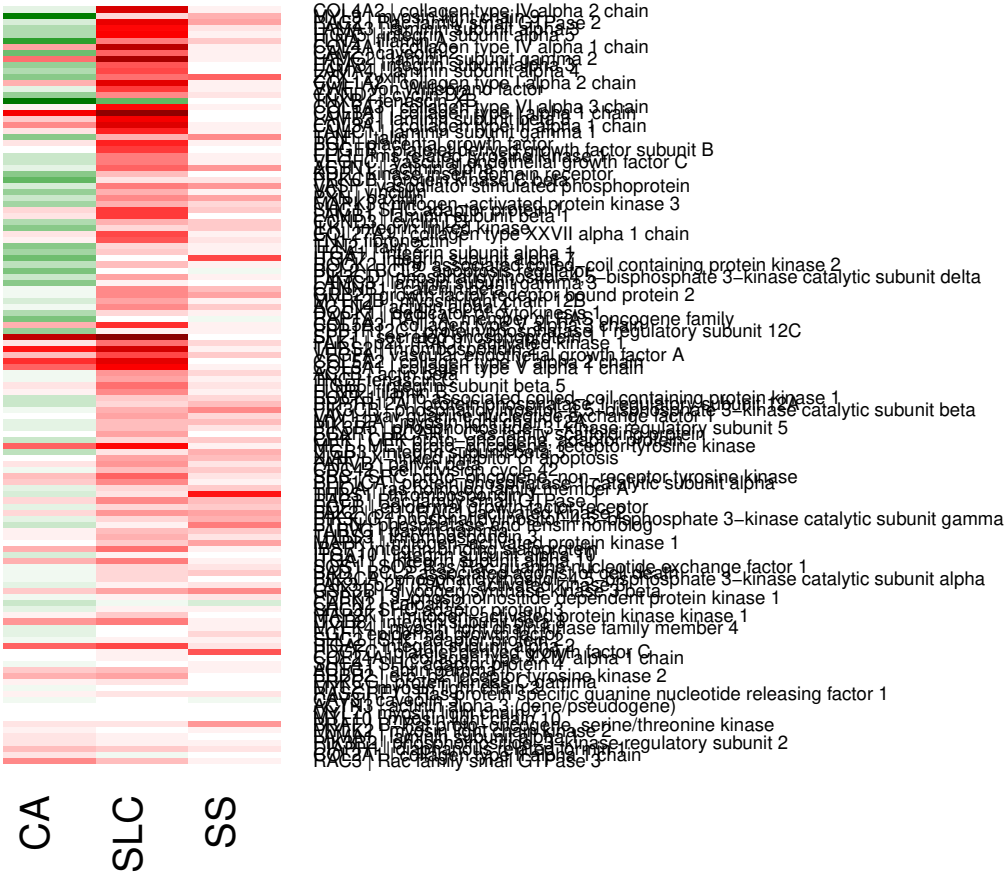

Other

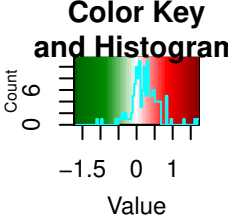

Adherens junction
hsa04520

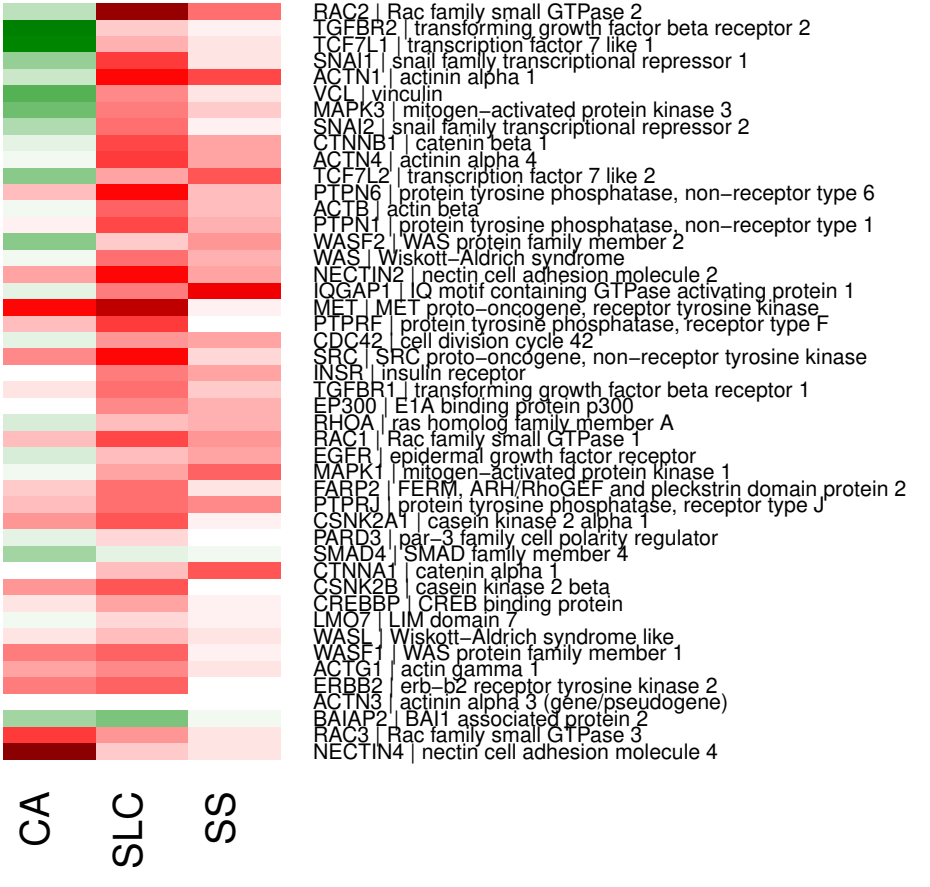

Other

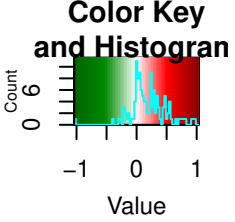

Synaptic vesicle cycle
hsa04721

VAMP2 | vesicle associated membrane protein 2
AP2B1 | adaptor related protein complex 2 beta 1 subunit
TCIRG1 | T−cell immune regulator 1, ATPase H+ transporting V0 subunit a3
ATP6V1C1 | ATPase H+ transporting V1 subunit C1
ATP6V1E1 | ATPase H+ transporting V1 subunit E1
CPLX1 | complexin 1
AP2M1 | adaptor related protein complex 2 mu 1 subunit
DNM2 | dynamin 2
SYT1 | synaptotagmin 1
AP2A2 | adaptor related protein complex 2 alpha 2 subunit
ATP6V0A1 | ATPase H+ transporting V0 subunit a1
ATP6V0B | ATPase H+ transporting V0 subunit b
DNM1 | dynamin 1
CLTB | clathrin light chain B
CLTC | clathrin heavy chain
AP2A1 | adaptor related protein complex 2 alpha 1 subunit
ATP6V0E1 | ATPase H+ transporting V0 subunit e1
ATP6V1B2 | ATPase H+ transporting V1 subunit B2
NAPA | NSF attachment protein alpha
ATP6V0D1 | ATPase H+ transporting V0 subunit d1
STX1A | syntaxin 1A
SNAP25 | synaptosome associated protein 25
AP2S1 | adaptor related protein complex 2 sigma 1 subunit
ATP6V0C | ATPase H+ transporting V0 subunit c
DNM3 | dynamin 3
STX3 | syntaxin 3
CLTA | clathrin light chain A
ATP6V1A | ATPase H+ transporting V1 subunit A
ATP6V1H | ATPase H+ transporting V1 subunit H
SLC18A1 | solute carrier family 18 member A1
STX1B | syntaxin 1B
ATP6V1B1 | ATPase H+ transporting V1 subunit B1
SLC17A6 | solute carrier family 17 member 6
NSF | N−ethylmaleimide sensitive factor, vesicle fusing ATPase
RIMS1 | regulating synaptic membrane exocytosis 1
CLTCL1 | clathrin heavy chain like 1
ATP6V1F | ATPase H+ transporting V1 subunit F
UNC13A | unc−13 homolog A
SLC18A3 | solute carrier family 18 member A3
ATP6V1C2 | ATPase H+ transporting V1 subunit C2
ATP6V0E2 | ATPase H+ transporting V0 subunit e2

Other

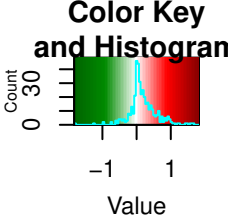

Regulation of actin cytoskeleton
hsa04810

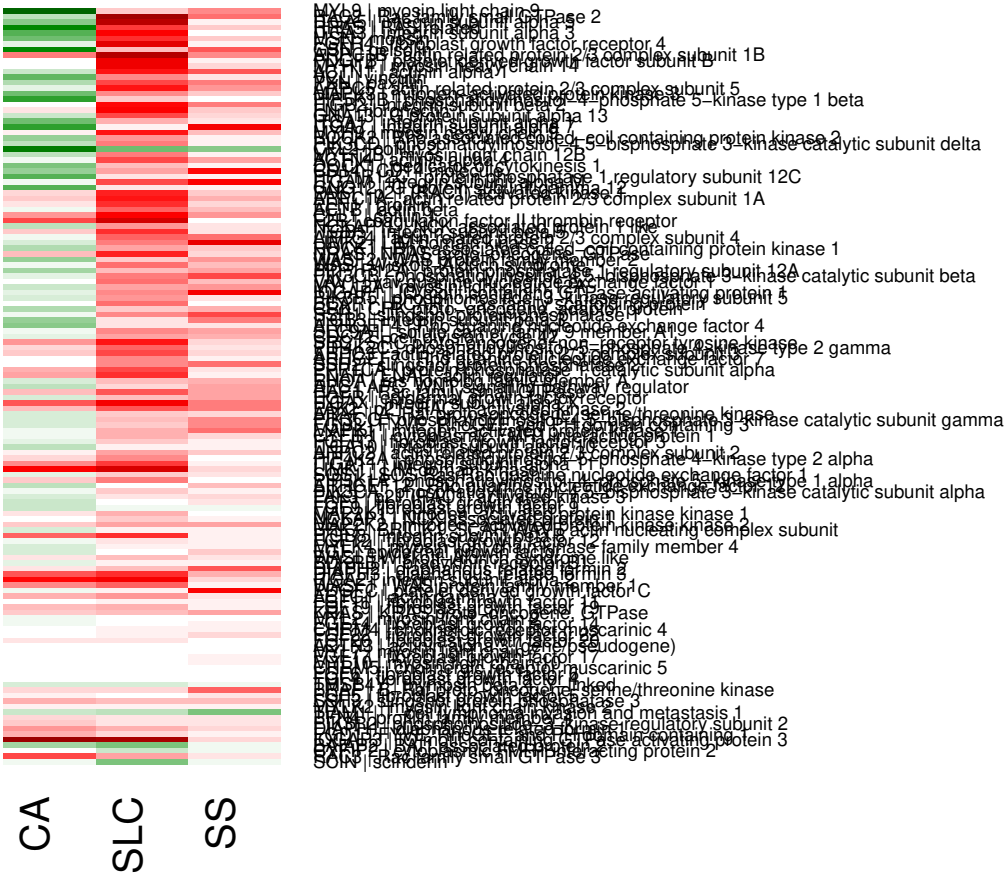

Other

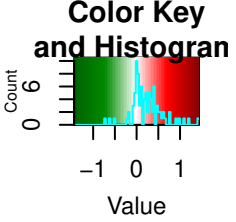

Amyotrophic lateral sclerosis (ALS)
hsa05014

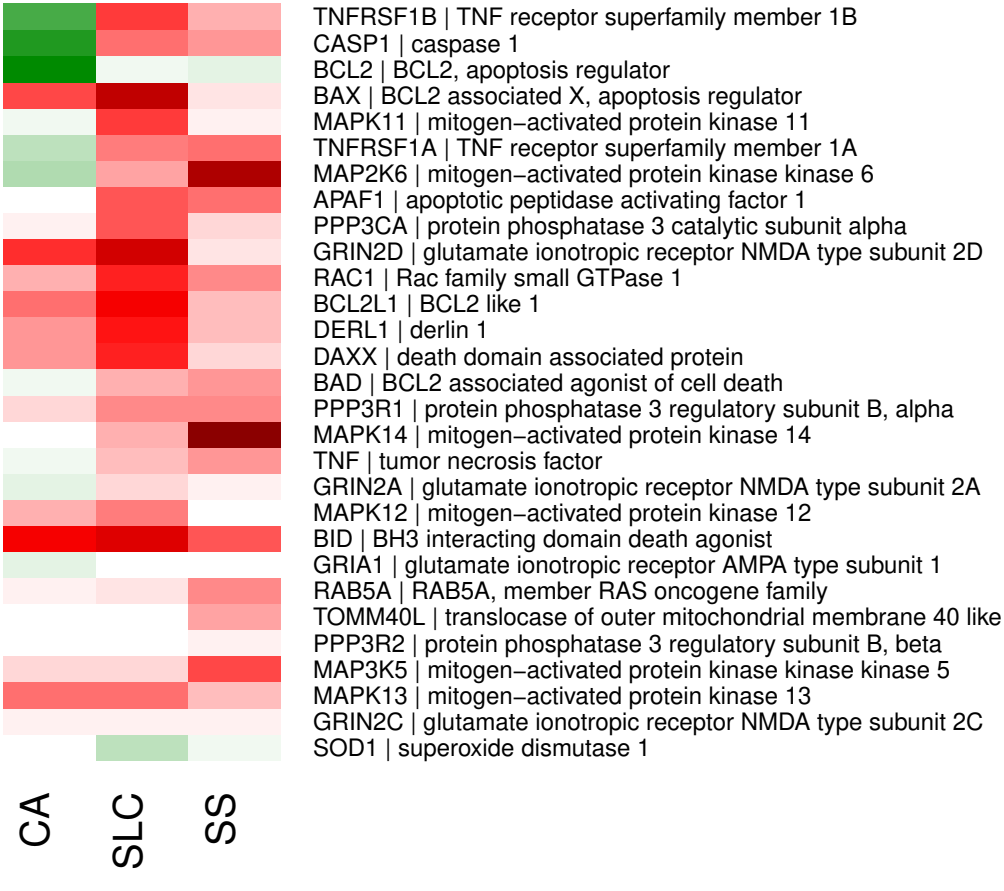

Other

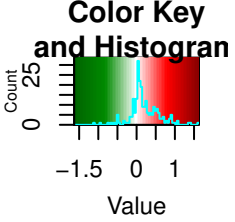

Alcoholism
hsa05034

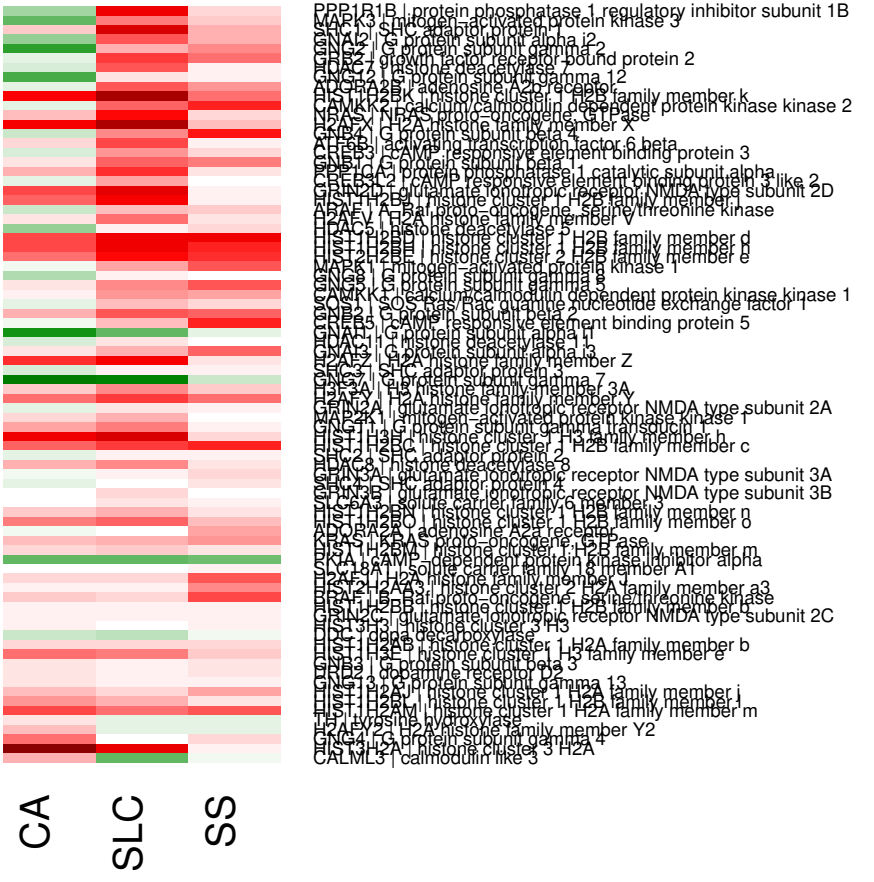

Other

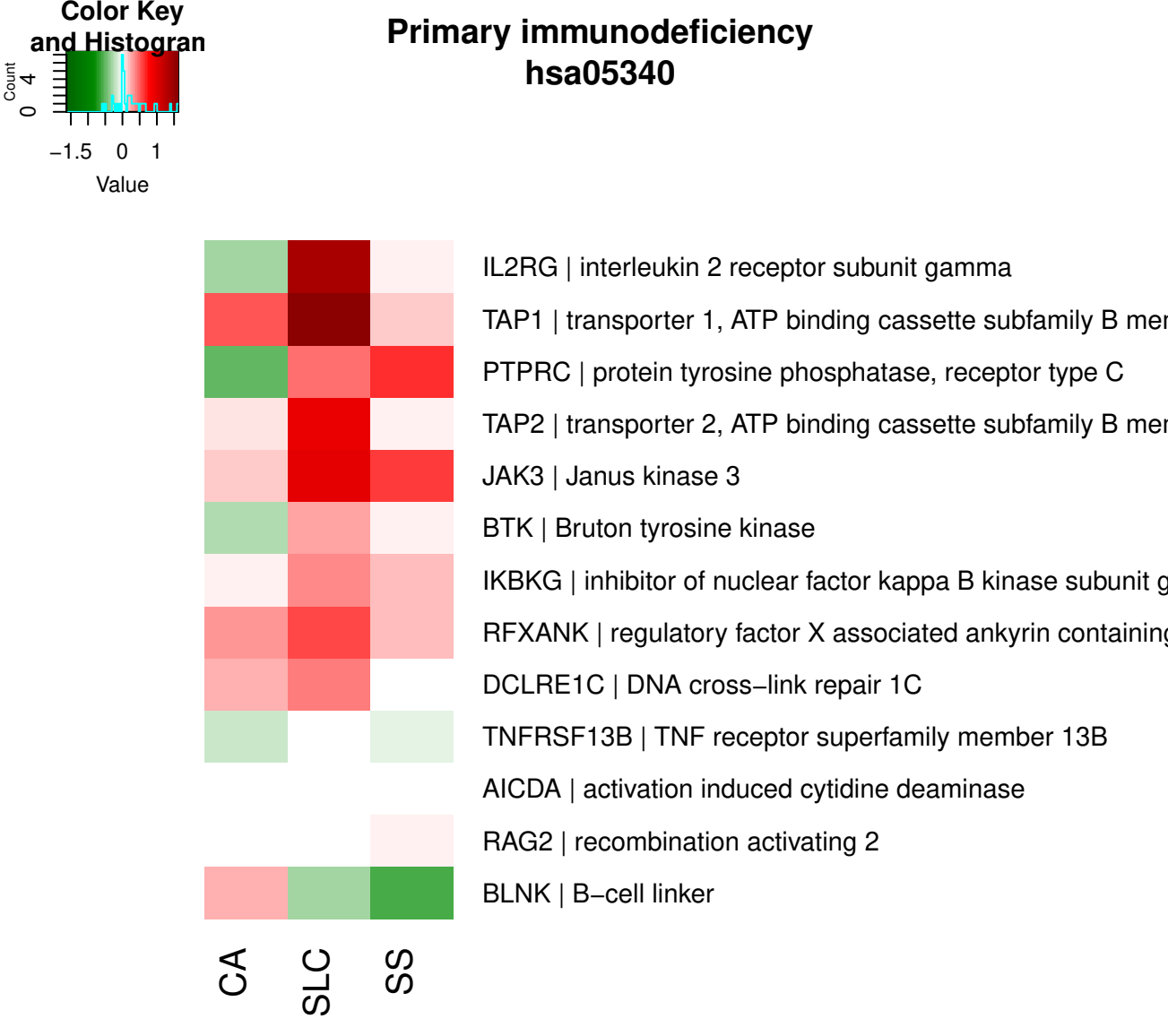
Color Key
and Histogram
Count
0
4
−1.5
0
1
Value
Primary immunodeficiency
hsa05340
IL2RG | interleukin 2 receptor subunit gamma
TAP1 | transporter 1, ATP binding cassette subfamily B mem
PTPRC | protein tyrosine phosphatase, receptor type C
TAP2 | transporter 2, ATP binding cassette subfamily B mem
JAK3 | Janus kinase 3
BTK | Bruton tyrosine kinase
IKBKG | inhibitor of nuclear factor kappa B kinase subunit g
RFXANK | regulatory factor X associated ankyrin containing
DCLRE1C | DNA cross−link repair 1C
TNFRSF13B | TNF receptor superfamily member 13B
AICDA | activation induced cytidine deaminase
RAG2 | recombination activating 2
BLNK | B−cell linker
CA
SLC
SS

Other

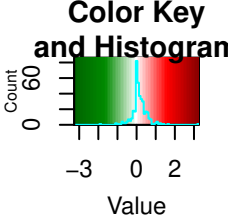

MAPK signaling pathway
hsa04010

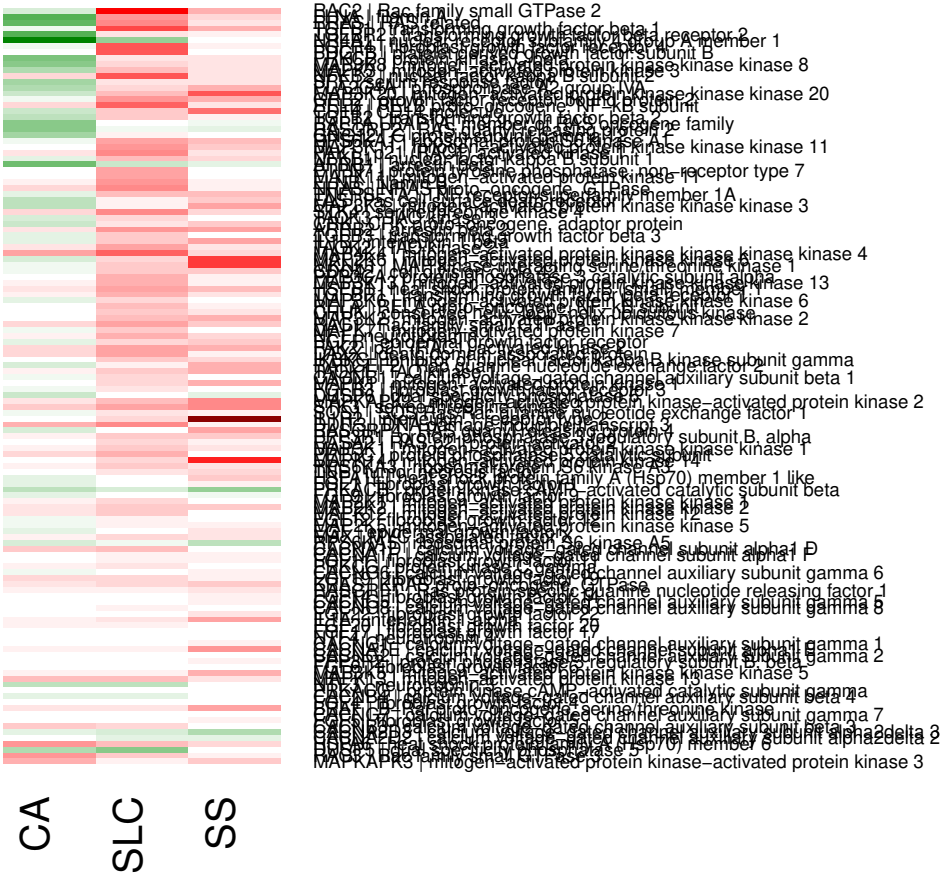

Signal transduction

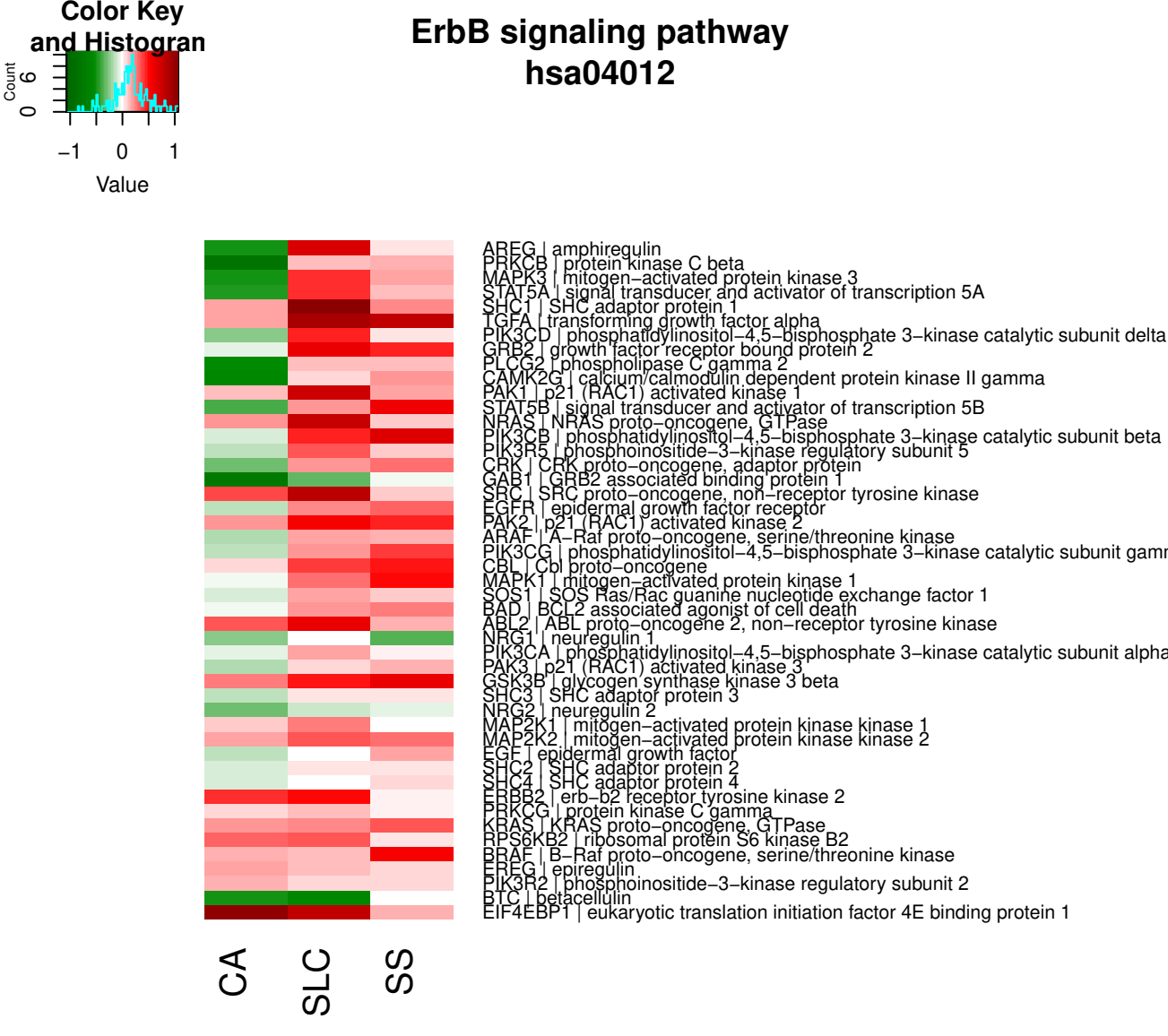

Signal transduction

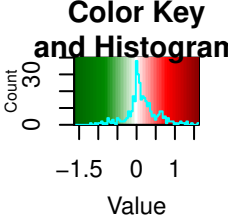

Rap1 signaling pathway
hsa04015

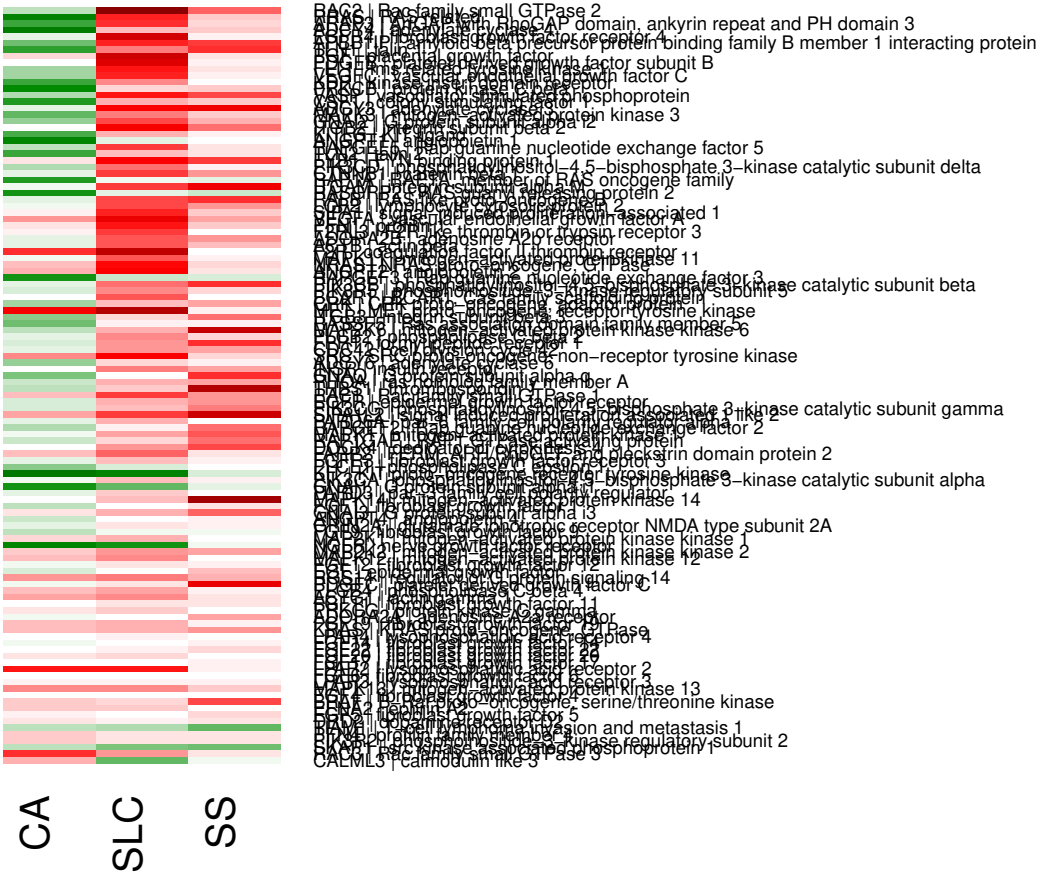

Signal transduction

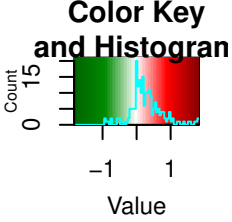

HIF−1 signaling pathway
hsa04066

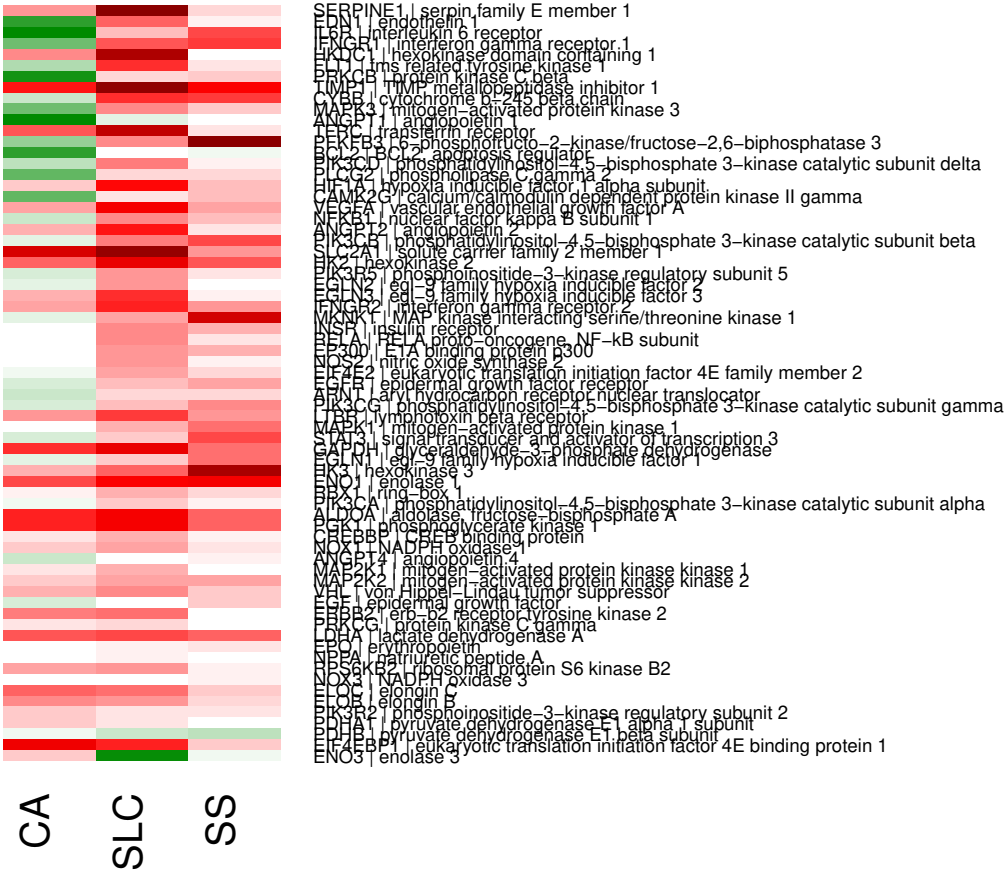

Signal transduction

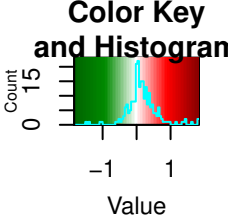

FoxO signaling pathway
hsa04068

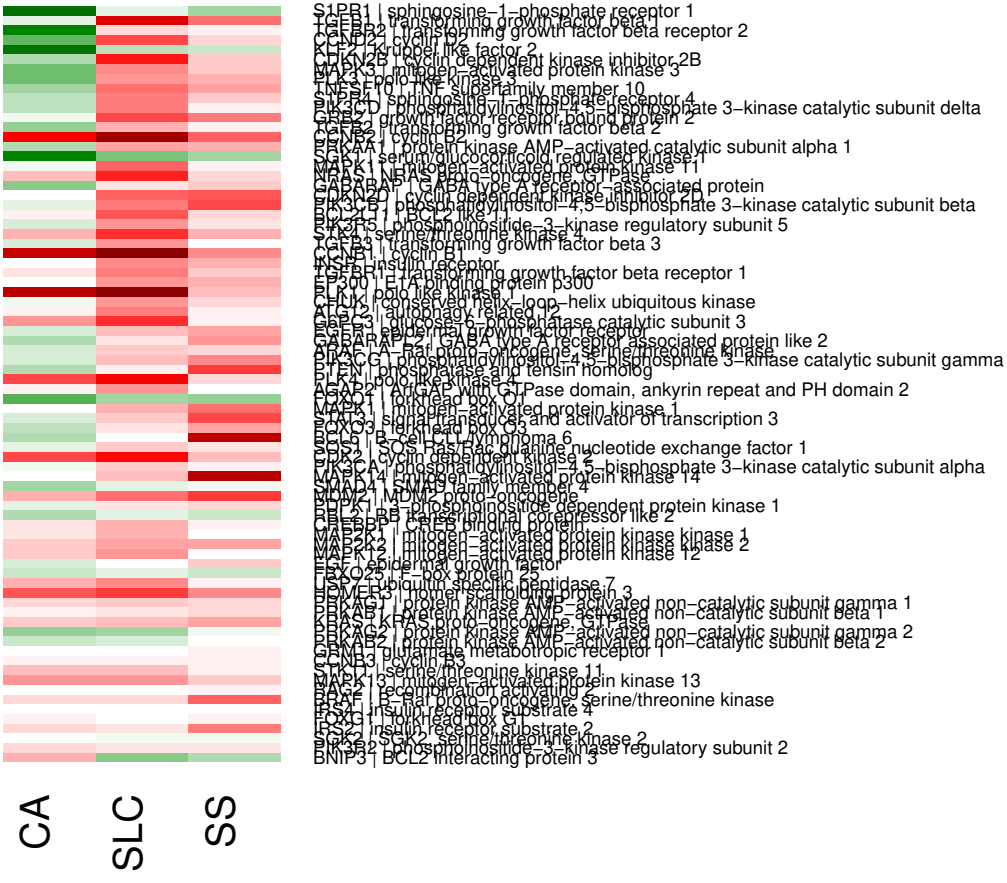

Signal transduction

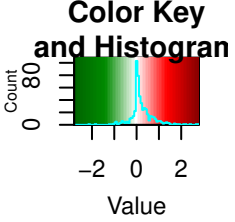

PI3K−Akt signaling pathway
hsa04151

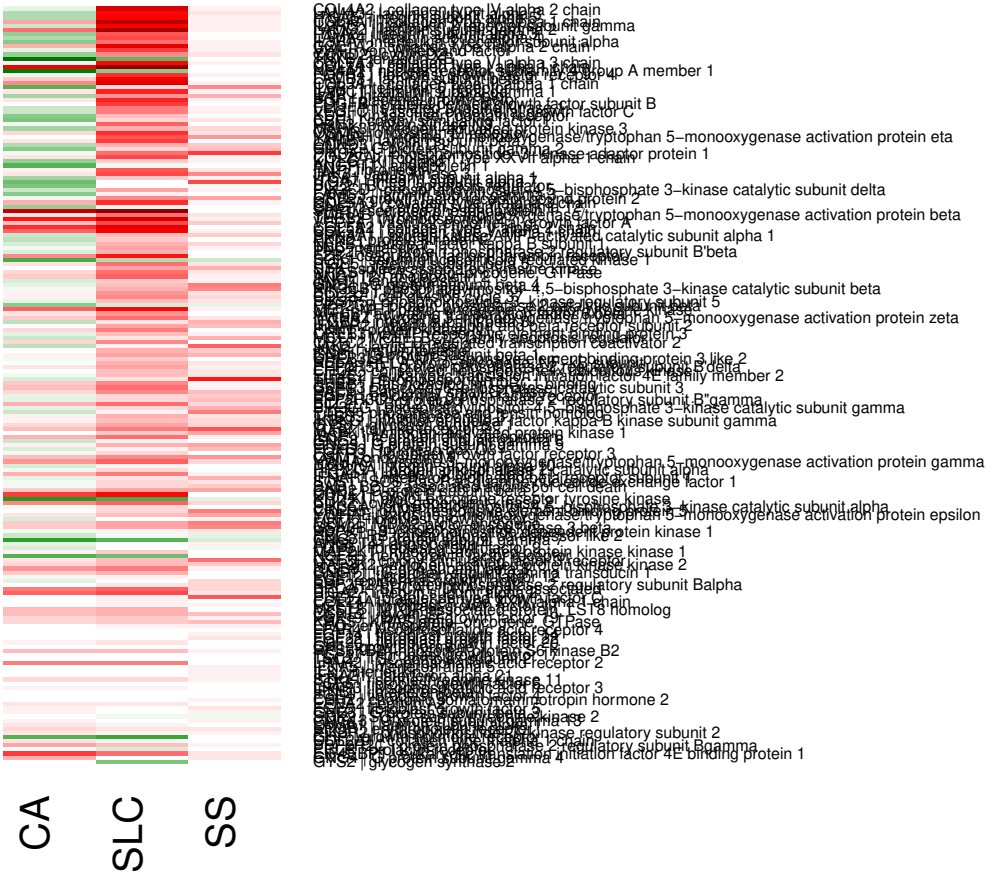

Signal transduction

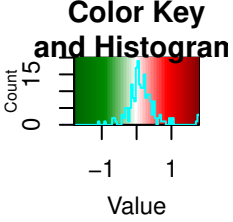

AMPK signaling pathway
hsa04152

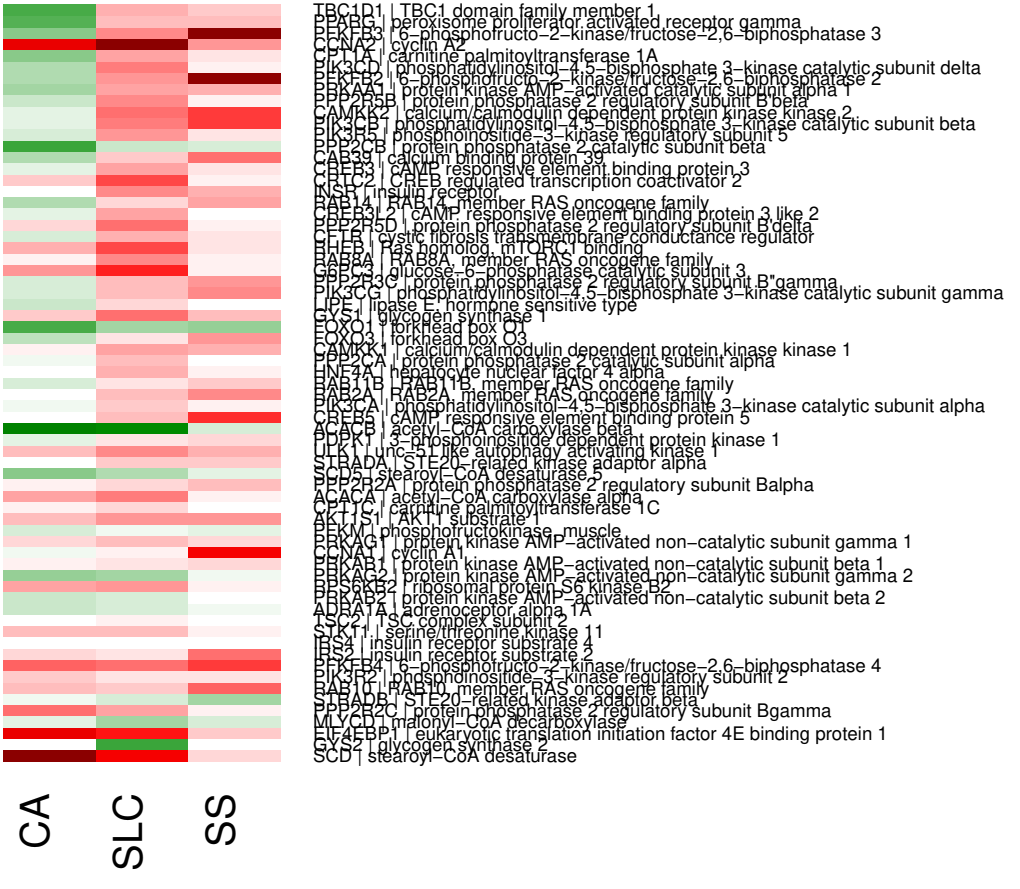

Signal transduction

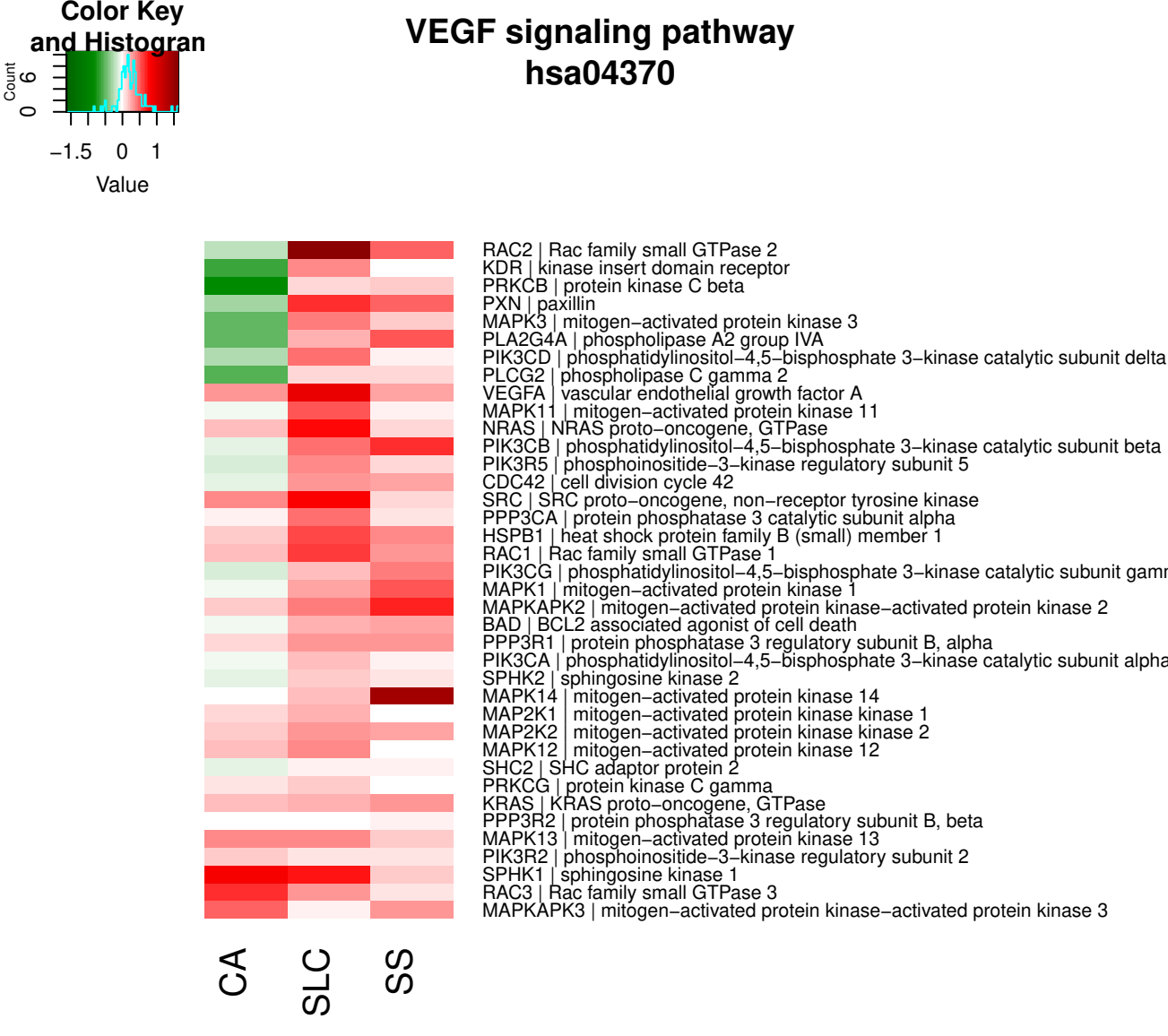

Signal transduction

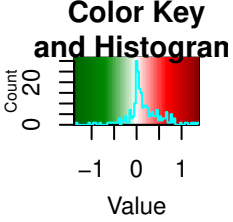

Jak−STAT signaling pathway
hsa04630

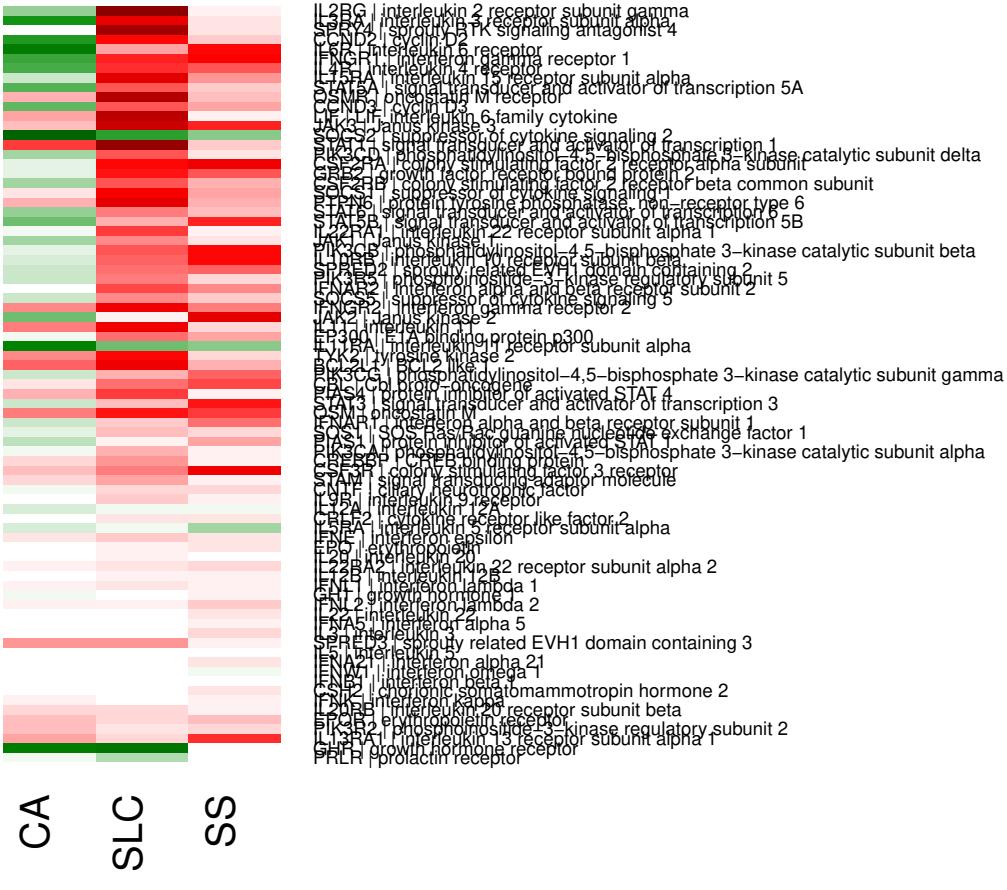

Signal transduction

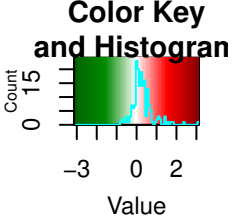

TNF signaling pathway
hsa04668

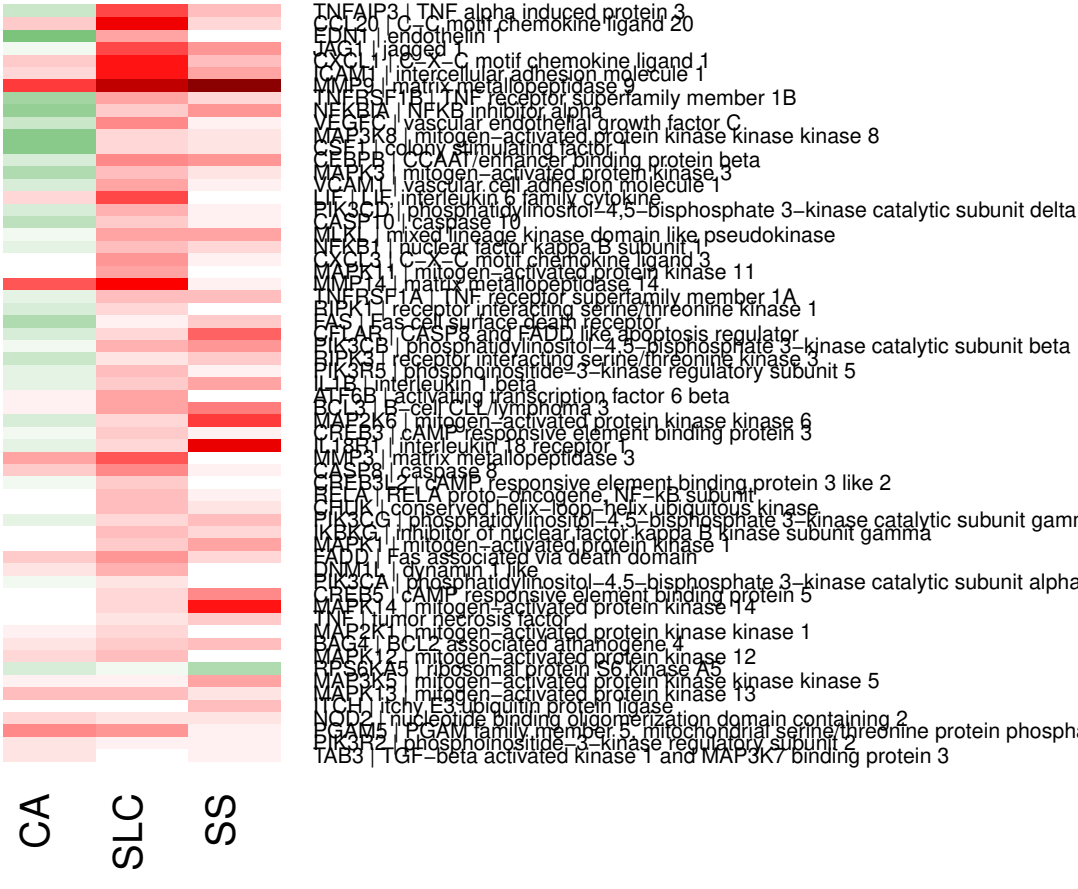

Signal transduction

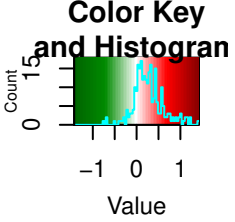

Lysosome
hsa04142

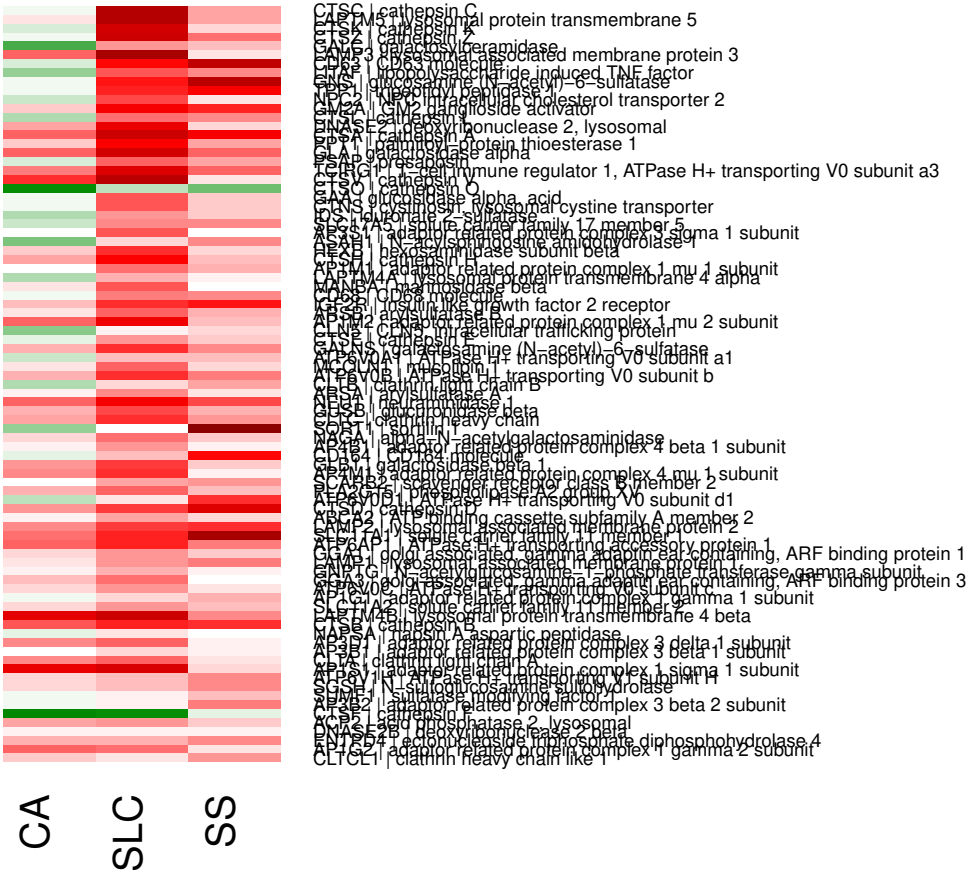

Transport and catabolism

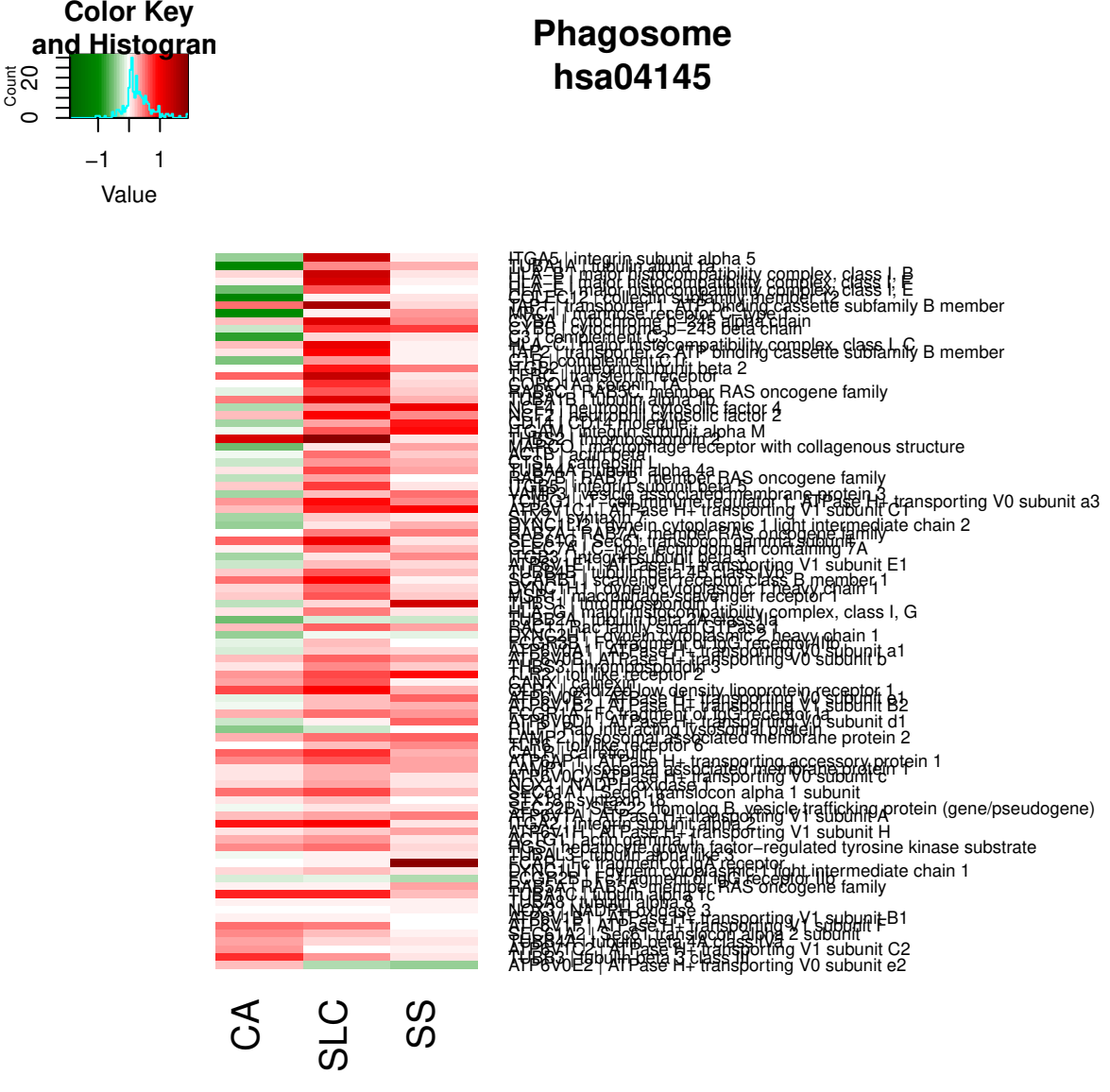
Color Key
and Histogram
Count
0
20
−1
1
Value
Phagosome
hsa04145
ITGA5 | integrin subunit alpha 5
TUBA1A | tubulin alpha 1a
HLA−B | major histocompatibility complex, class I, B
HLA−E | major histocompatibility complex, class I, E
HLA−F | major histocompatibility complex, class I, F
CD1E | CD1E antigen, e polypeptide
CD1D | CD1D antigen, d polypeptide
ABCB1 | transporter 1, ATP binding cassette subfamily B member
MRC1 | mannose receptor, C type 1
CYBB | cytochrome b−245 beta chain
C3 | complement C3
HLA−C | major histocompatibility complex, class I, C
TAP2 | transporter 2, ATP binding cassette subfamily B member
C7 | complement C7
ITGB2 | integrin subunit beta 2
TCR | transferrin receptor
C6 | complement C6
RAB7A | RAB7A, member RAS oncogene family
TUBA1B | tubulin alpha 1b
NCF4 | neutrophil cytosolic factor 4
NCF2 | neutrophil cytosolic factor 2
C9 | complement C9
ITGAM | integrin subunit alpha M
THBS2 | thrombospondin 2
MARCO | macrophage receptor with collagenous structure
CTSB | cathepsin B
CTSD | cathepsin D
TUBA4A | tubulin alpha 4a
RAB5B | RAB5B, member RAS oncogene family
ITGB3 | integrin subunit beta 3
VAMP3 | vesicle associated membrane protein 3
ATP6V0A1 | ATPase H+ transporting V0 subunit a1
ATP6V1C1 | ATPase H+ transporting V1 subunit C1
SYNCRIP | cytoplasmic 1 light intermediate chain 2
RAB7A | RAB7A, member RAS oncogene family
CD36 | CD36 antigen
TCEB2 | transcription elongation factor B (SIII), polypeptide 2 (p18, elongin B)
ITGB7 | integrin subunit beta 7
ATP6V1E1 | ATPase H+ transporting V1 subunit E1
TUBB4B | tubulin beta 4B class IVb
SCARB1 | scavenger receptor class B member 1
DYNC1H1 | dynein cytoplasmic 1 heavy chain 1
MSR1 | macrophage scavenger receptor 1
THBS1 | thrombospondin 1
HLA−G | major histocompatibility complex, class I, G
TUBB4A | tubulin beta 4A class IVa
DYNC2H1 | dynein cytoplasmic 2 heavy chain 1
DYNC1H1 | dynein cytoplasmic 1 heavy chain 1
ATP6V0A1 | ATPase H+ transporting V0 subunit a1
ATP6V0B | ATPase H+ transporting V0 subunit b
THBS3 | thrombospondin 3
TLR2 | toll like receptor 2
CANX | calnexin
SCARB2 | scavenger receptor class B member 2
ATP6V0D1 | ATPase H+ transporting V0 subunit d1
ATP6V1B2 | ATPase H+ transporting V1 subunit B2
ATP6V1C1 | ATPase H+ transporting V1 subunit C1
ATP6V1D | ATPase H+ transporting V1 subunit D
RILP | Rab interacting lysosomal protein
TMEM2 | transmembrane protein 2
TLR6 | toll like receptor 6
CALR | calreticulin
ATP6AP1 | ATPase H+ transporting accessory protein 1
LAMP1 | lysosomal associated membrane protein 1
ATP6V0C | ATPase H+ transporting V0 subunit c
NOX4 | NADPH oxidase 4
SLC9A1 | solute carrier family 9 (sodium/hydrogen exchanger), member 1
SLC25A5 | solute carrier family 25 (mitochondrial carrier; adenine nucleotide translocator), member 5
SEC22B | SEC22 homolog B, vesicle trafficking protein (gene/pseudogene)
ITGA2 | integrin subunit alpha 2
ATP6V1A | ATPase H+ transporting V1 subunit A
ATP6V1H | ATPase H+ transporting V1 subunit H
ACTG1 | actin gamma 1
HGS | hepatocyte growth factor−regulated tyrosine kinase substrate
TUBA1C | tubulin alpha 1c
FCGR2B | Fc fragment of IgG receptor
FCGR2A | Fc fragment of IgG receptor IIa
DYNLRB1 | dynein cytoplasmic 1 light intermediate chain 1
FCGR2B | Fc fragment of IgG receptor IIb
RAB5C | RAB5C, member RAS oncogene family
TUBA1C | tubulin alpha 1c
TUBA3 | tubulin alpha 3
NEDD4 | NEDD4 E3 ubiquitin protein ligase
ATP6V1B1 | ATPase H+ transporting V1 subunit B1
ATP6V1F | ATPase H+ transporting V1 subunit F
SLC9A1A2 | solute carrier family 9 (sodium/hydrogen exchanger), member 1 (antiporter, exchanger) pseudogene 2
TUBB4A | tubulin beta 4A class IVa
ATP6V1C2 | ATPase H+ transporting V1 subunit C2
TUBB3 | tubulin beta 3 class III
ATP6V0E2 | ATPase H+ transporting V0 subunit e2
CA
SLC
SS
Transport and catabolism